

MINERALOGIA – SPECIAL PAPERS

Volume 49, 2019

Abstracts and field trip guide

XXVIth Meeting of the Petrology Group of the Mineralogical Society of Poland



Session:

“Versatile Petrology in the Earth Sciences Research”

24-27 October, 2019
CHEĆCINY

Organised by:

Polish Geological Institute – National Research Institute
University of Warsaw, Faculty of Geology



PAŃSTWOWY
INSTYTUT
GEOLOGICZNY



Editor of the series:

Marek MICHALIK

Institute of Geological Sciences, Jagiellonian University
Gronostajowa 30, 30-387 Kraków, Poland

Editors of Volume 49:

Magdalena PAŃCZYK-NAWROCKA, Łukasz BORKOWSKI

Polish Geological Institute – National Research Institute
Rakowiecka 4, 00-975 Warszawa, Poland

Organising committee

Chairs:

Bogusław BAGIŃSKI (University of Warsaw, Faculty of Geology)

Magdalena PAŃCZYK-NAWROCKA (Polish Geological Institute – NRI)

Secretaries:

Paweł DERKOWSKI (Polish Geological Institute – NRI)

Anna GRABARCZYK (University of Warsaw, Faculty of Geology)

Members:

Agnieszka MARCINOWSKA (University of Warsaw, Faculty of Geology)

Sylwester SALWA (Polish Geological Institute – NRI)

Piotr LENIK (Polish Geological Institute – NRI)

Rafał SIUDA (University of Warsaw, Faculty of Geology)

Sławomir ILNICKI (University of Warsaw, Faculty of Geology)

Monika CYRKLEWICZ (Polish Geological Institute – NRI)

Łukasz BORKOWSKI (Polish Geological Institute – NRI)

Anna BAGIŃSKA (Polish Geological Institute – NRI)

Katarzyna ZBOIŃSKA (Polish Geological Institute – NRI)

Oliwia GRAFKA (University of Warsaw, Faculty of Geology)

Małgorzata CEGIEŁKA (University of Warsaw, Faculty of Geology)

Anna MACIOCH (University of Warsaw, Faculty of Geology)

Maciej KAŁASKA (University of Warsaw, Faculty of Geology)

PL ISSN 1899-8518

Wydawnictwo Naukowe “Akapit”, Kraków

Kom. 608 024 572

e-mail: wn@akapit.krakow.pl; www.akapit.krakow.pl

XXVIth Meeting of the Petrology Group of the Mineralogical Society of Poland

SPONSORS

General Sponsors:



Official Sponsors:



Table of Contents

INVITED SPEAKERS	13
Daniel J. DUNKLEY, Martin J. WHITEHOUSE, Monika A. KUSIAK, Simon A. WILDE A precarious dance: observation and inference in the zirconology of the Eoarchean of the North Atlantic Craton	15
Urs KLÖTZLI, Jolanta BURDA, Quili LI Petrochronology: insights into the evolution of rocks by combining petrology and geochronology	20
Grazina SKRIDLAITE, Laurynas SILIAUSKAS, Sabina PRUSINSKIENE, Bogusław BAGIŃSKI Enigmatic origin of the Varena Iron Ore deposit in the crystalline basement of southern Lithuania: implications from microtextures and mineral chemistry of the carbonate and silicate rocks	22
Krzysztof WOŹNIAK A Century after the Braggs – Mineralogy Based on Aspherical Atoms/Ions	23
ABSTRACTS	25
Bogusław BAGIŃSKI, Daniel HARLOV, Petras JOKUBAUSKAS, Witold MATYSZCZAK, Ray MACDONALD Hydrothermal breakdown of chevkinite-(Ce) – evidence from experiments	27
Wojciech BARTZ, Jolanta RATUSZNA Mineralogical analysis and provenance of Gothic stone sculptures from the Teutonic Order in Prussia	28
Łukasz BIRSKI, Richard WIRTH, Bartosz BUDZYŃ, Anja SCHREIBER TEM constraints on experimental fluid-induced phase transformation of monazite and xenotime	29
Michał BUCHA, Łukasz PLEŚNIAK, Mikołaj PIETRAS, Anna DETMAN, Aleksandra CHOJNACKA, Mariusz O. JĘDRYSEK, Anna SIKORA, Leszek MARYNOWSKI Microbial methane formation from different lithotypes of Miocene lignites from Konin and Sieniawa region, Poland	30
Daniel BUCZKO, Magdalena MATUSIAK-MAŁEK, Brian UPTON, Theodoros NTAFLLOS, Sonja AULBACH, Michel GRÉGOIRE, Jacek PUZIEWICZ Magmatic and metasomatic processes beneath Hebridean Terrane recorded in non-peridotitic xenoliths and megacrysts – Loch Roag monchiquite dyke (Outer Hebrides, UK) case study	31

Bartosz BUDZYŃ, Jiří SLÁMA U-Pb isotopic constraints on experimentally re-equilibrated xenotime	32
Jolanta BURDA, Urs KLÖTZLI, Beata WOSKOWICZ-ŚLĘZAK, Quili LI Geochronological insights into the evolution of the Chopok granodiorite (Dumbier Crystalline Complex, Lower Tatra Mts., W. Carpathians, Slovakia)	33
Małgorzata CEGIEŁKA, Bogusław BAGIŃSKI, Ray MACDONALD Primary and secondary mineralogy of the peralkaline granite of the Ilímaussaq Complex, South Greenland	34
Andrzej CHMIELEWSKI, Sławomir OSZCZEPALSKI Zonation of copper sulphides within the uppermost part of the Rote Fäule oxidation front in the Kupferschiefer series of SW Poland	35
Jakub CIAZELA, Bartosz PIETEREK, Marta GRABOWSKA, Andrzej MUSZYŃSKI, Hubert MAZUREK, Levente PATKO Towards global model of enrichment in sulfides along the crust-mantle transition zone	36
Justyna CIESIELCZUK, Janusz JANECZEK, Mateusz DULSKI, Tomasz KRZYKAWSKI, Eligiusz SZEŁĘG Cobalt- and zinc hydrous arsenates from Miedzianka, Sudetes Mts., Poland	37
Anna CZARNECKA-SKWAREK, Agnieszka ROŻEK, Emilia WÓJCIK Thermally modified and acidic activated clay minerals with microbiological quality in cosmetics industry applications	38
Justyna DOMAŃSKA-SIUJA, Krzysztof NEJBERT Textural and geochemical evidence for mixing within rapakivi-like granitoids from Krasnopol intrusion, Mesoproterozoic Mazury Complex, NE Poland	39
Grzegorz GIL, Bogusław BAGIŃSKI, Piotr GUNIA, Stanisław MADEJ, Zdzisław BELKA The origin of Nb mineralization in nephrites of the Ślęza Ophiolite	40
Maciej GÓRKA, Wojciech BARTZ, Alisa SKURIDINA, Anna POTYSZ Mineralogical and geochemical interpretation of atmospheric aerosols collected on <i>Populus nigra Italica</i> leaves in the JSC Almalyk Mining and Metallurgical Combine (Uzbekistan) area	41
Magdalena GORYL, Kamila BANASIK, Justyna SMOLAREK-LACH, Leszek MARYNOWSKI Estimation of thermal maturity of the Ediacaran organic matter from the East European Craton. Comprehensiveness of using GC-MS and Raman Spectroscopy techniques	42

Anna GRABARCZYK, Janina WISZNIEWSKA, Ewa KRZEMIŃSKA, Talat AHMAD New insights into mineralogy and geochemistry of the Aravalli mafic sequence, Rajasthan, India	43
Thomas HADLARI Sedimentary inheritance of detrital zircon age spectra	44
Sławomir ILNICKI, Ilona SEKUDEWICZ, Yan LIU, Grzegorz GIL Preliminary U-Pb dating and O isotope study of zircons from hornblendite from Bystrzyca Górna (Góry Sowie Massif, SW Poland)	45
Sławomir ILNICKI, Jacek SZCZEPAŃSKI Lawsonite pseudomorphs in metapelites and eclogites from the Kamieniec Metamorphic Belt (Sudetes, SW Poland): evidence of HP-LT conditions of prograde Variscan metamorphism	46
Petras JOKUBAUSKAS New software to improve the baseline accuracy of elemental composition measurements on SXFiveFE at University of Warsaw	47
Dominik JURA, Justyna CIESIELCZUK, Monika FABIAŃSKA, Magdalena MISZ-KENNAN, Joanna NOWIK Burned out coal seam No. 505 covered by red beds in sub-crop of the Saddle Beds in the southern part of the Chwałowice Syncline (Upper Silesian Coal Basin, Poland)	48
Maciej KAŁASKA, Marcin SYCZEWSKI, Jakub KOTOWSKI, Miłosz GIERSZ Chemical analysis of metal fragments from Castillo de Huarmey (Peru) using FE-SEM-EDS and FE-EMPA	49
Katarzyna KĄDZIOŁKA, Anna PIETRANIK, Jakub KIERCZAK, Anna POTYSZ Thermochemistry of disequilibrium silicate melts: reconstruction of smelting and cooling temperatures in slags	50
Piotr KENIS, Jacek SKURZYŃSKI, Zdzisław JARY Composition of heavy minerals in loess from Złota, using automated QEMSCAN analysis	51
Karolina KOŚMIŃSKA, Jane GILOTTI, William MCCLELLAND, Matthew COBLE P-T-t evolution of the Petersen Bay assemblage, Ellesmere Island: Insight into Pearya – Laurentia accretion	52
Jakub KOTOWSKI Application of rutile thermometer as a provenance indicator of Albian sands from southern Poland	53

Łukasz KRUSZEWSKI, Wojciech SIERNY Radlin coal fire heap: thiosulfate- and dithionate-bearing alkaline mineralization; Cu, Fe, As, and P mineralization; and second worldwide occurrence of tsaregorodtsevite	54
Łukasz KRUSZEWSKI, Rafał SIUDA, Mateusz ŚWIERK, Eligiusz SZEŁĘG New occurrences of secondary minerals from Fore-Sudetic Monocline copper deposits: juangodoyite (Rudna IX mine) and rapidcreekite/brushite (Lubin Główny mine)	55
Łukasz KRUSZEWSKI, Rafał SIUDA, Patryk KOSAŁKA, Paweł ŻOCHOWSKI, Beata MARCINIAK-MALISZEWSKA, Ewa DEPUT Copper and manganese minerals from “Hans” mine in Przygórze (Lower Silesia, SW Poland) – preliminary results	56
Ewa KRZEMIŃSKA, Leszek KRZEMIŃSKI, Ryszard HABRYN, Jolanta PACZEŚNA, Grzegorz ZIELIŃSKI The age of youngest detrital grains of clastic sediments and their interpretation – the cases of active versus passive tectonic settings	57
Piotr LENIK, Sylwester SALWA , Jakub BAZARNIK Ni,Co-pyrites (bravoites) from the Holy Cross Mountains, Poland	58
Piotr LENIK, Sylwester SALWA, Jakub BAZARNIK Thiospinels (siegenite, fletcherite) from the Holy Cross Mountains, Poland – preliminary results	59
Łukasz MACIĄG, Bernard CEDRO, Anna CEDRO Pegmatitic granite from Manikyangsa, Wangdue Phodrang, central Bhutan	60
Łukasz MACIĄG, Dominik ZAWADZKI Ferromanganese crusts from the Clarion-Clipperton polymetallic nodules deposit, equatorial Pacific, Interoceanmetal (IOM) claim area	61
Anna MACIOCH A comparison of vivianite-group minerals from the Kletno and Złoty Stok deposits (SW Poland)	62
Jarosław MAJKA Could contact metamorphism cause the Marinoan glaciation?	63
Rafał MAŁEK, Stanisław Z. MIKULSKI The critical and associated elements enrichment in cassiterite-sulphide mineralization from the stratiform tin deposits in the Stara Kamienica Schist Belt (Sudetes, SW Poland)	64
Dariusz MARCINIAK, Jacek SZCZEPAŃSKI Single-element geothermobarometry of selected rocks from the Doboszowice Metamorphic Complex (Fore-Sudetic Block)	65

Beata MARCINIAK-MALISZEWSKA Detrital Cr-spinel from Arafura Sea sediments (eastern Indonesia) as a tool in provenance studies of modern sand	66
Barbara MASSALSKA, Oliwia GRAFKA, Anna POSZYTEK Insights into the origin of organic matter and paleoenvironmental conditions of the Zechstein Limestone basinal facies from the Rudna copper mine (Fore-Sudetic Monocline, Poland) as a potential source of natural gas	67
Piotr MATCZUK, Magdalena MATUSIAK-MAŁEK, Brian G.J. UPTON, Theodoros NTAFLS, Sonja AULBACH A glance at lower crust beneath S Scotland – preliminary results on pyroxenitic xenoliths from Midland Valley and Southern Uplands	68
Hubert MAZUREK, Jakub CIAZELA, Magdalena MATUSIAK-MAŁEK, Jacek PUZIEWICZ, Theodoros NTAFLS, Anna KUKUŁA, Bartosz PIETEREK Melt-rock reaction and metal enrichment in the subcontinental lithospheric mantle: the Wilcza Góra xenoliths (SW Poland) case study	69
Jakub MIKRUT, Magdalena MATUSIAK-MAŁEK, Theodoros NTAFLS, Michel GREGOIRE, Leif JOHANSSON, Jacek PUZIEWICZ Cumulate xenoliths from S Sweden – tholeiitic intrusion in deep crust?	70
Magdalena PAŃCZYK, Jerzy NAWROCKI, Wiesław KOZDRÓJ, Małgorzata ZIÓŁKOWSKA-KOZDRÓJ, Krystian WÓJCIK New U-Pb ages of magmatic succession from Los Humeros Geothermal Field (E Mexico)	71
Magdalena PAŃCZYK, Jerzy NAWROCKI , Grzegorz ZIELIŃSKI Dating of charnockite-series rocks from Litynskiy complex (Podolian block, Ukraine) – preliminary results	72
Artur PĘDZIWIATR, Łukasz UZAROWICZ, Anna POTYSZ Mineralogy and properties of coal and wood combustion products from home stoves – preliminary results	73
Bartosz PIETEREK, Jakub CIAZELA, Riccardo TRIBUZIO Sulfide-rich melt-mantle reaction zones in the Balmuccia peridotite massif (NW Italy)	74
Anna POTYSZ, Jakub KIERCZAK Biologically and chemically mediated dissolution of copper metallurgical slags ...	75
Arkadiusz PRZYBYŁO, Anna PIETRANIK Zircon populations in rhyolitic rocks from Central Europe: insight from SEM-MLA analyses	76
Maciej RYBICKI, Leszek MARYNOWSKI, Bernd R.T. SIMONEIT Organic tracers from Miocene lignite burning	77

Sylwester SALWA The pyrophyllite – a new mineral of the metamorphic rocks from the Holy Cross Mountains, Poland	78
Sylwester SALWA, Wiesław TRELA Lower Ordovician (Tremadocian) tuffaceous mudstones from the Holy Cross Mountains, Poland: mineral composition and early diagenetic silicification	79
Magdalena SEK, Elżbieta HYCNAR Influence of sorbent texture and structure on sorption properties relative to SO ₂ – the case of dolomites	80
Mateusz SEK, Adam PIECZKA Remobilization of Ca and Ti during the contact metamorphism of Karkonosze Granite on basis of tourmaline of the Ca-series from Budniki near Kowary	81
Magdalena SITARZ, Piotr JELEŃ, Bożena GOŁĘBIEWSKA, Krzysztof NEJBERT Methane inclusions in Western Tatra Mountains mineralization: study by Raman spectroscopy	82
Rafał SIUDA, Bożena GOŁĘBIEWSKA, Adam PIECZKA, Paweł JELEŃ, Jan PARAFINIUK Walkilldellite-(Fe) from Rzędziny (Rudawy Janowickie Mts., SW Poland) – a preliminary report	83
Piotr SŁOMSKI, Jacek SZCZEPAŃSKI Numerical simulation of geological CO ₂ sequestration: case study of selected mudstones from the Baltic Basin	84
Justyna SMOLAREK-LACH, Leszek MARYNOWSKI, Wiesław TRELA , Paul B. WIGNALL Mercury as a proxy for large-scale volcanism during the Late Ordovician mass extinction	85
Marcin STACHOWICZ X-ray diffraction and photoelectron spectroscopy studies of chemically complex mineral chevkinite-(Ce)	86
Jacek SZCZEPAŃSKI, Robert ANCZKIEWICZ, Gabriela KASZUBA Detrital zircon provenance of volcano-sedimentary succession from the Kamieniec Metamorphic Belt (the Sudetes, SW Poland): preliminary data	87
Jacek SZCZEPAŃSKI, Xin ZHONG, Marcin DĄBROWSKI, Haozheng WANG, Marcin GOLEŃ P-T evolution of HP metapelites from the Kamieniec Metamorphic Belt, the Sudetes, SW Poland: evidence from raman spectroscopy of quartz inclusions in garnet and modelling of garnet zoning	88

Sylvin S. T. TEDONKENFACK, Jacek PUZIEWICZ, Theodoros NTAFLÓS, Sonja AULBACH, Anna KUKUŁA, Magdalena MATUSIAK-MAŁEK, Małgorzata ZIOBRO First data on mantle xenoliths from Befang (Oku Massif) in the Cameroon Volcanic Line	89
Fabian TRAMM, Grzegorz RZEPA, Bartosz BUDZYŃ, Gabriela A. KOZUB-BUDZYŃ Micro-Raman spectroscopy of experimentally altered monazite and xenotime	90
Katarzyna WALCZAK, Jarosław MAJKA, David G. GEE, Iwona KLONOWSKA, Christopher BARNES First geochronological evidence for the Finnmarkian orogenic event in the central Scandinavian Caledonides	91
Katarzyna ZBOIŃSKA, Anna POTYSZ, Wojciech BARTZ, Felix SCHMIDT, Markus LENZ Bioweathering processes of the Cretaceous joint sandstones from the North-Sudetic Basin	92
Karol ZGLINICKI, Gustaw KONOPKA, Krzysztof SZAMAŁEK REE minerals in the cassiterite processing tailings from Indonesian Tin Islands	93
Grzegorz ZIELIŃSKI, Petras JOKUBAUSKAS, Ewa KRZEMIŃSKA, Dominik GURBA, Paweł DERKOWSKI Chemical (U-Th-Pb) dating of monazite: standards and application	94
Grzegorz ZIEMNIAK, Jarosław MAJKA, Maciej MANECKI, Katarzyna WALCZAK, Karolina KOŚMIŃSKA Retrograde monazite records Early Devonian sinistral strike-slip shearing in the Müllernesset Formation, SW Svalbard	95
Małgorzata ZIOBRO, Jacek PUZIEWICZ, Theodoros NTAFLÓS, Sonja AULBACH, Magdalena MATUSIAK-MAŁEK Preliminary data on lithospheric mantle underlying Mid-German Crystalline High Variscan unit: Breitenborn (Vogelsberg) case study	96
FIELD TRIP GUIDE	97
Rafał SIUDA, Justyna DOMAŃSKA-SIUDA STOP 1: Miedzianka deposit – one of the oldest mining centres in Poland	99
Piotr LENIK, Sylwester SALWA STOP 2: Hematite mineralization in Zachełmie quarry, Holy Cross Mts.	104
Jerzy NAWROCKI, Magdalena PAŃCZYK Stop 3: Bardo diabase – Prągowiec	108
AUTHORS' INDEX	111

**XXVIth Meeting of the Petrology Group
of the Mineralogical Society of Poland**

Invited Speakers



A precarious dance: observation and inference in the zirconology of the Eoarchean of the North Atlantic Craton

Daniel J. DUNKLEY¹, Martin J. WHITEHOUSE², Monika A. KUSIAK³, Simon A. WILDE⁴

¹*Faculty of Earth Sciences, University of Silesia in Katowice, Sosnowiec, Poland;*
e-mail: daniel.dunkley@es.edu.pl

²*Swedish Museum of Natural History, Stockholm, Sweden*

³*Institute of Geophysics, Polish Academy of Sciences, Warsaw, Poland*

⁴*School of Earth & Planetary Sciences, Curtin University, Perth, Australia*

In high-grade gneissic terranes, much of the interpretation of geological history is made from microbeam dating (especially Secondary Ion Mass Spectrometry, or SIMS) of zircon, especially where it is the only mineral that survives multiple insults of metamorphism and deformation. This is the case in the Eoarchean record of crustal development, since all rocks of this age have been converted into amphibolite to granulite-facies gneisses, including those in the western part of the North Atlantic Craton (NAC, Fig. 1), which includes the best-preserved geological field relationships in the Isua region of SW Greenland (Nutman et al. 2019). Through careful dating, linked with interpretation of growth and modification structures in zircon, the pervasive Neoproterozoic metamorphism and deformation that occurred during the formation of the NAC can be ‘seen through’ to identify an assembly of Eoarchean terranes during a ca. 3.6 Ga orogeny that produced the Itsaq Gneiss Complex, and by inference the world’s first ‘supercontinent’, called Isukaqia by Nutman et al. (2015).

Further west, on the edge of the NAC, the Saglek Block of northern Labrador preserves Eoarchean gneisses that are mostly tonalite-trondhjemite-granodiorite (TTG). New SIMS data from the ~100 km section of coast between Ramah Bay and Hebron Fjord, when combined with recent work by Kusiak et al. (2018), Sałacińska et al. (2018, 2019), Vezinet et al. (2018) and Dunkley et al. (2019), along with earlier high-precision studies, reveal the dominance of ages between 3.75 and 3.70 Ga in the TTG Uivak Gneiss, with subsequent high-grade metamorphism at ca. 3.6 Ga (Fig. 2).

The difference in the Eoarchean record of the Saglek Block with that of the Isukasia Terrane of SW Greenland, where distinct domains of crust were assembled from 3660 Ma, leads us to propose a new ‘Uivak Terrane’ with an independent history before the formation of Isukaqia. Age elements from the ‘Uivak Terrane’ that are found in the complexly deformed Færingehavn Terrane, including remnants of pre-3.85 Ga TTG crust, may be an indication that the latter incorporates components of the ‘Uivak’ and Isukasia Terranes.

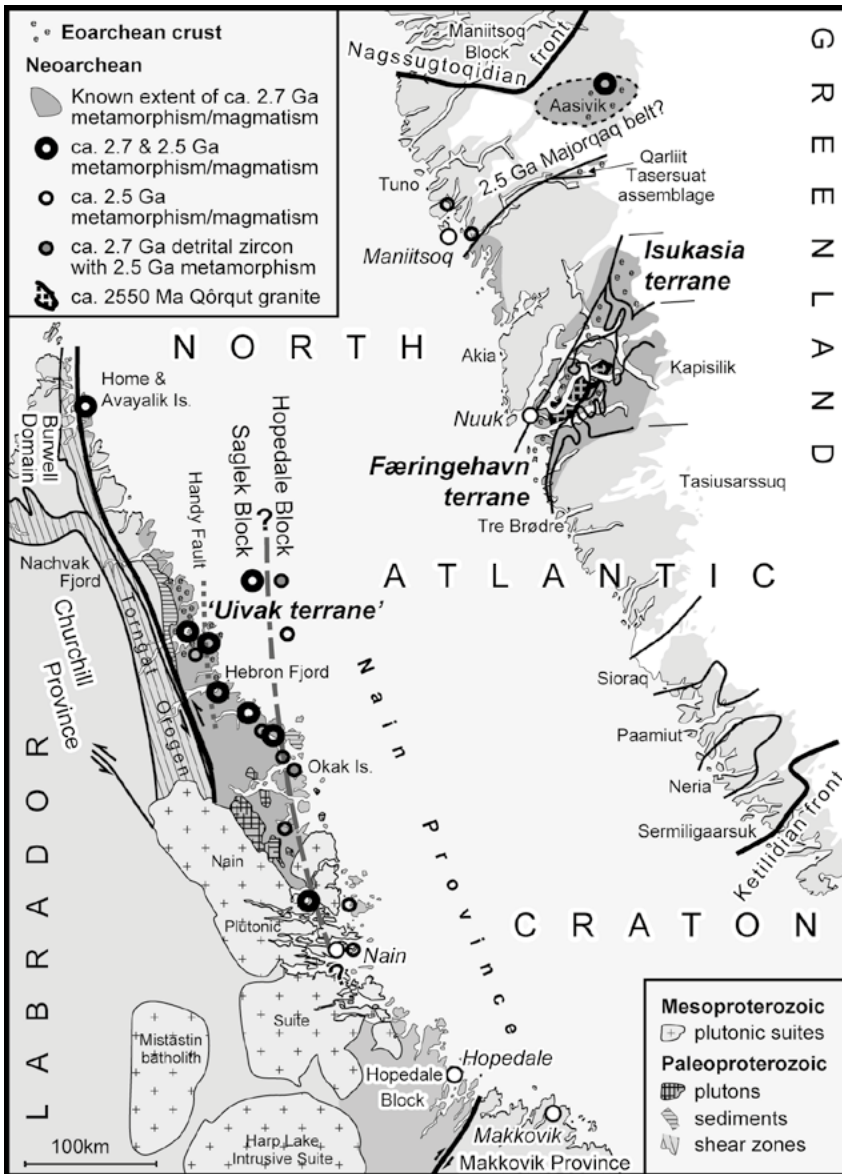


Fig. 1. Reconstructed western North Atlantic Craton (NAC) modified after Dunkley et al. (2019).

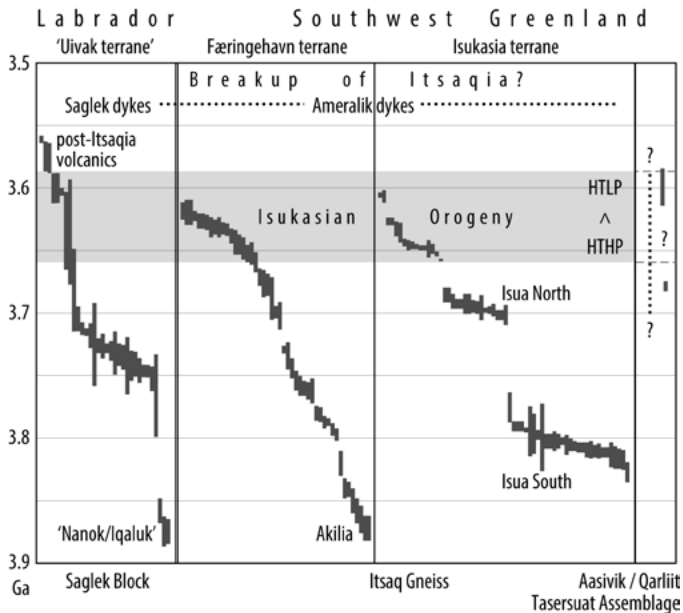


Fig. 2. Eoarchean protolith and metamorphic ages in the western part of the North Atlantic craton, modified after Sałacińska et al. (2018), with additional data from Sałacińska et al (2019) and unpublished SIMS data. The assembly of terranes in the Itsaq Gneiss Complex of SW Greenland during the Isukasian Orogeny also involved Eoarchean crust in the Saglek Block of northern Labrador, as demonstrated by the presence of metamorphic zircon at ca. 3.6 Ga. A distinct generation of TTG crustal growth between 3.75 and 3.70 Ga is here regarded as a separate 'Uivak terrane'.

The precarious dance

The 'age plateau' seen in data from the Uivak Gneiss is not seen in the more continuous 'prolonged granitoid formation' proposed by Komiya et al. (2017) on the basis of zircon dating by Laser Ablation Ion-Coupled Plasma Mass Spectrometry (LA-ICPMS). This is because the latter study lacks precision in analytical protocols and a neglect of statistical reproducibility in age estimates. A loose approach to analysis and interpretation has led the same team to claim evidence of life in supposedly >3.95 Ga supracrustal rocks from the Saglek Block (Tashiro et al. 2018). However, such claims are based on undemonstrated assumptions, in both field relationships and the interpretation of zircon textures and ages, and contradict evidence from earlier studies (Whitehouse et al. 2019). This includes arbitrary 'cherry-picking' of >3.9 Ga analyses from an imprecise dataset, which contains a subset of statistically equivalent data that yield a more robust 'maximum' age of ca. 3870 Ma. Rather than dating protolith formation, zircon of this age found in metagranite that postdates gneiss formation was used by Shimojo et al. (2016) to constrain the time of metamorphism. Re-analysis of the TTG gneiss (Fig. 3) and metagranite transposed into the dominant gneissosity provides a ca. 3870 Ma age for protolith formation, and reveals an additional generation of ca. 2710 Ma magmatic zircon in syn-tectonic granite. Thus, the estimated age for granitic magmatism and metamorphism obtained by Shimojo et al. (2016) is derived from xenocrystic zircon incorporated into a much younger melt. This case study demonstrates the confusion that can arise when the essential interplay between observation and inference in zirconology is neglected.

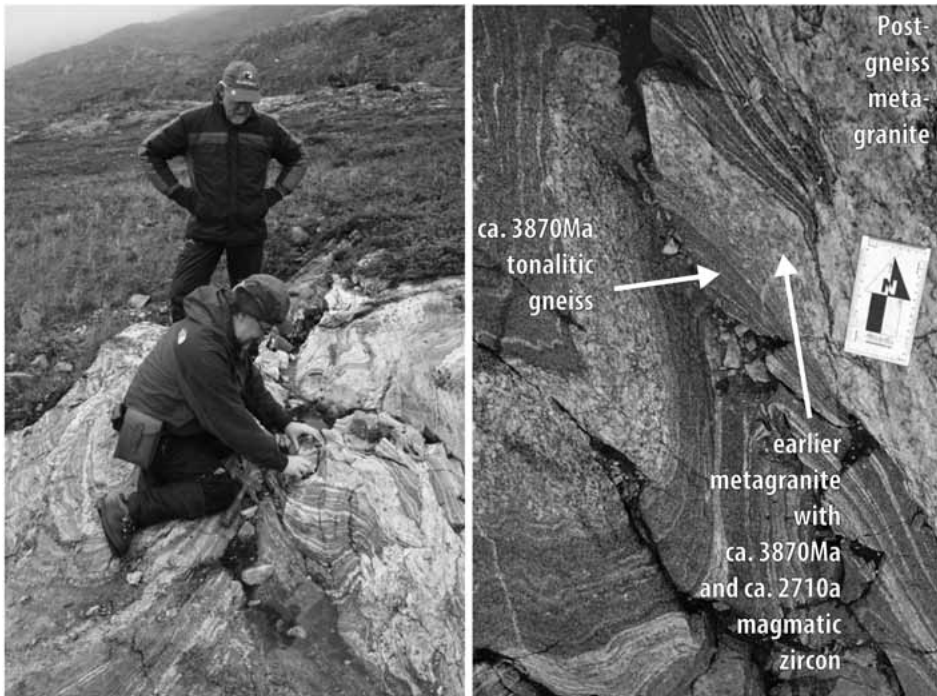


Fig. 3. Resampling of gneisses interpreted by Shimojo et al. (2016) to have >3.9 Ga protoliths metamorphosed at ca. 3.87 Ga. Re-analysis reveals gneiss formation at ca. 2.7 Ga.

Acknowledgments. DJD: POLONEZ fellowship UMO-2016/23/P/ST10/01214 from the National Science Center (NCN), funded through EU Horizon 2020 under Marie Skłodowska-Curie grant agreement No. 665778. MAK: NCN grant UMO2016/21/B/ST10/02067. MJW: Grants from the Knut and Alice Wallenberg Foundation (2012.0097) and the Swedish Research Council (2012-4370); SAW: funding from the Australian Research Council Centre of Excellence for Core to Crust Fluid Systems (CCFS).

References

- Dunkley, D.J., Kusiak, M.A., Wilde, S.A., Whitehouse, M.J., Sałacińska, A., Kielman, R. & Konečný, P. (2019). Two Neoproterozoic tectonothermal events on the western edge of the North Atlantic Craton, as revealed by SIMS dating of the Saglek Block, Nain Province, Labrador. *Journal of the Geological Society*. <https://doi.org/10.1144/jgs2018-153>.
- Komiya, T., Yamamoto, S., Aoki, S., Koshida, K., Shimojo, M., Sawaki, Y., Aoki, K., Sakata, S., Yokoyama, T.D., Maki, K., Ishikawa, A., Hirata, T. & Collerson, K.D. (2017). A prolonged granitoid formation in Saglek Block, Labrador: Zonal growth and crustal reworking of continental crust in the Eoarchean. *Geoscience Frontiers*, 8, 355–385.
- Kusiak, M.A., Dunkley, D.J., Whitehouse, M.J., Wilde, S.A., Sałacińska, A., Konečný, P., Szopa, K., Gawęda, A. & Chew D. (2018). Peak to post-peak thermal history of the Saglek Block of Labrador: a multiphase and multi-instrumental approach to geochronology. *Chemical Geology*, 484, 210–223.
- Nutman, A.P., Friend, C.R.L., Barker, S.S. & McGregor, V.R. (2004). Inventory and assessment of Palaeoproterozoic gneiss terrains and detrital zircons in southern West Greenland. *Precambrian Research*, 135, 281–314.

- Nutman, A.P., Bennett, V.C. & Friend, C.R.L. (2015). Proposal for a continent 'Itsaqia' amalgamated at 3.66 Ga and rifted apart from 3.53 Ga: initiation of a Wilson Cycle near the start of the rock record. *American Journal of Science*, *315*, 509-536.
- Nutman, A.P. & Bennett, V.C. (2019). The 3.9–3.6 Ga Itsaq Gneiss Complex of Greenland. In: van Kranendonk, M., Bennett, V.C. & Hoffmann, J.E. (Eds), *The World's Oldest Rocks*, 2nd Ed., Elsevier, Amsterdam, Chapter 17, 375–399.
- Sałacińska, A., Kusiak, M.A., Whitehouse, M.J., Dunkley, D.J., Wilde, S.A. & Kielman, R. (2018). Complexity of the early Archean Uivak Gneiss: Insights from Tigigagkyuk Inlet, Saglek Block, Labrador, Canada and possible correlations with south West Greenland. *Precambrian Research*, *315*, 103–119.
- Sałacińska, A., Kusiak, M.A., Whitehouse, M.J., Dunkley, D.J., Wilde, S.A., Kielman, R. & Król, P. (2019). Gneiss forming events in the Saglek Block, Labrador: a reappraisal of the Uivak Gneiss. *International Journal of Earth Sciences*, *108*, 753–778.
- Shimojo, M., Yamamoto, S., Sakata, S., Yokoyama, T. D., Maki, K., Sawaki, Y., Ishikawa, A., Aoki, K., Aoki, S., Koshida, K., Tashiro, T., Hirata, T., Collerson, K. D. & Komiya, T. (2016). Occurrence and geochronology of the Eoarchean, ~3.9 Ga, Iqaluk Gneiss in the Saglek Block, northern Labrador, Canada: Evidence for the oldest supracrustal rocks in the world. *Precambrian Research*, *278*, 218–243.
- Tashiro, T., Ishida, A., Hori, M., Igisu, M., Koike, M., Méjean, P., Takahata, N., Sano, Y., Komiya, T. (2017). Early trace of life from 3.95 Ga sedimentary rocks in Labrador, Canada. *Nature*, *549*, 516–518.
- Vežinet, A., Pearson, D. G., Thomassot, E., Stern, R. A., Sarkar, C., Luo, Y., Fisher, C. M. (2018). Hydrothermally-altered mafic crust as source for early Earth TTG: Pb/Hf/O isotope and trace element evidence in zircon from TTG of the Eoarchean Saglek Block, N. Labrador. *Earth and Planetary Science Letters*, *503*, 95–107.
- Whitehouse, M. J., Dunkley, D. J., Kusiak, M. A., Wilde, S.A. (2019). On the true antiquity of Eoarchean chemofossils – assessing the claim for Earth's oldest biogenic graphite in the Saglek Block of Labrador. *Precambrian Research*, *323*, 70–81.



Petrochronology: insights into the evolution of rocks by combining petrology and geochronology

Urs KLÖTZLI¹, Jolanta BURDA², Quili LI³

¹Department of Lithospheric Research, University of Vienna, Althanstrasse 14, 1090 Vienna, Austria;
e-mail: urs.kloetzli@univie.ac.at

²Faculty of Earth Sciences, University of Silesia, Będzińska st. 60, 41-200 Sosnowiec, Poland;
e-mail: jolanta.burda@us.edu.pl

³State Key Laboratory of Lithospheric Evolution, Institute of Geology and Geophysics,
Chinese Academy of Sciences, Beijing 100029, China; e-mail: liqiuli@mail.iggcas.ac.cn

The progress of geoscience research in our understanding of System Earth depends on the proper quantification of processes working on Earth. Most descriptions of System Earth processes incorporate some sort of quantification of time and time scales and thus process rates. For instance, the understanding of timescales of heating, cooling and exhumation of metamorphic and igneous basement units is a key problem in tectonics. The determination of the rates and timescales of processes that form, overprint and exhume metamorphic and igneous rocks depends on the knowledge of (a) the absolute age and (b) the P-T-X-d conditions to which these ages are related to.

In order to set the frame for the present account, we restrict the further discussion to metamorphic processes acting on the continental crust

Absolute age data collected from accessory minerals (hereafter AM) such as zircon, monazite, xenotime, apatite, allanite, rutile, baddeleyite, and titanite are preferentially used to derive the ages and rates of processes forming and overprinting continental crust. But despite the emphasis placed on these age data, our understanding of how to relate the timing of growth, textural and geochemical evolution and consumption of AM to an evolving rock remains in its infancy. Of major importance thereby is the determination of whether the geochronologically important AM form, for instance, during igneous activity, prograde metamorphism, during suprasolidus melting at or around peak temperature, or during the retro-grade post-peak temperature overprint at supra- or sub-solidus conditions.

Another fundamental problem is that especially in former studies AM chemistry “fingerprinting” was used as a proxy to the respective petrology of major mineral phases: The samples P-T-X-t evolution is derived by classical thermobarometry or forward modelling from major mineral phases only which are not directly dated. The age data on the other hand is provided by in-situ dating of AM. The link between petrology of the major mineral phases, and hence the whole rock P-T data and absolute AM ages is then made by mineral chemistry. For instance, the Y behaviour in garnet and monazite is used as a proxy to gain some insight into the petrological relation of the AM and major mineral phases in P-T-X-t space. In any case, using this classical approach of combining independently derived petrological and geochronological data, the correlation of absolute age and petrology s.l. remains ambiguous at best.

So even in spite of the immense amount of published radiometric age and petrologic data, the unification thereof enabling a more objective quantification of orogenic processes remains to be a challenge.

This is where the field of petrochronology comes into play: Petrochronology is the interpretation of (mostly radiometric) absolute ages in the light of complementary elemental or isotopic information from the same mineral(s) thus combining petrology and geochronology. Petrochronology basically combines geochemistry, textures, and thermodynamic modelling and absolute ages in a petrogenetic context of individual crystals or crystal domains. Examples in metamorphic systems include the use of crystal domain-specific trace element patterns or thermometers in minerals like zircon, monazite, xenotime, apatite, allanite, titanite, rutile, etc. to link an age to a rocks P-T-d evolution. The field of petrochronology is expanding rapidly to exploit in-situ trace elements and Hf isotopes in zircon, trace elements and Nd-Hf isotopes in monazite, apatite and xenotime, trace elements, Sm-Nd and Sr isotopes in titanite, and trace elements and Hf isotopes in rutile, to name but a few. Although primarily founded in metamorphic studies, petrochronology has numerous other applications to igneous and detrital mineral studies as well. All of these approaches are founded on the same principle: that the combination of absolute ages and elemental/isotopic mineral systematics provides a powerful methodology to enhance our understanding of Earth System processes.

There are a number of components to petrochronology that can be used to varying degrees of success in different minerals. The textural setup of a mineral helps to identify the reactions that formed, recrystallized, or partially consumed the mineral or identify deformation or fluid flow coincident with such. The elemental and isotopic zoning of a mineral, assessed through CL and BSE imaging or direct chemical mapping (LASS (MC-) ICP-MS, LA-(MC-) ICP-MS, SIMS, EMPA), can assist in matching mineral (re-)crystallization to specific igneous, metamorphic or deformation events, or the presence or absence of other minerals. The volume proportion of an accessory phase can be used as a qualitative barometer or thermometer in favourable circumstances when accompanied by pseudosection modelling. The concentrations of trace elements (e.g. Ti, Zr, and Y) can be used to estimate ambient temperatures.

One important fact to keep in mind is that petrochronology mainly deals with the estimation of “temperature ages” in T-t space. Providing reliable age estimates for ambient pressures is inevitably imprecise to impossible. This is due to the fact that the applied geochronometers are principally based on the transport of atoms, be it by crystal growth, simple volume diffusion s.l., fluid mediated transport, and/or recrystallization. And the rates, that is the effectiveness of these transport mechanisms, are to a high extent temperature dominated.

To date the most widely employed minerals for petrochronological investigations are zircon, monazite, titanite and rutile. These four accessory phases are found in a broad range of rocks and can persist through multiple sedimentary transport cycles, metamorphic and igneous events that span a wide range of pressures, temperatures, deformation and fluid conditions. They often grow in response to changes in these parameters and may record these changes in distinct compositional domains that can be related to mineral-forming reactions and dated.

Each of these accessories, plus for example xenotime and apatite, is readily dated in-situ by the U-Th-Pb dating methods as U and/or Th and Pb concentrations are high enough to permit the determination of precise and accurate in-situ ages at the scale of a few microns. U and Th are effectively immobile and Pb has sufficiently low diffusivities over geologic time to allow age information from multiple episodes of growth, dissolution and re-precipitation to be preserved within single crystals. Also, the U-Th-Pb system has the advantage over other mineral chronometers (e.g. Rb-Sr, Sm-Nd, Lu-Hf, Re-Os) of allowing internal consistency testing. This permits to identify open system behaviour and makes possible a more stringent age data interpretation.

In short, petrochronological investigations can deliver a plethora of new insights into the T-X-t(-P-d) evolution of crystalline rocks thus allowing to identify and quantify more realistically System Earth processes and process rates.



Enigmatic origin of the Varena Iron Ore deposit in the crystalline basement of southern Lithuania: implications from microtextures and mineral chemistry of the carbonate and silicate rocks

Grazina SKRIDLAITE^{1,2}, Laurynas SILIAUSKAS¹, Sabina PRUSINSKIENE¹, Bogusław BAGIŃSKI³

¹*Institute of Geology and Geography, Nature Research Centre, Akademijos 2, LT-08412 Vilnius, Lithuania; e-mail: grazina.skridlaite@gamtc.lt*

²*Institute of Geosciences, Faculty of Chemistry and Geosciences, Vilnius University, M.K. Ciurlionio 21/27, LT-03225 Vilnius, Lithuania*

³*Institute of Geochemistry, Mineralogy and Petrology, Faculty of Geology of the University of Warsaw, Al. Żwirki i Wigury, 93, PL-02-089 Warszawa, Poland; e-mail: B.baginski@uw.edu.pl*

The Varena Iron Ore deposit (VIOD) yields from 71 to 219.6 million tons of iron ore according to different economic evaluations. In early nineties, the ores were assumed to be of metasomatic and hydrothermal origin, however several other hypotheses explaining the VIOZ origin, e.g. as a layered mafic, ultramafic or carbonatite intrusion were later suggested.

The VIOD in the crystalline basement of western East European Craton, S Lithuania, is situated predominantly in former dolostones, that accumulated in a shelf environment along an earlier, established after ca. 1.84 Ga (Bogdanova et al. 2015), continental margin. They were pure dolostones or contained variable amounts of cherts or clastic sediments. The metasediments are hosted by metamorphosed magmatic rocks of felsic and intermediate composition.

During the recent rock and mineral studies by SEM and EPMA approaches, high-grade skarns (forsterite, enstatite, spinel and diopside) produced in a closed system during metamorphism at 750° C and 5-6 kbar were distinguished. The X_{CO_2} concentrations, proximity to a contact with alumina-silicate rocks and silica, magnesium and calcium transportation in circulating fluids have caused the observed zonation. They were followed by water-consuming and amphibole (tremolite, actinolite, anthophyllite etc.) producing reactions during the later uplift.

The low-temperature (ca. 400-300°C) water fluid-influx caused a voluminous serpentinization, iddingsite and chlorite formation as well as brought iron, sulphides, and other mineralizations. Small homogeneous monazite grains and rims in the studied calciphyre yielded ca. 1.54 Ga, coinciding with the emplacement of voluminous AMCG suites such as the Mazury complex and the Kabeliai intrusions further south. To establish a relationship between the abundant sulphide, iron oxide and REE mineralizations in the Mazurys complex and in the VIOD would enhance considerably a potential of mineral resources in the whole region.

References

- Bogdanova, S., Gorbatshev, R., Skridlaite G., Soesoo A. & Taran L. D. K. (2015). Trans-Baltic Palaeoproterozoic correlations towards the reconstruction of supercontinent Columbia/Nuna. *Precambrian Research* 259, 5-33.



A Century after the Braggs – Mineralogy Based on Aspherical Atoms/Ions

Krzysztof WOŹNIAK¹

¹*Department of Chemistry, University of Warsaw, Pasteura 1, 02-093 Warszawa, Poland;
e-mail: kwozniak@chem.uw.edu.pl*

There is quite a paradox that a century after the introduction of the Independent Atom Model (IAM – Bragg 1914), 97% of all ca. 1.5 mln known crystal structures have been refined using IAM which has some methodological deficiencies including almost all minerals (with exception of ca. 30 of them). In the IAM atoms are spheres which do not exchange electron density. In my presentation, I will present different approaches to localization and refinement of H-atoms including applications of spherical Independent Atom Model (Sanjuan-Szklarz et al. 2016) and aspherical approaches such as the Hansen-Coppens pseudoatom formalism applied in multipole modeling (Hoser et al. 2009) and Hirshfeld Atom Refinement (HAR; Woińska et al. 2016). I will present a detailed comparison of the results obtained with different approaches as a function of data resolution and models of electron density and compare these with the results of neutron diffraction and theoretical computations. I will discuss the accuracy and precision of different refinement results. Additionally, I will present how H-atom ADPs change with data resolution and electron density models.

I will also present results of our successful experimental quantitative charge density feasibility study of grossular under high pressure. X-ray data collection for grossular was conducted on the CRISTAL beamline at the SOLEIL synchrotron (Paris, France). We studied single crystal of a natural mineral grossular – $\text{Ca}_3\text{Al}_2(\text{SiO}_3)_4$, which crystallizes in the space group Ia-3d of the cubic crystal system. The beamline parameters such as beam wavelength (0.41 Angstrom) and a special type of Diamond Anvil Cell (DAC) with the opening angle 110 deg. let us collect data with the resolution up to 0.35 Å (with 100% completeness up to 0.39 Å). We have compared our results with experimental charge densities obtained for grossular at ambient conditions and those obtained for pyrope – $\text{Mg}_3\text{Al}_2(\text{SiO}_3)_4$ (isostructural with grossular), measured at low temperature, 30K (Destro et al. 2017). In the case of our measurements for grossular, the calculated properties of the charge density at the (3, -1) BCPs as well as the net atomic charges are comparable. We think that thanks to the new type of DACs with wider opening angle and access to synchrotron radiations for some types of high symmetry compounds charge density distribution can be determined experimentally (Gajda et al. 2019). Up to our knowledge this is the first successful determination of quantitative charge distribution in crystal under high pressure (Fig. 1). This opens a new field of mineralogical subatomic studies of different mineralogical processes in the Earth mantle in laboratory conditions.



Fig. 1. (left) Redistribution of electron density at O and Al ions under high pressure, and (right) the 3D SiO₄ deformation electron density maps at ambient conditions – isosurfaces: blue colour +0.1 e/A³, red colour -0.1e/A³.

References

- Destro, R., Ruffo, R., Roversi, P., Soave, R., Loconte, L. & Presti, L.L. (2017). *Acta Crystallographica*, *B73*, 722-736.
- Gajda, R., Stachowicz, M., Makal, A., Sutula, S., Parafiniuk, J., Fertey, P. & Woźniak, K. (2019). Successful Experimental Quantitative Charge Density Feasibility Study of Grossular Under High Pressure, *IUCr Journal* (in press).
- Hoser, A.A., Dominiak P.M. & Woźniak K. (2009) .*Acta Crystallographica*, *A65*, 300-311.
- Sanjuan-Szklarz, W.F., Hoser, A. A., Gutmann, M., Madsen A.Ø. & Woźniak K. (2016). Yes, one can obtain better quality structures from routine X-ray data collection. *IUCr Journal*, *3*, 61-70.
- Woińska, M., Grabowsky, S., Dominiak, P.M., Woźniak, K. & Jayatilaka D. (2016). Hydrogen atoms can be located accurately and precisely by x-ray crystallography. *Science Advances*, *2*(5), e1600192.

**XXVIth Meeting of the Petrology Group
of the Mineralogical Society of Poland**

Abstracts



Hydrothermal breakdown of chevkinite-(Ce) – evidence from experiments

Bogusław BAGIŃSKI¹, Daniel HARLOV², Petras JOKUBAUSKAS¹, Witold MATYSZCZAK¹, Ray MACDONALD¹

¹*Institute of Geochemistry, Mineralogy and Petrology, Faculty of Geology, University of Warsaw, al. Żwirki i Wigury 93, 02-089 Warszawa, Poland; e-mail: b.baginski@uw.edu.pl*

²*GeoForschungsZentrum Potsdam, Telegrafenberg, D-14473 Potsdam, Germany; e-mail: dharlov@gfz-potsdam.de*

During hydrothermal alteration, the REE-bearing minerals of the chevkinite group (CGM) have the potential to release, not only REE but also high field-strength elements and the actinides. A commonly observed alteration sequence in natural rocks is chevkinite → titanite plus a REE phase, such as allanite and bastnäsite. To provide quantitative information on such reactions, we have experimentally subjected a natural chevkinite-(Ce) from the Diamer District, Pakistan to fluid-induced alteration involving a Ca(OH)₂-bearing hydrous fluid. The experimental conditions were: temperature 600°C; pressure 400 MPa; duration 21 days. Small amounts of natural albite and quartz were added to the charge to simulate natural rock-forming conditions more closely.

Significant reaction between the chevkinite-(Ce) and fluid occurred, with the formation of titanite and britholite-(Ce), plus minor hedenbergite. The nature of the reaction zones was very variable. Commonly, the rims of chevkinite-(Ce) were replaced by thin zones comprised first of britholite-(Ce) followed by titanite. Such a structure is similar to that experimentally produced by dissolution-reprecipitation in monazite and apatite by Harlov and colleagues. In the present case, chevkinite-(Ce) was dissolved by the fluid until it became saturated with britholite-(Ce) and then with titanite. With time, the reaction proceeded inwards into the chevkinite via a coupled dissolution reprecipitation process.

A second type of alteration is seen along cracks. Here britholite-(Ce) forms along the walls with titanite crystallizing centrally, often as beautifully euhedral crystals. The titanite occasionally formed “veinlets” away from the cracks, which cut across the chevkinite-(Ce). This attests to a remarkable mobility of the titanite component.

A puzzling result of the experiment is that we are so far unaware of any natural example where a CGM has broken down to titanite and britholite. Ongoing experiments using different combinations of ligands in the fluids and P-T-time conditions are aimed at creating a full record of the mechanisms and products of CGM alteration.

Acknowledgements. Study was financed from the National Science Centre, Poland; grant no. 2017/26/M/ST10/00407.



Mineralogical analysis and provenance of Gothic stone sculptures from the Teutonic Order in Prussia

Wojciech BARTZ¹, Jolanta RATUSZNA²

¹University of Wrocław, Institute of Geological Sciences, pl. M. Borna 9, 50-204, Poland;
e-mail: wojciech.bartz@uwr.edu.pl

²The Castle Museum in Malbork, Conservation Laboratory, ul. Starościńska 1, 82-200 Malbork, Poland;
e-mail: j.ratuszna@zamek.malbork.pl

A characteristic group of stone sculptures, dated back to ca. 1380-1400, showing a unity of convention and a high level of workmanship, was distinguished within the art of the state of the Teutonic Order in Prussia. All of these sculptures were carved in a golden-grey, unusual to Prussia and of unspecified lithology. Therefore a mineralogical analysis was planned in order to assess petrology of raw material and its provenance. A total of fifteen sculptures were selected for a more detailed study. A combination of mineralogical methods has been applied i.e.: optical microscopy (OM) scanning microscopy (SEM-EDX), X-ray diffraction (XRD), thermal analysis (DSC-TG).

Our study revealed that all investigated sculptures were made of a mineralogically similar marlstone. It is an extremely fine-grained rock, from pale-yellow to golden-yellow in color. The rock matrix consists of a microcrystalline silica-carbonate mass. The carbonates play a minor role and do not exceed ca. 30-35 wt.%. A microcrystalline iron oxyhydroxide occurs, but in small quantities (up to 5 wt.%). A more abundant constituents are flakes of clay minerals, represented mostly by kaolinite and subordinate illite. These occur in a form of single crystals, as well as small (up to 30-40 µm in diameter) aggregates of randomly oriented flakes. Kaolinite of concertina-type is uncommon. Single bioclasts, both carbonatitic and silica in nature, as well as detrital k-feldspar, quartz grains and glauconite aggregates are randomly disseminated within the matrix (up to ca. 50 µm).

The mineralogical character of investigated samples fits well to a Cretaceous marlstone, cropping out across the Europe. Samples of two varieties were chosen for comparative study: 1) marlstone from Přední Kopanina (Czech Republic) and 2) Baumberger Kalksandstein (Germany), both of them extensively used as building or as sculptural stone in the past. As a result, we found out that if the first one is mineralogically very similar to the investigated samples, the second one is significantly different. Comparing to the Přední Kopanina marlstone as well as investigated samples, it is stated that the rock is: 1) enriched in carbonates and carbonatitic bioclasts (the rock contains at least 55 wt.% of CaCO₃) at the expense of silica, 2) free from K-feldspar grains, 3) strongly depleted in clay-minerals.

Our study proved that the use of a multi-technique approach allows the best possible discrimination of source for raw-material. Moreover, it clearly indicates that rock quarried in Přední Kopanina was used as a raw-material for carving all of investigated sculptures.

Acknowledgements. The financial support from The Castle Museum in Malbork is acknowledged.



TEM constraints on experimental fluid-induced phase transformation of monazite and xenotime

Łukasz BIRSKI¹, Richard WIRTH², Bartosz BUDZYŃ¹, Anja SCHREIBER²

¹*Institute of Geological Sciences, Polish Academy of Sciences, Warszawa, Poland;*
e-mail: l.birski@twarda.pan.pl

²*GeoForschungsZentrum Potsdam (GFZ), Telegrafenberg, Potsdam, 14473, Germany*

Experimentally metasomatized monazite and xenotime (from Budzyń et al. 2017) have been evaluated by TEM to determine mechanisms of fluid-induced phase transformations in nanoscale. Six foils of altered monazite grains (experiments at 450°C, 400 MPa; 650°C, 1000 MPa; 750°C, 200 MPa) and three of altered xenotime (350°C, 400 MPa; 650°C, 200 MPa; 650°C, 1000 MPa) have been investigated. Two additional foils for monazite and xenotime were cut from the starting materials, as references to identify transformations of both phosphates. The TEM imaging modes of bright field (BF), dark field (DF) and lattice fringe imaging were used.

The TEM revealed extensive monazite alterations, and two types of transformations have been distinguished. The first is dissolution of the monazite and precipitation of steacyite at 450°C, or britholite and cheralite nanocrystals at 650–750°C. Alteration process initiated with removal of REE and Th from the monazite and precipitation of britholite, followed by nucleation of cheralite when Th concentration in fluid reached its saturation. The second type of phase transformation is penetration of the monazite by fluids migrating through the cracks along the cleavage planes of (100) and (001) (runs at 650–750°C). Traces of recrystallization are demonstrated as differences in the BF images contrast and developed extensive nano-porosity resulting from the fluid-induced coupled dissolution-reprecipitation process. Traces of this alteration within the entire monazite grains indicate that the process may be considered extremely effective. However, no changes in composition of the monazite altered along cleavages were detected by TEM-EDX analysis.

In the case of xenotime, the TEM observations revealed only the first type of alterations listed above. The britholite is the only alteration product, crystallizing from amorphous phase formed due to dissolution of the xenotime. The britholite precipitated in the form of numerous nano-crystals growing independently of each other.

The nanoscale TEM observations revealed differences in alterations of monazite and xenotime, providing new insights on their transformation mechanisms and remobilization of Th and REE during metasomatic processes.

Acknowledgements. The project was funded by the NCN grant no. 2017/27/B/ST10/00813.

References

- Budzyń, B., Harlov, D.E., Kozub-Budzyń, G.A. & Majka, J. (2017). Experimental constraints on the relative stabilities of the two systems monazite-(Ce) – allanite-(Ce) – fluorapatite and xenotime-(Y) – (Y,HREE)-rich epidote – (Y,HREE)-rich fluorapatite, in high Ca and Na-Ca environments under P-T conditions of 200–1000 MPa and 450–750 °C. *Mineralogy and Petrology*, *111*, 183–217.



Microbial methane formation from different lithotypes of Miocene lignites from Konin and Sieniawa region, Poland

Michał BUCHA¹, Łukasz PLEŚNIAK², Mikołaj PIETRAS², Anna DETMAN³, Aleksandra CHOJNACKA³, Mariusz O. JĘDRYSEK², Anna SIKORA³, Leszek MARYNOWSKI¹

¹Faculty of Earth Sciences, University of Silesia, Sosnowiec, Poland; e-mail: michal.bucha@gmail.com

²Faculty of Earth Sciences and Environmental Management, University of Wrocław, Wrocław, Poland

³Institute of Biochemistry and Biophysics, Polish Academy of Sciences, Warszawa, Poland

The main objective of the study was to determine and compare yield of microbial methane production from different lithotypes of Miocene lignites from Konin and Sieniawa region in Poland. For this purpose, a series of batch experiments inoculated with natural lignite microflora and microorganisms from an external source (e.g. sludge from a biogas plant, sewage sludge) were carried out. Detritic and xylitic lignites were used as substrates for biodegradation under anaerobic conditions. Biogas was analyzed to determine volume, concentration and stable carbon isotopes of microbial methane. The main analytical methods used in the study were gas chromatography (GC) and gas chromatography-combustion-isotope ratio mass spectrometry (GC-C-IRMS).

Our results showed that the natural microflora present in collected lignite samples from Konin and Sieniawa region is able to degrade lignin and cellulose. Unfortunately, in the batch experiments with using of natural microflora methane was not present. In case of batch experiments with using of methanogenic consortium from biogas plants and sewage sludge methane was produced from lignites of both: Konin and Sieniawa region. We found that xylite (fossil wood) is a slightly better raw material for the microbial methane production than detritic lignites. Methane yield for detritic lignite was equal 7.6 $\mu\text{mol CH}_4/\text{g}$ of sample, where for xylite it was 8.2 $\mu\text{mol CH}_4/\text{g}$ of sample. The mean $\delta^{13}\text{C}(\text{CH}_4)$ value in experiments with detritic coal from Konin was equal -36.3‰, where for fossil wood fragments it was -47.2‰ (well preserved trunks), and -42.4‰ (fibrous xylite). We suppose that differences in the mean $\delta^{13}\text{C}(\text{CH}_4)$ values from biodegradation of the different lithotypes of lignite from Konin region are depended most probably on the cellulose content (%). In analysed samples of detritic and xylitic lignites from Konin region the mean holocellulose content is equal 3.0% and 35.9%, respectively. The main gaseous product from biodegradation of lignite from Sieniawa region was nitrogen. This batch experiment was characterized by the mean $\delta^{13}\text{C}(\text{CH}_4)$ value equaled -55.3‰. The possible reason of enrichment of methane in light carbon isotopes, when compared to values obtained in experiment with lignite from Konin region, is partial fermentation of fresh sewage sludge. These results will be verified by culture-independent molecular biology techniques – metagenomics.

Acknowledgements. Funding: the National Science Center (Projects: DEC-2015/16/S/ST10/00430 and 2018/31/B/ST10/00284).



Magmatic and metasomatic processes beneath Hebridean Terrane recorded in non-peridotitic xenoliths and megacrysts – Loch Roag monchiquite dyke (Outer Hebrides, UK) case study.

Daniel BUCZKO¹, Magdalena MATUSIAK-MAŁEK¹, Brian G.J. UPTON², Theodoros NTAFLIOS³, Sonja AULBACH⁴, Michel GRÉGOIRE⁵, Jacek PUZIEWICZ¹

¹ Institute of Geological Sciences, University of Wrocław, pl. Maxa Borna 9, 50-204 Wrocław, Poland;

² Grant Institute, University of Edinburgh, James Hutton Rd., EH9 3FE Edinburgh, Scotland;

³ Department of Lithospheric Research, University of Vienna, Althanstraße 14, 1090 Wien, Austria;

⁴ Department of Geosciences, Goethe University Frankfurt, 60323 Frankfurt am Main, Germany;

⁵ Géosciences Environnement Toulouse, CNRS-CNES-IRD Université Toulouse III, OMP, Toulouse

An Eocene (Faithfull et al. 2012) monchiquite dyke near Loch Roag (N Scotland, Hebridean terrane) is rich in xenoliths (mantle and crustal) and a broad spectrum of megacrysts. Here we consider possible origins of dioritic and mica-clinopyroxenitic xenoliths and megacrysts of alkali feldspar and clinopyroxene from the dyke.

Dioritic xenoliths comprise plagioclase with of An₃₀₋₄₀ and clinopyroxene (Al-augite/diopside; Mg# =50-76). Clinopyroxene in biotite/phlogopite-bearing clinopyroxenites is Al-augite/diopside with Mg#=66-81. Megacrysts of alkali feldspar have Or₆₆₋₉₈ and may contain inclusions of clinopyroxene (Al,Ti-diopside; Mg# =54-63), biotite and apatite. Clinopyroxene megacryst is Al,Ti-diopside with Mg# =59-64 and contains inclusions of apatite and biotite.

The clinopyroxene in xenoliths is LREE-enriched: in the dioritic ones its (La/Lu)_N is 1-3, while in clinopyroxenitic xenoliths the ratios are 6-17. Clinopyroxene in both types of xenoliths are characterized by negative Nb-Ta, Zr-Hf and Ti anomalies; in dioritic clinopyroxene negative Eu negative anomaly is also present. Megacrystic clinopyroxene has (La/Lu)_N=8.75 and negative Ti anomalies. Both the plagioclase in the diorite and alkali feldspar megacrysts are LREE-enriched with (La/Lu)_N=66-320 and 202, respectively; feldspars in both have distinct positive Eu anomaly.

Two genetic models may be suggested for the studied suite of samples: 1) “metasomatic” model assumes metasomatism of diorites and clinopyroxenites by melts responsible for megacrysts crystallization; 2) “magmatic” model assumes origin of all the xenoliths and megacrysts from the same magmatic source, chemical and modal variation of the samples would record different stages of evolution of magmatic system. Future work focusing on radiogenic isotopes in clinopyroxene will help distinguish between these possibilities.

Acknowledgements. Funded by Polish National Science Centre grant no. UMO-2016/23/B/ST10/01905 and supported by the Polish-Austrian project WTZ PL 08/2018.

References

Faithfull, J.W., Timmerman M.J., Upton B.G.J. & Rumsey M. (2012). Mid-Eocene renewal of magmatism in NW Scotland: the Loch Roag Dyke, Outer Hebrides. *Journal of Geological Society*, 169, 115-118.



U-Pb isotopic constraints on experimentally re-equilibrated xenotime

Bartosz BUDZYŃ¹, Jiří SLÁMA²

¹*Institute of Geological Sciences, Polish Academy of Sciences (ING PAN), Research Centre in Kraków, Senacka 1, PL-31002 Kraków, Poland; ndbudzyn@cyf-kr.edu.pl*

²*Institute of Geology, ASCR (The Czech Academy of Sciences), Rozvojová 269, Prague 6 16500, Czechia*

The LA-ICP-MS U-Pb age constraints have been conducted on the xenotime from five experiments at 250°C, 200 MPa; 450°C, 600 MPa; 550°C, 800 MPa; 650°C, 200 and 600 MPa (experimental products from Budzyń, Kozub-Budzyń 2015; Budzyń et al. 2017) to evaluate potential re-equilibration of U-Pb isotopic system in xenotime induced by alkali-rich fluids. The experimental starting materials included xenotime (LA-ICP-MS U-Pb age of 38.37 ± 0.64 Ma), albite, K-feldspar, biotite, muscovite, garnet, SiO₂, CaF₂, Na₂Si₂O₇ and H₂O. The experimental setup roughly replicated granitic to metapelitic composition with high Na, Ca, Si and F activities in the fluid to enhance alterations of xenotime. The xenotime has been partially replaced by (Y,REE)-rich fluorapatite to Y-rich fluorocalciobrotholite in all experiments, and by an unnamed (Y,HREE)-rich silicate at 250°C and 200 MPa. The LA-ICP-MS analysis revealed no ²⁰⁶Pb/²³⁸U age disturbance in the xenotime from runs at 250°C, 200 MPa; 450°C, 600 MPa; and 650°C, 200 MPa. Faint to moderate patchy zoning with U and Pb depletion in altered domains of the xenotime developed only in two experiments at 550°C, 800 MPa and 650°C, 600 MPa. The re-equilibrated xenotime domains via coupled dissolution-precipitation reactions yielded ²⁰⁶Pb/²³⁸U dates of ca. 15–34 Ma demonstrating partial resetting of the age record.

The U-Pb data for the first time experimentally confirm that alkali-rich fluid/melt-induced re-equilibration of xenotime via coupled dissolution-precipitation reactions can result in removal of radiogenic Pb. These findings provide crucial implications for applications of U-Pb xenotime dating of igneous (particularly in pegmatites) and metamorphic processes.

Acknowledgements. The project was funded by the National Science Centre of Poland, grant no. 2017/27/B/ST10/00813.

References

- Budzyń, B. & Kozub-Budzyń, G.A. (2015). The stability of xenotime in high Ca and Ca-Na systems under experimental conditions of 250–350°C and 200–400 MPa: the implications for fluid-mediated low-temperature processes in granitic rocks. *Geological Quarterly*, 59, 316–324.
- Budzyń, B., Harlov, D.E., Kozub-Budzyń, G.A. & Majka, J. (2017). Experimental constraints on the relative stabilities of the two systems monazite-(Ce) – allanite-(Ce) – fluorapatite and xenotime-(Y) – (Y,HREE)-rich epidote – (Y,HREE)-rich fluorapatite, in high Ca and Na-Ca environments under P-T conditions of 200–1000 MPa and 450–750 °C. *Mineralogy and Petrology*, 111, 183–217.



Geochronological insights into the evolution of the Chopok granodiorite (Dumbier Crystalline Complex, Lower Tatra Mts., W. Carpathians, Slovakia)

Jolanta BURDA¹, Urs KLÖTZLI², Beata WOSKOWICZ-ŚLĘZAK¹, Quili LI³

¹Faculty of Earth Sciences, University of Silesia, Będzińska st. 60, 41-200 Sosnowiec, Poland; e-mail: jolanta.burda@us.edu.pl

²Department of Lithospheric Research, University of Vienna, Althanstrasse 14, 1090 Vienna, Austria; e-mail: urs.kloetzli@univie.ac.at

³State Key Laboratory of Lithospheric Evolution, Institute of Geology and Geophysics, Chinese Academy of Sciences, Beijing 100029, China. e-mail: liqiuli@mail.iggcas.ac.cn

Former attempts to date the igneous formation (aka intrusion) of the Chopok granodiorite by conventional Rb/Sr mineral dating and in-situ LA-ICP-MS U/Pb zircon dating were not successful. On the other hand the combination of in-context (in thin section) U/Th/Pb dating of zircon, monazite and xenotime by SIMS and EMPA allows to decipher the complex evolutionary path of the rock. Five major age components are recorded, either in single crystals or in crystal domains:

- a) **Cambrian** and **pre-Cambrian** ages for zircons (> 512 Ma) interpreted as being inherited with a major contribution (ca. 50%) from a Cadomian source (684 ±12 Ma).
- b) Two distinct **lower Ordovician** igneous growth episodes are recorded in zircon:
 - i) 479.3 ±2.6 Ma (igneous zircon domains with Th/U <0.15)
 - ii) 473.2 ±2.6 Ma (igneous zircon domains with Th/U >0.15)

These two zircon growth episodes are statistically distinguishable by their respective zircon Th/U ratios but are certainly related to only one major magmatic event. Identical Ordovician igneous monazite and xenotime domains (474.7 ±7.2 Ma) date the same major magmatic event but cannot be directly attributed to either one of the zircon growth episodes.

c) A first **Carboniferous** (Variscan) metasomatic and/or hydrothermal overprinting event is dated by domains of overgrowth and recrystallization in all three minerals (351.1 ±4.2 Ma, $T_{\text{xnt-mnz}} = 560 \pm 45$ °C).

d) A second **Upper Permian to Lower Triassic** metasomatic and/or hydrothermal imprint is also dated by domains of overgrowth and recrystallization in all three minerals (246.4 ±6.9 Ma, $T_{\text{xnt-mnz}} = 455 \pm 15$ °C).

Conclusions

a) The Chopok granodiorite has to be interpreted as a lower Palaeozoic intrusion into a Cambrian to pre-Cambrian basement. The Variscan orogeny only resulted in metasomatic/hydrothermal and structural overprinting of the Chopok granodiorite.

b) In-context multi mineral geochronology allows to successfully decipher the complex high-temperature evolution of petrographically seemingly simple rocks.



Primary and secondary mineralogy of the peralkaline granite of the Ilímaussaq Complex, South Greenland

Małgorzata CEGIEŁKA¹, Bogusław BAGIŃSKI¹, Ray MACDONALD¹

¹*Institute of Geochemistry, Mineralogy and Petrology, Faculty of Geology, University of Warsaw, Żwirki i Wigury 93, 02-089, Warszawa, Poland; e-mail: malgorzata.cegielka@student.uw.edu.pl*

The peralkaline “Green Granite” is an early component of the agpaitic Ilímaussaq Complex in the Gardar alkaline province of South Greenland. Emplacement of the intrusion took place around 1160 ± 5 Ma (Krumrei et al. 2006) and consisted of at least three stages of magma intrusion (Sørensen 2001; Upton 2013). Prolonged fractional crystallization of a large body of magma made possible by its high halogen content and consequent low viscosity (Marks, Markl 2015) resulted in unique mineral assemblages. The main goal of this research is a detailed description of the complex mineralogical assemblage comprising the Green Granite. For this purpose multiple analytical methods were used, including optical microscopy, scanning microscopy (SEM/EDS), electron microprobe analysis (EPMA), mass spectrometry (ICP-MS) and X-ray diffraction (XRD). The main focus was the determination of empirical formulas, textural relationships and crystallization paths of the minerals present in the granite. Over 30 phases were identified, with chevkinite-(Ce), ekanite and henrymeyerite being recorded for the first time at Ilímaussaq.

The Green Granite is holocrystalline, porphyritic and massive without any visible orientation of crystals. The texture is characterized by subhedral perthitic alkali feldspars. The primary minerals are alkali feldspar, quartz, amphibole (richterite to arfvedsonite) and aenigmatite. The accessory phases include: aegirine, astrophyllite, britholite-(Ce), catapleite, chevkinite-(Ce), ekanite, elpidite, fluorite, henrymeyerite, Fe-poor Ba-titanate, ilmenite, leucosphenite, lorenzenite, monazite-(Ce), narsarsukite, neptunite, pectolite, pyrochlore, thorite, titanite, zircon and five unidentified phases. The granite records the transition from miaskitic to agpaitic assemblages and estimated conditions ranged from magmatic to hydrothermal.

References.

- Krumrei, T.V., Villa, I.M., Marks, M.A.W. & Markl, G. (2006). A $^{40}\text{Ar}/^{39}\text{Ar}$ and U/Pb isotopic study of the Ilímaussaq complex, South Greenland: Implications for the ^{40}K decay constant and for the duration of magmatic activity in a peralkaline complex. *Chemical Geology* 227, 258-273.
- Marks, M. A. W. & Markl, G. (2015). The Ilímaussaq Alkaline Complex, South Greenland. *Springer Geology*, 649-691.
- Sørensen, H. (2001). Brief introduction to the geology of the Ilímaussaq alkaline complex, South Greenland, and its exploration history. *Geology of Greenland Survey Bulletin* 190, 7-23.
- Upton, B.G.J. (2013). Tectono-magmatic evolution of the younger Gardar southern rift, South Greenland. *Geological Survey of Denmark and Greenland Bulletin* 29.



Zonation of copper sulphides within the uppermost part of the Rote Fäule oxidation front in the Kupferschiefer series of SW Poland

Andrzej CHMIELEWSKI¹, Sławomir OSZCZEPALSKI¹

¹Państwowy Instytut Geologiczny – Państwowy Instytut Badawczy, Rakowiecka 4 Str., 00-975 Warszawa, Poland; e-mail: andrzej.chmielewski@pgi.gov.pl, sosz@pgi.gov.pl

This paper concerns the petrographic examination of altered copper sulphides in the Kupferschiefer series within few areas (Bogdaj–Uciechów, Czmoń, Grochowice, Grodzisk, Jawor, Łuszczanów, Mieszków, Paproć, Radlin, Żabno) of the Fore-Sudetic Monocline in SW Poland. Relationships between the variability of mineral textures and the degree of alteration of copper sulphides were investigated. New outcomes are based on a compilation of reflected-light microscopy and electron microprobe studies. Within the research area, the mineralized profiles are characterized by the predominance of copper sulphides from the Cu-S group, where chalcocite prevails quantitatively over digenite, covellite accompanied by bornite and chalcopyrite. The presence of oxidized geochemical facies (Rote Fäule), barren with ore minerals but significantly enriched with hematite, was confirmed in all of the examined profiles. Particular attention was paid to the uppermost part of oxidized profiles representing transition zone from strongly oxidized rocks to ore series, where slightly altered, mostly copper sulphides from CuS and Cu-Fe-S groups are encountered. The transition zone is distinguished by remnant copper sulphides and minor hematite. The Cu-sulphides exhibit features characteristic for weak oxidative alteration represented by covellitization process. Gradual Cu depletion in Cu-S group minerals towards the Rote Fäule center is also registered. The Cu-S sulphides zonation pattern is oriented radially and concentrically outwards from the most oxidized to less altered parts in the following order: covellite (CuS) – yarrowite (Cu₉S₈) – spionkopite (Cu₃₉S₂₈) – geerite (Cu₈S₅) – anilite (Cu₇S₄) – digenite (Cu₉S₅) – djurleite (Cu₃₁S₁₆) – chalcocite (Cu₂S), expressing progressive alteration of chalcocite. Additionally, microprobe examination has shown decreased concentrations of Ag (up to 0.8 wt.%) in covellite replacing Cu-S and Cu-Fe-S minerals in comparison to Ag content in latter sulphides (up to 5 wt.%). Furthermore, elevated concentration of Se in covellite (up to 4 wt.%) in comparison to values in the replacing copper sulphides (up to 0.7 wt.%) are also noted. Replacements of copper sulphides by covellite indicate foremost oxidative alteration processes with step-wise loss of copper. Microscopic and microprobe studies display clearly that copper sulphides replacement by covellite, gradual decrease in Cu content in copper sulphides as well as Cu-S mineral zonation towards the Rote Fäule zone are an effect of the evolution of mineralizing processes during expansion of ore fluids. As their oxidative potential diminished, in the outer parts of the oxidized zones weaker processes of ore minerals alteration took place. In summary, the evolution of mineralization system resulted in progressive changes in mineralogical composition close to the redox interface that is characterized by a gradual alteration of the Cu-S sulphides. This alteration pattern corresponds to increasing copper depletion in the copper minerals towards the Rote Fäule.



Towards global model of enrichment in sulfides along the crust-mantle transition zone

Jakub CIAZELA^{1,2}, Bartosz PIETEREK², Marta GRABOWSKA³, Andrzej MUSZYNSKI², Hubert MAZUREK⁴, Levente PATKO⁵

¹Space Research Center, Polish Academy of Sciences, Warsaw, Poland, e-mail: jc@cbk.pan.wroc.pl

²Institute of Geology, Adam Mickiewicz University, Poznań, Poland

³Centre for Research in Earth Sciences, University of Plymouth, United Kingdom

⁴Institute of Geological Sciences, University of Wrocław, Poland

⁵Lithosphere Fluid Research Lab (LRG), Eötvös Loránd University, Budapest, Hungary

Cu-rich sulfide ore deposits of economic importance in ophiolites often occur along the crust-mantle transition zones (e.g. Begemann et al. 2010), where the relics of magmatic sulfides indicate igneous nature of metal enrichment. In fact, crust-mantle transition zones in situ in the oceans have been recently suggested to be enriched in sulfides and chalcophile metals due to melt-peridotite reaction (Ciazela et al. 2017; 2018). The enrichment seems to be ubiquitous along the oceanic crust-mantle transition zone (Ciazela et al. 2018), and might be expected even at the continental Moho. This is possible as sulfides precipitate during melt-peridotite reaction independently on pressure. The reaction yields sulfides at low pressures (0.1-0.2 GPa) of the oceanic crust-mantle transition zones, medium pressures (~1 GPa) of the continental crust-mantle transition zone (Pieterik et al., this issue), and even high pressures (up to 2.5 GPa) recorded in mantle xenoliths (Mazurek et al. this issue, Patko et al. last issue). This, of course, affects the metal budget of the lithosphere and secondary ore-forming processes. To better understand how other key physicochemical parameters (melt and mantle composition, oxygen fugacity, temperature) control the amount and composition of yielded sulfides, we are starting a systematic study of the best exposed crust-mantle transition zone in the Oman ophiolite recently drilled by the ICDP OmanDP program (2017/2018). We have collected 120 samples from the OmanDP cores that represent the upper mantle and lower crust of the Oman ophiolite sequence, including 40 samples from the crust-mantle transition zone.

References

- Begemann, F., Hauptmann, A., Schmitt-Strecker, S. & Weisgerber, G. (2010). Lead isotope and chemical signature of copper from Oman and its occurrence in Mesopotamia and sites on the Arabian Gulf coast. *Arabian Archaeology and Epigraphy*, 21, 135–169.
- Ciazela, J., Dick, H.J.B., Koepke, J., Pieterik, B., Muszynski, A., Botcharnikov, R. & Kuhn, T. (2017). Thin crust and exposed mantle control sulfide differentiation in slow-spreading ridge magmas. *Geology*, 45, 935–938.
- Ciazela, J., Koepke, J., Dick, H.J.B., Botcharnikov, R.E., Muszynski, A., Lazarov, M., Schuth, S., Pieterik, B. & Kuhn, T. (2018). Sulfide enrichment at an oceanic crust-mantle transition zone: Kane Megamullion (23°N, MAR). *Geochimica et Cosmochimica Acta*, 230, 155–189.



Cobalt- and zinc hydrous arsenates from Miedzianka, Sudetes Mts., Poland

Justyna CIESIELCZUK¹, Janusz JANECEK¹, Mateusz DULSKI², Tomasz KRZYKAWSKI¹, Eligiusz SZEŁĘG¹,

¹Faculty of Earth Sciences University of Silesia, 60 Będzińska, Sosnowiec, Poland;

e-mail: justyna.ciesielczuk@us.edu.pl

²Institute of Material Sciences, University of Silesia, 75 Pułku Piechoty 1a, 41–500 Chorzów, Poland

The oxidative supergene alteration zone in the Miedzianka polymetallic ore deposit is unique, because of the occurrence of numerous extended solid solutions among base-metal arsenates and phosphates (Siuda, Gołębiowska, 2011, Parafiniuk et al. 2016) including 77.5 mol. % cornwallite-pseudomalachite and 75 mol. % kipushite-philipsburgite solid solutions (Ciesielczuk et al. 2016). In this study, the extended erythrite-köttigite $(\text{Co}_{3-x}\text{Zn}_x)(\text{AsO}_4)_2(\text{H}_2\text{O})_8$ solid solution and possibly new $(\text{Co}_{3-x}\text{Zn}_x)(\text{AsO}_4)_2(\text{H}_2\text{O})_4$ solid solutions have been examined by SEM-EDS, EPMA, XRD, FT-IR, and Raman spectroscopy.

In the low P-T environments, it is the availability of chemical components that hinder the formation of solid solution among minerals within the same pH-Eh stability field. The extended Co- and Zn hydrous arsenates solid solutions reflect the chemical evolution of supergene fluids (gradual increase in Zn(II) activity related to the depletion in Co(II) caused by the precipitation of erythrite) in the oxidative zone of the ore deposit.

References

- Ciesielczuk, J., Janeczek, J., Dulski, M. & Krzykowski, T. (2016). Pseudomalachite–cornwallite and kipushite–philipsburgite solid solutions: chemical composition and Raman spectroscopy. *European Journal of Mineralogy*, 28, 555-569.
- Parafiniuk, J., Siuda, R. & Borkowski, A. (2016). Sulphate and arsenate minerals as environmental indicators in the weathering zones of selected ore deposits, Western Sudetes, Poland. *Acta Geologica Polonica*, 66(3), 493–508.
- Siuda, R. & Gołębiowska, B. (2011). New data on supergene minerals from Miedzianka-Ciechanowice deposit in the Rudawy Janowickie Mountains (Lower Silesia, Poland). *Przegląd Geologiczny*, 59, 226-234 (in Polish with English abstract).



Thermally modified and acidic activated clay minerals with microbiological quality in cosmetics industry applications

Anna CZARNECKA-SKWAREK¹, Agnieszka ROŻEK², Emilia WÓJCİK³

^{1,2} *Institute of Geochemistry, Mineralogy and Petrology, Faculty of Geology, University of Warsaw, Żwirki i Wigury 93, 02-089 Warsaw; e-mail: a.czarnecka6@uw.edu.pl, a.rozek@uw.edu.pl*

³ *Institute of Hydrogeology and Engineering Geology, Faculty of Geology, University of Warsaw, Żwirki i Wigury 93, 02-089 Warsaw; e-mail: wojcike@uw.edu.pl*

Clay minerals are widely used in the cosmetic and pharmaceutical industry as active substances or carriers and emulsifiers. The aim of this preliminary study was to indicate the optimal method for the preparation of new mineral material derived from natural clay, maintaining the microbiological quality standards. The presence of some microorganisms may have an impact on the reduction, or even elimination, of the dedicated action of the cosmetic. In addition, it has potentially adverse effects on the health of the people who use a given cosmetic product. Therefore, manufacturers of cosmetic preparations should ensure the lowest level of microbiological contamination of the final product.

The subject of the study was the sample of Neogene clay (mostly beidellite), which has been modified by thermal treatment and acidic activation. The samples were thermally modified at temperatures of 600, 700 and 750°C with 2h holding. Acidic activation of the samples was carried out using a 2M HCl solution. Specific Surface Area (SSA) was determined by the BET method. The changes in mineral composition were investigated by XRD and thermal analysis (DTA-DTG), while SEM was used to investigate the microstructure of newly prepared materials. Microbiological research included the determination of the total amount of both the mesophilic aerobic bacteria and the amount of yeast and mould in the starting material and subjected to thermal and acidic activation. Determination of the total number of aerobic mesophilic bacteria, yeasts and moulds was made by surface culture on two types of microbiological medium: for bacteria – Nutrient-Agar (BIOCORP), for yeast and mould – Sabouraud agar with dextrose and chloramphenicol, as an antibiotic inhibiting bacterial growth.

The results showed that the physical and chemical properties of clay were changed under the influence of temperature and acid. The results of the modification of the clay are: an increase of the specific surface area by approx. 30%, and changes in the microstructure and distribution of pore size. The results of the microbiological studies indicated that the total number of mesophilic bacteria in aerobic cultures carried out for the initial mineral sample was 2.2×10^6 cfu/ml, while fungi and moulds were respectively 3.1×10^3 cfu/ml. There was no growth of microorganisms on both nutrient and Sabourad medium, for samples subjected to thermal modification (regardless of the temperature used) or/and acidic activation. Application of the described methods of modification of the examined clay material leads to an inhibition of microbial growth and activity.



Textural and geochemical evidence for mixing within rapakivi-like granitoids from Krasnopol intrusion, Mesoproterozoic Mazury Complex, NE Poland

Justyna DOMAŃSKA-SIUDA¹, Krzysztof NEJBERT¹

¹Faculty of Geology, Warsaw University, Żwirki i Wigury 93, 02-089 Warsaw, Poland;
e-mail: j.domanska@uw.edu.pl; nejbert@uw.edu.pl

The Mazury Complex (NE Poland), composed of rapakivi-granitoid massifs (~1.54–1.49 Ma) of A-type affinity and anorthosite massifs consist of part of AMCG suite (Dörr et al. 2002; Bagiński et al. 2007; Wiszniewska et al. 2007).

The examined rocks from the Krasnopol PIG-6 drill core represent dominant porphyric, coarse-grained monzodiorite/granodiorite and numerous fine-grained dark enclaves, spatially associated with them. Enclaves range from and intermediate to basic rocks with monzonite, monzodiorite and monzogabbro in composition.

The contacts of the enclaves with granodiorite are sharp and/or partly diffuse. Their textural relations indicate the mixing/mingling processes. The interaction between the two magmas is marked by a fine-grained “chilled margin”. Sometimes dark enclaves are surrounded by narrow felsic halos. Some contacts are commonly underlined by the presence of mafic minerals. Large feldspar phenocrysts are observed to cross the contacts between enclaves and granodiorite, in addition to occurring inside them.

The geochemistry examined rocks may also indicate magma mixing/mingling processes. The SiO₂ content in the granodiorite rocks ranges from 56 to 62%; enclaves are characterized by a broad compositional range (from 45 to 57 wt.% SiO₂). Investigated rocks show well-defined, co-linear trends on the Harker diagrams.

To test the mixing hypothesis we performed geochemical modelling, both for major and trace elements. In this modelling, the equation of the mass equilibrium law was used. The proportions of the felsic and mafic melts in the hybrid rocks were ca. 61% and 39%, respectively.

References

- Bagiński, B., Duchesne, J.-C., Martin, H. & Wiszniewska, J. (2007). Isotopic and geochemical constraints on the evolution of the Mazury granitoids, NE Poland. *Granitoids in Poland, Archivum Mineralogiae Monograph, 1*, 11-30.
- Dörr, W., Belka, Z., Marheine D., Schastok, Valverde-Vaquelo P. & Wiszniewska J. (2002). U-Pb and Ar-Ar geochronology of anorogenic granite magmatism of the Mazury complex NE Poland. *Precambrian Research, 119*, 101-120.
- Wiszniewska, J., Kusiak, M., Krzemińska, E., Dörr, W. & Suzuki, K. (2007). Mesoproterozoic AMCG granitoids in the Mazury Complex, NE Poland – A geochronological update. *Granitoids in Poland, Archivum Mineralogiae Monograph, 1*, 31-39.



The origin of Nb mineralization in nephrites of the Ślęza Ophiolite

Grzegorz GIL^{1,2}, Bogusław BAGIŃSKI¹, Piotr GUNIA², Stanisław MADEJ², Zdzisław BELKA³

¹Faculty of Geology, University of Warsaw, Żwirki i Wigury 93, 02-089 Warsaw, Poland;
e-mail: g.gil2@uw.edu.pl

²Institute of Geological Sciences, University of Wrocław, Maksa Borna 9, 50-204 Wrocław, Poland;
e-mail: grzegorz.gil2@uwr.edu.pl

³Isotope Laboratory, Adam Mickiewicz University, Krygowskiiego 10, 61-680, Poznań;
e-mail: zbelka@amu.edu.pl

The Ślęza Ophiolite (Central Sudetes, SW Poland) hosts abundant nephrite deposits. The chemical composition and Sr isotope ratios of these nephrites, and of selected wall-rocks, were measured in order to track the fluid history.

The F, Sr and Nb contents of the nephrites are relatively constant (42–54 ppm F, 6.3–15.4 ppm Sr, <0.1 to 8.7 ppm Nb), with the exception of an unusually enriched, dark green nephrite sample from Jordanów Śląski (392 ppm F, 61.7 ppm Sr, 18.7 ppm Nb). Moreover, an initial ⁸⁷Sr/⁸⁶Sr ratio (⁸⁷Sr/⁸⁶Sr₍₀₎: 0.7031 to 0.7070) of nephrites corresponds with the Niemcza granitoids or metabasites of the Ślęza Ophiolite. However, the unusually enriched nephrite is characterized by a significantly higher ⁸⁷Sr/⁸⁶Sr ratio (⁸⁷Sr/⁸⁶Sr₍₀₎ = 0.7081), which is more similar to the ~305 Ma two-mica granite of the Strzegom-Sobótka batholith (⁸⁷Sr/⁸⁶Sr₍₀₎: 0.7061–0.7088, Pin et al. 1989, recalculated according to the age of Turniak et al. 2014). In this enriched nephrite, we observed later, microscopic clinozoisite veins, in which clinozoisite has notable Sr contents (0.04–0.17 wt.% SrO, 0.08 wt.% on average). Thus, elevated F, Sr and ⁸⁷Sr/⁸⁶Sr₍₀₎ correlates with the presence of clinozoisite veins, which are probably related to the intrusion of a two-mica granite (105 ppm F, 81.6 ppm Sr) of the Strzegom-Sobótka pluton. Moreover, the highly elevated Nb content of this clinozoisite-veined nephrite also correlates with the two-mica granite (19.6 ppm Nb). The elevated Nb content is associated with the presence of a Nb-titanite in this nephrite sample, and, interestingly, lacks correlation with the enrichment in Ta (0.7 ppm Ta).

Summing up, Nb mineralization in some of the nephrite samples from the Ślęza Ophiolite is shown by the presence of Nb-titanite. Nb was introduced jointly with F and Sr – although without Ta – via clinozoisite veins, probably related to the intrusion of the ~305 Ma two-mica granite of the Strzegom-Sobótka pluton.

Acknowledgements. Study was financed from the NCN grant no. 2016/20/S/ST10/00137.

References

- Pin, C., Puziewicz, J., Duthou, J.L. (1989). Ages and origins of a composite granitic massif in the Variscan belt: A Rb-Sr study of the Strzegom-Sobotka Massif, W. Sudetes (Poland). *Neues Jahrbuch für Mineralogie-Abhandlungen*, 160(1), 71–82.
- Turniak, K., Mazur, S., Domańska-Siuda, J., Szuszkiewicz, A. (2014). SHRIMP U-Pb zircon dating for granitoids from the Strzegom-Sobótka Massif, SW Poland: Constraints on the initial time of Permo-Mesozoic lithosphere thinning beneath Central Europe. *Lithos*, 208–209, 415–429.



Mineralogical and geochemical interpretation of atmospheric aerosols collected on *Populus nigra Italica* leaves in the JSC Almalyk Mining and Metallurgical Combine (Uzbekistan) area

Maciej GÓRKA¹, Wojciech BARTZ¹, Alisa SKURIDINA¹, Anna POTYSZ¹

¹Faculty of Earth Science and Environmental Management, University of Wrocław, Cybulskiego 32, 50-205 Wrocław, Poland; e-mail: maciej.gorka@uwr.edu.pl

Metal mining and smelting industry significantly influences local environment. Atmospheric pollutants e.g. PAHs, metal-bearing particles and toxic gases directly by breathe or indirectly by contamination of local soils and surface waters impair human health. Atmospheric particles are collected either using passive samplers or active pumping in the form of suspended (from fine to coarse) fraction (Górka et al. 2018). The bioindicators (pine needles, spider webs) can be a potential passive samplers of atmospheric particles (Teper 2009; Górka et al. 2018). Currently, we propose *Populus nigra Italica* leaves as a potentially useful bio-passive collectors of atmospheric aerosols in atypical to normal sampling areas. The Almalyk mining and smelting industrial facility in Uzbekistan is one of the metallurgical complexes that negatively influences both the local atmosphere and soil (Shukurov et al. 2012). Moreover, the classical air pollutants sampling methods were not possible to apply in this area. Therefore, the 9 leaves of *Populus nigra Italica* and 3 soil samples were gathered in August 2018 in the JSC Almalyk MMC area. In our study, we applied two analytical techniques: SEM-EDX (to determine a mineralogical composition of aerosols and soils based on SEM-EDX and size distribution based on scaled SEM photography) as well as ICP-MS (to determine elements concentration in soils). Our preliminary investigations indicate that (i) spatial distribution of aerosols are connected with industry centres which both influence anthropogenic/crustal aerosols ratio as well as size distribution and mineralogical character of analysed particles; (ii) increased metal concentrations (Cu, Pb, Zn, Cd, Mo and Au) are unambiguously connected with specific non-ferrous metal processing centres.

Mineralogical and geochemical data allowed us to indicate polluted areas as well as to assess anthropogenic impact based on our newly proposed bio-passive environmental tool.

References

- Górka M., Bartz W. & Rybak J. (2018). The mineralogical interpretation of particulate matter deposited on *Agelenidae* and *Pholcidae* spider webs in the city of Wrocław (SW Poland): A preliminary case study. *Journal of Aerosol Science*, 123, 63-75.
- Shukurov N., Kodirov O., Peitzsch M., Kersten M., Pen-Mouratov S. & Steinberger Y. (2014). Coupling geochemical, mineralogical and microbiological approaches to assess the health of contaminated soil around the Almalyk mining and smelter complex, Uzbekistan. *Science of the Total Environment*, 476–477, 447–459.
- Teper E. (2009). Dust-particle migration around flotation tailings ponds: pine needles as passive samplers. *Environ Monit Assess*, 154(1–4), 383–391.



Estimation of thermal maturity of the Ediacaran organic matter from the East European Craton. Comprehensiveness of using GC-MS and Raman Spectroscopy techniques

Magdalena GORYL¹, Kamila BANASIK², Justyna SMOLAREK-LACH², Leszek MARYNOWSKI²

¹*Institute of Geological Sciences, Polish Academy of Sciences, Research Centre in Kraków, Poland;*

e-mail: m.goryl@ingpan.krakow.pl

²*Faculty of Earth Sciences, University of Silesia, Sosnowiec, Poland*

Thermal maturity of the Ediacaran organic matter from western margin of the East European Craton was estimated using two separate methods: (i) gas chromatography-mass spectrometry (GC-MS), which is based on extractable organic matter, and (ii) Raman spectroscopy, which is based on organic particles measurement. To avoid extensive operator interaction and potential manipulation of the data for Raman analysis, IFORS software recommended by Lünsdorf and Lünsdorf (2016) for peak decomposition was used.

Here, we present the correlation of Raman spectra with the homohopane C31 22S/(S+R) ratio as a parameter equivalent to vitrinite reflectance (Ro) as well as the potential and limitations of the application of several Raman parameters commonly used in thermal maturity estimates in the case of organic-lean and relatively immature samples (Goryl et al. 2019).

Whereas based on Raman parameters, two distinctive groups of samples were observed: immature (from NE Russia, Belarus, and Lithuania) and mature (from SE Ukraine and SW Poland), according to biomarker data (homohopane C31 22S/(S+R) ratio) three groups of samples can be distinguished: immature (from Russia and Belarus), marginally mature (from Lithuania), and thermally mature (from Ukraine and Poland). The difference between GC-MS results and Raman spectra may also indicate the utility of the latter as a tool for the diagnosis of drill core contamination.

Acknowledgements. Authors acknowledge financial support from the Polish National Science Centre MAESTRO grant 2013/10/A/ST10/00050.

References

- Lünsdorf, N. K., & Lünsdorf, J. O. (2016). Evaluating Raman spectra of carbonaceous matter by automated, iterative curve-fitting. *International Journal of Coal Geology*, 160, 51–62.
- Goryl, M., Banasik, K., Smolarek-Lach, J., & Marynowski, L. (2019). Utility of Raman spectroscopy in estimates of the thermal maturity of Ediacaran organic matter: An example from the East European Craton. *Geochemistry*, (*in press*) doi: <https://doi.org/10.1016/j.chemer.2019.06.001>



New insights into mineralogy and geochemistry of the Aravalli mafic sequence, Rajasthan, India

Anna GRABARCZYK¹, Janina WISZNIEWSKA², Ewa KRZEMIŃSKA², Talat AHMAD³

¹University of Warsaw, Faculty of Geology, Institute of Geochemistry, Mineralogy and Petrology, Żwirki i Wigury 93, 02-089 Warsaw, Poland; e-mail: anna.grabarczyk@student.uw.edu.pl

²Polish Geological Institute, Rakowiecka 4, 00-975 Warsaw, Poland; e-mail: jwis@pgi.gov.pl, ekrz@pgi.gov.pl

³Department of Geology, University of Delhi, Delhi-110007, India; e-mail: tahmad001@yahoo.co.in

The Precambrian rocks of the Aravalli Craton, NW India are separated into three units: (1) The Banded Gneiss Complex (3.5-2.5 Ga); (2) the Aravalli sequence (2.5-2.0 Ga) and (3) the Delhi Supergroup (2.0-1.7 Ga), composed of arenaceous and calcareous sediments (Ahmad, Tarney 1994).

Mafic metavolcanic rocks from Aravalli sequence have been recognized as pillow lavas with a coarse-grained core. A spinifex-like texture has been observed at the margins of the pillows, which suggests fast quenching of lava underwater. The rocks are composed of fine-grained plagioclase (oligoclase and andesine) and elongated amphibole grains, mainly magnesio-(ferri-) hornblende. No relicts of olivine or pyroxene have been found. The amphibole geothermobarometer gives temperatures not exceeding 550°C, with pressure in the range 1.5-2.5 GPa, implying a moderate thermal regime for amphibole crystallization. Chlorite was used for defining the last stage of metamorphism, indicating temperatures from 290 to 330°C. These rocks have been altered in the greenschist to lower amphibolite facies. The olivine/pyroxene crystals have been replaced by hornblende, epidote, chlorite and occasional carbonate preserving pseudo-spinifex texture.

The whole-rock composition indicates a wide range of Mg# from 0.24 to 0.55, with MgO contents from 5.32 to 16.85 wt.%. The Ti content is relatively low (<2.5 wt.% TiO₂). The sum of alkalis usually do not exceed 3 wt.%. Rocks are also enriched in incompatible elements and LREE with the range for (Ce/Yb)_N ratios being 2.3 to 6.9 and (Gd/Yb)_N ratios 1.4 to 2.7 (characteristic of Barberton-type komatiites). The negative Ce anomalies suggest additional fluid-induced alteration processes during metamorphism.

On a Zr/Y vs. Zr diagram the Aravalli rocks plot in the WPB field. On the AFM plot samples show a typical tholeiitic Fe-enrichment trend. Lavas of the Aravalli rocks were rather less Mg-rich than the komatiites from other Archaean greenstone belts. Positive correlation in Zr/Y and Al₂O₃/TiO₂ ratio and negative Nb anomalies may confirm crustal contamination caused by the thermal influence of mafic magma during the ascent, which changed the chemical composition of magma.

References

- Ahmad, T. & Tarney, J. (1994). Geochemistry and petrogenesis of Late Archaean Aravalli Volcanics, basement enclaves and granitoids, Rajasthan. *Precambrian Research*, 65, 1-23.



Sedimentary inheritance of detrital zircon age spectra

Thomas HADLARI¹

¹*Geological Survey of Canada, Calgary, AB, Canada; e-mail: thomas.hadlari@canada.ca*

The likelihood of sedimentary recycling can present a fundamental flaw for any sedimentary provenance study. Reviewing detrital zircon age spectra from Paleoproterozoic to Late Cretaceous strata of the northern Canadian Cordillera provides insights on: billion year patterns in recycling of zircon; the duality of “syn-tectonic” detrital zircon signatures as a function of basin geometry, particularly between the orogenic and flexural margins of foreland basins; and relatively local recycling of sediment during transgressions, such as recorded by Cambrian sandstones.

Erosion of sedimentary rocks will yield sediment that generally has the same age spectrum of zircon as that sedimentary rock. It follows that after the first cycle of erosion from an ultimate source, that detrital zircon grains in sedimentary reservoirs form proximate sources are spatially decoupled from ultimate sources. The main conclusion is that to harness the power of ultrahigh-n and somewhat random sampling of regional sources of zircon by the sedimentary system, any provenance study should start with a catalog of detrital zircon age spectra from older strata near the sedimentary basin being studied, and then develop basin reconstructions so that provenance interpretations have an improved chance of being accurate.

References

- Hadlari, T., Swindles, G.T., Galloway, J.M., Bell, K.M., Sulphur, K.C., Heaman, L.M., Beranek, L.P. & Fallas, K.M. (2015). 1.8 billion years of detrital zircon recycling calibrates a refractory part of Earth’s sedimentary cycle. *PLoS ONE*, 10(12): e0144727.



Preliminary U-Pb dating and O isotope study of zircons from hornblende from Bystrzyca Górna (Góry Sowie Massif, SW Poland)

Sławomir ILNICKI¹, Ilona SEKUDEWICZ¹, Yan LIU², Grzegorz GIL^{1,3}

¹ Institute of Geochemistry, Mineralogy and Petrology, Faculty of Geology, University of Warsaw, Al. Żwirki i Wigury 93, 02-089 Warszawa, Poland; e-mail: slawomir.ilnicki@uw.edu.pl

² Institute of Geology, Chinese Academy of Geological Sciences, Beijing 100037, China; e-mail: ly@cags.ac.cn

³ Institute of Geological Sciences, University of Wrocław, pl. Maksa Borna 9, 50-204 Wrocław, Poland; e-mail: g.gil2@uw.edu.pl, grzegorz.gil2@uwr.edu.pl

The Góry Sowie massif (GSM) comprises gneisses and migmatites with dispersed HP granulites and eclogites, amphibolites, meta-ultramafites and pegmatites. The studied hornblende, together with serpentinite, forms bodies embedded in the gneiss-hosted high-grade granulites. The rock is coarse-grained in the central part of the body and gradationally passes into finer varieties at the margins. It is composed of predominant pargasite accompanied by phlogopite, aggregates of F-rich apatite with allanite-(Ce), titanite and zircon as accessories. Geochemical features of the hornblende suggest its magmatic origin and derivation from a hydrous mantle source metasomatized by subducted slab-derived components.

Zircons in the hornblende are mostly euhedral with common oscillatory zoning, typical of magmatic origin. The ion microprobe U-Pb dating and O isotope ratio measurements were performed in thick, oscillatory-zoned zircon rims. Out of the analyzed zircons batch, 10 spot analyzes were rejected due to high common ²⁰⁶Pb or discordance, and the remaining 55 spots yield concordant age of 388.3 ± 0.8 Ma (2σ, MSWD = 0.18, probability = 0.67). This age is slightly older than the U-Pb magmatic ages of intrusive and anatectic rocks from GSM (ca. 369–383 Ma; e.g. Aftalion, Bowes 2002). However, it is close to the age of the HP conditions recorded by the GSM eclogites and granulites (ca. 389–395 Ma) and postulated tectonic incorporation of mantle rocks into the GSM gneisses (389 ± 1.6 Ma; e.g., Nejbert et al. 2013). Furthermore, the oxygen isotope ratios (δ¹⁸O values span 2.3 to 6.5‰, average δ¹⁸O = 5.7‰; n = 66) indicate mantle origin of the hornblende zircons, thus excluding the assimilation from the adjacent gneisses, granulites or pegmatites. Therefore, it appears that the ca. 388 Ma mantle-derived intrusion of the Bystrzyca Górna hornblendites coincides with the climax of crustal subduction and predates major magmatic activity recorded in GSM.

References

- Aftalion, M. & Bowes, D.R. (2002). U–Pb zircon isotopic evidence for mid-Devonian migmatite formation in the Góry Sowie domain of the Bohemian Massif, Sudeten Mountains, SW Poland. *Neues Jahrbuch für Mineralogie Monatshefte*, 4, 182–192.
- Nejbert, K., Ilnicki S., Anczkiewicz R., Pieczka A., Szełęg E., Szuszkiewicz A. & Turniak K. (2013). Geochronological constraints on metamorphism of eclogites from Piława Górna (Góry Sowie block, Sudetes). *Mineralogia – Special Papers*, 41, 66.



Lawsonite pseudomorphs in metapelites and eclogites from the Kamieniec Metamorphic Belt (Sudetes, SW Poland): evidence of HP-LT conditions of prograde Variscan metamorphism

Sławomir ILNICKI¹, Jacek SZCZEPAŃSKI²

¹*Institute of Geochemistry, Mineralogy and Petrology, Faculty of Geology, University of Warsaw, Al. Żwirki i Wigury 93, 02-089 Warszawa, Poland; e-mail: slawomir.ilnicki@uw.edu.pl*

²*Institute of Geological Sciences, University of Wrocław, pl. Maksa Borna 9, 50-204 Wrocław, Poland; e-mail: jacek.szczepanski@uwr.edu.pl*

The volcano-sedimentary succession of the Kamieniec Metamorphic Belt (KMB) situated at the NE margin of the Bohemian Massif (Fore-Sudetic Block, SW Poland) is recognized as a portion of the Variscan collision zone between the Saxothuringian and Brunovistulian domains. As the details of the tectonometamorphic evolution remain debatable, our recent petrological studies focused on reconstruction of P–T trajectories in the predominant metapelites of KMB and dispersed in them eclogite bodies. Crystals of high-Si white mica (Si⁴⁺ up to 3.48 a.p.f.u. in metapelites and eclogites), inclusions of chloritoid in metapelite garnets and decompression textures (sodic diopside + albite symplectites) in eclogites imply that both lithologies underwent HP conditions of metamorphism. The results of thermodynamic modelling of phase equilibria show that metapelites recorded conditions of ca. 16–18 kbar and 470°C followed by decompression to 6–8 kbar and 550–600°C, while eclogites experienced baric peak of 2.4–2.8 GPa at temperatures of 550–570°C. In both cases the models predict the presence of lawsonite in their respective HP-LT mineral assemblages (up to ca. 3–5 vol.% in metapelites and ca. 6 vol.% in eclogites), however, in neither of these lithologies the mineral was found. Due to its pivotal role in the models, the research focused on recognition of the post-lawsonite pseudomorphs. The detailed SEM and EPMA inspection has shown that metapelitic and eclogitic garnets comprise polymineral aggregates, which in metapelites comprise margarite + clinozoisite or zoisite + paragonite, while in eclogites these are composed of clinozoisite (or epidote) + paragonite + phengite (pseudomorphed by biotite and plagioclase intergrowths) ± quartz ± albite; rarely kyanite is also present. Based on that mineral-textural evidence and available literature data, these aggregates are interpreted as post-lawsonite pseudomorphs. Their presence validates the calculated phase diagrams and P–T inferences on development of metamorphic conditions. Moreover, these pseudomorphs attest to cold conditions of burial (ca. 6–7°C/km), definitely cooler than in HP units of the Sudetes located in the vicinity of the KMB and represented by the Góry Sowie Massif and the Orlica-Śnieżnik Dome.

Acknowledgements. The study was financed by the grant no UMO-2015/17/B/ST10/02212 from the National Science Centre.



New software to improve the baseline accuracy of elemental composition measurements on SXFiveFE at University of Warsaw

Petras JOKUBAUSKAS¹

¹Faculty of Geology, University of Warsaw, Żwirki i Wigury 93, Warsaw, Poland;
e-mail: p.jokubauskas@uw.edu.pl

A new generation Cameca SxFiveFE electron microprobe (EMP), installed at the Faculty of Geology at the University of Warsaw, is equipped with 5 WDS spectrometers, where 4 are equipped with large diffracting crystal pairs. Currently the main task of the instrument is to measure REE and trace element concentrations in complex minerals (up to 30-40 elements per mineral). Accurate (trace) element measurements are possible only when natural and artificial spectral effects are clearly understood and counter-measured, particularly when using large diff. crystals. X-ray spectra originating from complex minerals often suffer from complete or partial spectral overlaps, which, if overlooked, can lead to negative or positive bias in any EMP analysis (in the range 10 ppm up to a few weight percent). In geological applications, such as chemical dating and geothermobarometry, this is of key importance. The WDS scan examination and stacking with stock software from Cameca – Peaksight – are cumbersome, tedious and not efficient. To make the described method more robust (or even possible) new software is being developed by author.

Proposed method. To check for every possible interference, multiple WDS scans are acquired from standard samples containing the highest element concentrations (preferably metals). The beam current should be set as high as possible, but not too high (to saturate but not to over-saturate the counters). The pulse height analyzer (PHA) should be configured to be at the integral mode. By overlaying/stacking multiple WDS scans (selected-by elements and constrained-to the single spectrometer) on the same axes the real overlaps can be visually examined and the optimal background position(s) can be defined for a given set of elements at the same time taking into consideration the possible overlap corrections. Hitherto, a similar method was applied sparingly to decompose some limited overlap situations, but the novelty proposed here is to make it robust and use it for all analytical work. Such detailed WDS scans should be acquired once per instrument and beam acceleration voltage, and can be consulted every time the new analytical setup is assembled or old setup is adjusted.

The software is still in its infancy (its scope is larger than this method), but it is already usable. It is being written in python and uses the pyqtgraph (www.pyqtgraph.org) plotting library. One of the major difficulties, which had to be overcome, was reading the proprietary binary WDS file format produced with Cameca's Peaksight software. The format had to be reverse engineered to be loadable with this new software, and at the present stage this limits loading functionality only to files produced with 6.0 to 6.4 versions of Peaksight. The active code development takes place at <https://github.com/sem-geologist/QSEM-viewer>. Any contributions are welcome.



Burned out coal seam No. 505 covered by red beds in sub-crop of the Saddle Beds in the southern part of the Chwałowice Syncline (Upper Silesian Coal Basin, Poland)

Dominik JURA¹, Justyna CIESIELCZUK¹, Monika FABIAŃSKA¹, Magdalena MISZ-KENNAN¹, Joanna NOWIK²

¹University of Silesia, Będzińska 60, 41-200 Sosnowiec, Poland, e-mail: dominik.jura@us.edu.pl

²PGG SA KWK ROW Ruch Marcel

In the southern part of the Chwałowice Syncline (the western part of the Upper Silesian Coal Basin, Poland) the coal seam No. 505, belonging to the Saddle Beds, shows the reduced thicknesses from about 3 m to 0.5 m. It is exposed in a testing gallery in the Marcel Coal Mine at the depth 300 m with overlying white and reddish claystones and collapse breccias. The mineralogy, petrology, and geochemistry of 3 samples of coal and 7 samples of associated rocks has been determined by XRD, SEM-EDS, GC-MS, XRF, and RLOM.

Measured volatile contents range from ca 10-12% for rocks and 37.8-40.4 % for coals. Carbon Preference Index values (ca 1.50) indicate organic matter at the middle catagenic stage of thermal maturity; this is confirmed by C₃₁ hopane ratios of ca 0.55. Pr/Ph values fall within two different ranges, ~1.0 and 2.0-6.0. Those in the first range were deposited in anoxic-dysoxic conditions and those in the second in oxic conditions and/or with high inputs of terrestrial material. However, distributions of *n*-alkanes fall into two different sample subsets – monomodal, comprising coal and bimodal found in gangue rocks samples.

The mineral composition of claystones is quartz (21-62%), kaolinite group (14-57%), illite/sericite (0-40%) with traces of feldspars and carbonates (calcite or siderite-magnesite). Secondary minerals such as alunite, natroalunite, anatase, mullite, hematite, titanite, tridymite, and cristobalite reflect heating. The mineralogy of a collapse breccia filling the partly burned out coal No. 505 seam was previously described by Muszyński et al. (2006).

Subbituminous coal (high volatile, type 31.2) is composed of vitrinite (48.8 and 38%), liptinite (9.6 and 8.6%), inertinite (40.8 and 52.2%) macerals with random reflectance values of 0.85 and 0.87%. Total carbon value ranges from 63.40% to 66.30%. Ash content is about 2%. The coal samples contain barite and gypsum, confirmed by Ba and Sr contents 10 times higher than the average for the region. Isotope $\delta^{13}\text{C}$ ranges from -23.64 to -23.05.

The origin of the minerals can be assigned to different processes likely related to a complex overlapping history of variable weathering, heating due to local endogenic fires with and without oxygen access, and metasomatism.

Acknowledgements. The project was funded from grant 2016/21/B/ST10/02293 from the National Science Centre, Poland.

References

Muszyński, M., Skowroński, A. & Lipiarski, I. (2006). Red beds of the collapse-type breccia from the “Marcel” Coal Mine (Upper Silesian Coal Basin, Poland). *Kwartalnik AGH Geologia*, 32(3), 345-367.



Chemical analysis of metal fragments from Castillo de Huarmey (Peru) using FE-SEM-EDS and FE-EMPA

Maciej KAŁASKA¹, Marcin SYCZEWSKI¹, Jakub KOTOWSKI¹, Miłosz GIERSZ²

¹Institute of Geochemistry, Mineralogy and Petrology, Faculty of Geology, University of Warsaw, Żwirki i Wigury 93, 02-089, Warszawa, Poland; e-mail: maciek-kalaska@wp.pl

²Institute of Archaeology, Faculty of History, Warsaw University, Krakowskie Przedmieście 26/28, 00-927, Warszawa, Poland; e-mail: mgiersz@uw.edu.pl

The subject of the research is small fragments of metals originating from the tomb of the culture elite Wari (Middle Horizon), located at the archaeological site of Castillo de Huarmey. These objects were subjected to chemical analysis using a scanning electron microscope with energy-dispersive X-ray and field emission (FE-SEM-EDS) and electron microprobe analyzer with field emission (FE-EPMA). Analyses of the chemical composition of the alloys revealed that in the case of objects made of copper we were dealing with four different alloys differing in the content of arsenic. The first type of alloy is virtually pure copper in which the arsenic content is below the limit of detection. The second is a low alloy of As (0.2 - 0.6 wt.%). This is copper arsenic alloy. The third type is an alloy containing from 1.1 to 2.4 wt.% arsenic. The last type contains between 3.4 and 6.6 wt.% As. The third and fourth types of alloy are high arsenic – arsenic brown. In the silver alloys, two different alloys differing in the form of the copper content in the alloy and the inclusion of copper oxides. In the first type, the Cu content is in the range of 0.2 - 0.6 wt.%. In the second type, the Cu content is at the level of 1.8 - 3.0 wt.%. There were also 6 types of inclusions contained in copper alloys: Cu_xO_y , $\text{Cu}_x\text{As}_y\text{O}_z$, $\text{Pb}_x\text{Cu}_y\text{As}_z\text{O}_q$, $\text{Pb}_x\text{Bi}_y\text{Cu}_z\text{As}_q\text{O}_w$, $\text{Bi}_x\text{Cu}_y\text{Sb}_z\text{As}_q\text{O}_w$ and $\text{Pb}_x\text{Bi}_y\text{Cu}_z\text{Sb}_q\text{As}_w\text{O}_e$. In the silver alloys, 8 types of inclusions were distinguished: Cu_xO_y , Pb_xO_y , $\text{Pb}_x\text{Cu}_y\text{O}_z$, $\text{Pb}_x\text{Ag}_y\text{O}_z$, $\text{Pb}_x\text{Bi}_y\text{O}_z$, $\text{Pb}_x\text{Bi}_y\text{Cu}_z\text{O}_q$. Based on the results of chemical analyses of alloys and inclusions contained therein, it was found that sulphide or oxidized ore was used for the production of pure copper alloys without the addition of arsenic-containing minerals. In the case of copper alloys containing arsenic, copper ores (e.g. sulphides, sulfosalt, oxidized forms) and arsenic ores (e.g. arsenopyrite) were probably used in their production. In the case of silver alloys, silver sulphides (e.g. acanthite, argentite) were probably used. In the case of the second type of alloy, apart from sulphides, it was also possible to use an ore containing sulfosalt Ag, Cu, Pb, Bi.

Acknowledgements. Research financially supported by NCN grant no: 2014/14/M/HS3/00865 and project POIG.02.02.00-00-025/09.



Thermochemistry of disequilibrium silicate melts: reconstruction of smelting and cooling temperatures in slags

Katarzyna KĄDZIOŁKA¹, Anna PIETRANIK¹, Jakub KIERCZAK¹, Anna POTYSZ¹

¹Institute of Geological Sciences, University of Wrocław, Maxa Born'a 9, 50-204 Wrocław, Poland;
e-mail: katarzyna.kadziolka2@uwr.edu.pl

Temperature is a crucial factor influencing the effectiveness of metal smelting process. When studied in historical slags it provides information on the evolution of smelting technologies over time and on approaches of humankind to metal recovery. Methodological approaches to the temperature reconstruction vary and this study serves as a first attempt to combine and compare nearly all available methods of temperature reconstructions using pyrometallurgical slags. A complex historical smelting site is used as an example of the application of the methods. The example includes silica-undersaturated, potassium-rich Cu slags from four locations in the Old Copper Basin, Poland, and is of particular interest because (a) K-rich slag compositions are not widely found and this provides additional challenge to temperature reconstruction approach and (b) the site provides material of different ages (18th, 19th and 20th century) and, therefore, gives insight into potentially different pyrometallurgical processes. Several methods are compared and include phase diagrams, geothermometry (Cpx-WR), thermodynamical modelling with MELTS software and thermal XRD analyses with the main implication that most of the methods have their merits, but modelling by MELTS software returns the most reliable estimates of liquidus (smelting) temperatures. However, our study proved that more elements of the thermal history may be reconstructed, both in the case of crystalline and amorphous samples.

Acknowledgements. The research was supported by Polish Ministry of Sciences and Higher Education within grant: Diamentowy Grant (decision: DI2015 023345).

References

- Kądziółka K., Pietranik A., Kierczak J., Potysz A. & Stolarczyk T. (2019). Towards better reconstruction of smelting temperatures: a methodological review of temperature reconstructions and the case of K-rich copper slags from the Old Copper Basin, Poland, *Journal of Archaeological Science*, *Submitted*



Composition of heavy minerals in loess from Złota, using automated QEMSCAN analysis

Piotr KENIS^{1,2}, Jacek SKURZYŃSKI², Zdzisław JARY²

¹*Łukasiewicz Research Center, Polish Center for Technology Development, Stalowicka St.147, 54-066 Wrocław, Poland, e-mail: piotr.kenis@port.org.pl*

²*Institute of Geography and Regional Development, University of Wrocław, 50-137, Wrocław, Poland, e-mail: piotr.kenis@uwr.edu.pl, jacek.skurzynski@uwr.edu.pl, zdzislaw.jary@uwr.edu.pl*

The loess section near Złota village is located in the southwestern part of Poland in the Vistula river valley (Moska et al. 2018). Aeolian sediments with a fraction not exceeding 500 microns are relatively difficult to investigate, especially when it comes to mineral composition. Separation of heavy minerals from this type of sediment is particularly complicated and time-consuming. By using the potential of SEM coupled with two EDS detectors and equipped with the QEMSCAN system, it is possible to identify over 100,000 particles per hour. Another advantage is that complicated separation processes are not necessary and all phases can be examined in one measurement, including grain size distribution based on digital image, without manual sieving. Application of this method for the study of heavy minerals in loess has been used by scientists from China (Nie, Peng 2014). Correct sample preparation and proper selection of measurement parameters allow to identify individual mineral phases even in previously archived samples. Application of QEMSCAN system allowed to identify minerals and intermetallic compounds previously not described in this location and therefore contributed to determining the origin of the source material and the main directions of loess transport. This methodology will be applied to the studies of heavy minerals from most important loess sections in Poland. According to this research it will be possible to reinterpretate previously identified loess characteristics in terms of mineralogical composition, with much greater accuracy and more detailed data acquisition.

References

- Nie, J. & Peng, W. (2014). Automated SEM–EDS heavy mineral analysis reveals no provenance shift between glacial loess and interglacial paleosol on the Chinese Loess Plateau. *Aeolian Research*, 13, 71-75.
- Moska, P., Adamiec, G., Jary, Z., Bluszcz, A., Poręba, G., Piotrowska, N., Krawczyk, M. & Skurzyński, J. (2018). Luminescence chronostratigraphy for the loess deposits in Złota, Poland, *Geochronometria*, 45(1), 44-55. doi: <https://doi.org/10.1515/geochr-2015-0073>



P-T-t evolution of the Petersen Bay assemblage, Ellesmere Island: Insight into Pearya – Laurentia accretion

Karolina KOŚMIŃSKA^{1,2}, Jane GILOTTI², William MCCLELLAND², Matthew COBLE³

¹Faculty of Geology, Geophysics and Environmental Protection, AGH University of Science and Technology, 30-059 Krakow, Poland; e-mail: karolina.kosminska@agh.edu.pl

²Department of Earth and Environmental Sciences, University of Iowa, Iowa City, IA 52242, USA

³Stanford-USGS Ion Microprobe Laboratory, Geological Sciences Department, Stanford, CA 94305, USA

Ellesmere Island, northernmost Canadian Arctic, is composed of the displaced Pearya terrane and the Laurentian passive margin. Although accretion of the Pearya terrane to the Laurentian margin plays an important role in paleogeographic reconstructions, the timing and conditions of this event are not well constrained. Here, we focus on the Petersen Bay assemblage (PBA), which crops out along an approximately 5 km wide belt between the crystalline basement of Pearya and the Clements Markham fold belt. The PBA represents a subduction-related complex comprising a variety of lithologies, such as: garnet-bearing schist, garbenschiefer, amphibolite, serpentinite, marble and metachert. The highest-grade metamorphic rocks, garnet-bearing garbenschiefer (sample 17-64) and garnet-kyanite schist (17-66), were chosen for pressure-temperature (P-T) studies and for in-situ monazite U-Pb dating by sensitive high resolution ion microprobe. Quartz in garnet (QuiG) isomekes together with Ti-in-biotite thermometry indicates garnet core growth at 7.5–8 kbar and 500–550°C for the garbenschiefer sample 17-64. The same geothermobarometers yield estimates of garnet core formation at 6.5–7.5 kbar and 540–600°C for the garnet-kyanite schist (sample 17-66). Thermodynamic modelling of 17-66 gives similar P-T conditions of 7.8–8.1 kbar and 590–610°C. The effective bulk composition and crosscutting isopleths indicate garnet rim growth at 8–9 kbar and 650–660°C. Based on the textural relationships and chemical zoning of monazite, 3 chemical domains are distinct. Monazite-I in 17-64 defines a weighted mean ²⁰⁶Pb/²³⁸U age of 394 ± 2 Ma (n = 11, MSWD = 0.6). Monazite-II yields an age of 388 ± 2 Ma (n = 7, MSWD = 0.8). A younger age of 374 ± 6 Ma is recorded by a slightly discordant Monazite-III population (n = 6, MSWD = 3.1). Monazite-I from 17-66 defines a weighted mean ²⁰⁶Pb/²³⁸U age of 397 ± 2 Ma (n = 18, MSWD = 1.6), whereas monazite-II gives an age of 385 ± 2 Ma (n = 19, MSWD = 1.5). The U/Pb monazite ages and P-T results are interpreted as recording Middle Devonian amphibolite facies metamorphism of the PBA, thus the juxtaposition of the Pearya basement and the northern margin of Laurentia is Middle Devonian or younger. This is significantly younger than previous estimates of Late Silurian (Tretin 1998) or Late Ordovician (Klaper 1992).

References

- Klaper, E.M. (1992). The Paleozoic tectonic evolution of the northern edge of North America: a structural study of northern Ellesmere Island. *Tectonics*, 11, 854–870.
- Tretin, H.P. (1998). Pre-Carboniferous geology of the northern part of the Arctic Islands. Northern Heiberg Fold Belt, Clements Markham and Pearya. *GSC Bulletin*, 425, 401p.



Application of rutile thermometer as a provenance indicator of Albian sands from southern Poland

Jakub KOTOWSKI¹

¹Faculty of Geology, University of Warsaw, ul. Żwirki i Wigury 93, 02-089 Warsaw;
e-mail: j.kotowski@uw.edu.pl

Siliciclastic Albian sediments in southern, extra-Carpathian Poland are developed mainly as quartz sands. Differences in the chemical composition of the heavy minerals, i.e. tourmaline (Kotowski et al. 2018), garnet, spinel and monazite (unpublished material) divide the study area into two sections: a western area (Miechów Trough) and an eastern (Lublin area in eastern Poland). Each of the areas has a distinctly different source of detrital material.

The Zr in rutile thermometer is a relatively new method and is used mainly for determining crystallization temperatures of rutile in various metamorphic rocks. This method can only be applied when the $\text{SiO}_2\text{-ZrO}_2\text{-TiO}_2$ system is in equilibrium and the most common, and likely, mineral assemblage is quartz-zircon-rutile (Zack et al. 2004). However, when studying detrital rutile in sedimentary rocks it cannot be known under which conditions it crystallized and if quartz and zircon/baddeleyite were also present during crystallization.

Under the assumption that the above mentioned constraint was fulfilled, rutile crystals from two zones were analyzed using a CAMECA SX Five electron microprobe at the Faculty of Geology, University of Warsaw. To avoid elevated Zr contents in rutile due to microinclusions of zircon, only analyses with $\text{Si} < 200$ ppm were considered valid.

Nearly 300 rutile grains were analyzed from the two zones. The distribution of calculated temperatures for the western zone is bimodal. Most temperatures fall into the granulite facies (800-1000°C) and only 30% of the analyzed rutile grains can be attributed to amphibolite facies (500-650°C). Rutile samples from the eastern zone give more uniform and lower temperatures than in the western zone. Calculated temperatures range from 450 to 800°C, with most analyses oscillating around 600°C. Only a few analyses exceed 800°C.

This distinction between rutile crystallization temperatures supports conclusions from previous heavy mineral studies and confirms the hypothesis of two zones with different source areas of Albian clastic sediments in southern Poland.

References

- Kotowski, J., Nejbert, K. & Olszewska-Nejbert D. (2018). Chemistry and provenance of tourmaline from Albian sands of southern Poland, Joint 5th Central-European Mineralogical Conference and 7th Mineral Sciences in the Carpathians Conference – book of abstracts, 54.
- Zack, T., Moraes, R. & Kronz, A. (2004). Temperature dependence of Zr in rutile: Empirical calibration of a rutile thermometer. *Contributions to Mineralogy and Petrology*, 148, 471-488.



Radlin coal fire heap: thiosulfate- and dithionate-bearing alkaline mineralization; Cu, Fe, As, and P mineralization; and second worldwide occurrence of tsaregorodtsevite

Łukasz KRUSZEWSKI¹, Wojciech SIERNY²

¹Institute of Geological Sciences, Polish Academy of Sciences, Twarda 51/55 Str., Warsaw, Poland; e-mail: lkruszewski@twarda.pan.pl

²Polska Grupa Górnicza (Polish Mining Group, PGG) S.A., ROW Section, Jastrzębska 10 Str., 44-253 Rybnik, Poland; e-mail: w.sierny@list.pl

Long-term study of the “Marcel” coal mine burning waste heap in Radlin allowed to detect over 100 mineral species (as characterized in previous papers of Kruszewski) resulting mainly from extremely dynamic hydrothermal/exhalative processes. New batch of samples confirms the occurrence of alkaline-sulfur mineralization, including (1) $K_5Na(S_2O_6)_2$ (a dithionate, *P4/mnc*) + $Na_2S_2O_3 \cdot 5H_2O$ (a thiosulfate, *P2₁/c*) + $(NH_4)_5(SO_4)(NO_3)_3$ (*P2₁*) + monoclinic (*P2₁/n*) polymorph of letovicite $(NH_4)_3H(SO_4)_2$; (2) thénardite-halite-blödite-löweite-vanhoffite with kogarkoite $Na_3(SO_4)F$; (3) tamarugite-rich one with hohmannite $Fe_2O(SO_4)_2 \cdot 8H_2O$, krausite $KFe(SO_4)_2 \cdot H_2O$, butlerite $Fe(SO_4)(OH) \cdot 2H_2O$, mendozite $NaAl(SO_4)_2 \cdot 11H_2O$, natrojarosite, coquimbite $FeFe(SO_4)_3 \cdot 9H_2O$, pseudowollastonite, and probable volaschioite $Fe_4O_2(SO_4)(OH)_6 \cdot 2H_2O$ and erdite $NaFeS_2 \cdot 2H_2O$; (4) görgeyite $K_2Ca_5(SO_4)_6 \cdot H_2O$ + kröhnkite $Na_2Cu(SO_4)_2 \cdot 2H_2O$ and likely alpersite $(Mg,Cu)(SO_4) \cdot 7H_2O$; and (5) villiamite NaF. Rich copper mineralization includes chalcantite, $(Cu_{0.99}Fe_{0.01})(SO_4) \cdot 5H_2O$ ($n=9$), dolerophanite (1st and 9th occurrence in Poland and worldwide, respectively), $(Cu_{1.96}Fe_{0.03})_{\Sigma 1.99}O_{1.03}(SO_4)_{0.98}$ ($n=15$), tenorite $(Cu_{1.99}Fe_{0.01})O$, cuprite, and a probable Se-rich variety of dolerophanite with > 15 wt.% SeO_2 , associated with minor euchlorine $KNaCu_3O(SO_4)_3$ (8th find worldwide), antlerite $Cu_3(SO_4)(OH)_4$, cyanochroite $K_2Cu(SO_4)_2 \cdot 6H_2O$, and probable paramelaconite $Cu_2Cu_2O_3$, eriochalcite $CuCl_2 \cdot 2H_2O$, and sanjuanite. Cu minerals may be paragenetically related to $(NH_4)[ZnCl_4]Cl$ – a new mineral currently under study. The most important Fe mineral find concerns rich accumulations of akaganeite $Fe_8(OH,Cl)_{16}Cl_{1.25} \cdot nH_2O$ associated, i.a., with an aenigmatite-group species. Phosphates confirmed are wagnerite $(Mg,Fe)_2(PO_4)F$, mejillonesite $HNaMg_2(PO_3OH)(PO_4)(OH) \cdot 2H_2O$ (2nd occurrence in the world), a graftonite-group species, $Na_2CaMg(PO_4)_2$ phase (*P-3m1*), and probable bobierrite $Mg_3(PO_4)_2 \cdot 8H_2O$, vivianite, and spheniscidite $(NH_4,K)(Fe,Al)_2(PO_4)_2(OH) \cdot 2H_2O$. Arsenic minerals include arsenolamprite (As, *Bmab*) associated with carobbiite (KF) and probably mansfieldite $AlAsO_4 \cdot 2H_2O$, and brassite $Mg(AsO_3OH) \cdot 4H_2O$. Tsaregorodtsevite – unique tetramethylammonium aluminosilicate – is confirmed. Another interesting Si species found is melanophlogite, a clathrasil, $46SiO_2 \cdot 6(N_2,CO_2) \cdot 2(CH_4,N_2)$. Brewsterite-group zeolite, brucite, chloritoid, pyrrhotite-5C, troilite-2H, and possible chlorartinite, kernite, pertlikite, shortite, and $FeFe_2(PO_3OH)_4(H_2O)_4$ and $Mn[PO(OH)_2]_2 \cdot H_2O$ (a phosphinate, i.e., hypophosphite) phases (*P2₁/n* for both) are some additional minerals identified.



New occurrences of secondary minerals from Fore-Sudetic Monocline copper deposits: juangodoyite (Rudna IX mine) and rapidcreekite/brushite (Lubin Główny mine)

Łukasz KRUSZEWSKI¹, Rafał SIUDA², Mateusz ŚWIERK³, Eligiusz SZEŁĘG⁴

¹Polish Academy of Sciences, Institute of Geological Sciences, Twarda 51/55 Str., Warsaw, Poland; e-mail: lkruszewski@twarda.pan.pl

²University of Warsaw, Faculty of Geology, Institute of Geochemistry, Mineralogy and Petrology, Żwirki i Wigury 93, 02-089, Warsaw, Poland

³University of Wrocław, Faculty of Earth Sciences and Environment Modeling, Institute of Geological Sciences, Kuźnicza 35 Str., 50-138 Wrocław, Poland

⁴University of Silesia, Faculty of Earth Sciences, Będzińska 60 Str., 41-200, Sosnowiec, Poland

This paper summarizes results of X-Ray Powder Diffraction and Electron Microprobe Analysis of secondary minerals from 1200 m level of Rudna IX mine (Polkowice area) and 610 m level of Lubin Główny mine, both located within the Fore-Sudetic Monocline (Lower Silesia, Poland). Mineralization from Rudna IX forms covering, encrustations and idiomorphic crystals on surfaces of cracked quartzeous chalcocite-bearing sandstones and dolomitic shales. Chalconatronite, with normalized formula $\text{Na}_{2.00}\text{Cu}_{1.00}(\text{CO}_3)_{2.00} \cdot 3\text{H}_2\text{O}$ forms azurite-like, dark blue, single or intergrown, prismatic, spear-like crystals. Juangodoyite, $\text{Na}_{2.00}\text{Cu}_{1.00}(\text{CO}_3)_{2.00}$ ($n=10$), crystallizes as light blue pseudomorphoses after chalconatronite or earthy masses and platy to isometric crystals. Malachite is usually represented by the formula $(\text{Cu}_{1.89}\text{Mg}_{0.11})_{\Sigma 2.00}(\text{CO}_3)_{1.00}(\text{OH})_{2.00}$ corresponding to 5% mean part of mcguinnessite molecule. It forms green botryoidal microcrystalline aggregates. Similar botryoids covering dolomitic shales may be composed of cornubite. Aragonite, $(\text{Ca}_{0.95}\text{Na}_{0.03}\text{Mg}_{0.02}\text{Sr}_{0.01})_{\Sigma 1.01}(\text{CO}_3)_{1.00}$ ($n=5$), is present as white (locally greenish-white) elongated, curved, socket-like aggregates usually in cores and overgrown by hydromagnesite, $(\text{Mg}_{4.90}\text{Cu}_{0.08}\text{Ca}_{0.02})_{\Sigma 5.00}(\text{CO}_3)_{4.00}(\text{OH})_{2.00} \cdot n\text{H}_2\text{O}$, with rims of a probable mixture of northupite (PXRD-confirmed), $\text{Na}_{3.15}(\text{Mg}_{1.93}\text{Cu}_{0.05}\text{Ca}_{0.02})_{\Sigma 2.00}(\text{CO}_3)_{3.00}\text{Cl}_{1.13}$, and magnesite. Azurite is a very minor phase occurring at malachite-chalcocite interface, empirical formula of which is $(\text{Cu}_{2.96}\text{Fe}_{0.04}\text{Ca}_{0.01})_{\Sigma 3.01}(\text{CO}_3)_{2.01}(\text{OH})_{2.00}$ ($n=1$). Greenish covering are veinlets and single crystals of botallackite, $(\text{Cu}_{1.96}\text{Mg}_{0.04})_{\Sigma 2.00}(\text{OH})_{3.01}\text{Cl}_{0.98}$ ($n=16$). Juangodoyite bears minor inclusions of a mica-like phase, possibly "oxymuscovite", $(\text{K}_{0.70}\text{Na}_{0.18}\text{Ca}_{0.07})_{\Sigma 0.94}(\text{Al}_{2.37}\text{Cu}_{0.36}\text{Mg}_{0.29}\text{Fe}_{0.04})_{\Sigma 3.06}\text{Si}_{3.99}\text{O}_{10.00}[\text{O}_{1.33}(\text{OH})_{0.58}\text{S}_{0.09}]_{\Sigma 2.00}$. Locally, austinite, $\text{CaZn}(\text{AsO}_4)(\text{OH})$, is also present. Lubin mineralization is still under study. It comes from a site known as C1B chamber. Here, close to a rock-mass-waters seepage (with slightly elevated water temperature), dolomite (contacting with sandstone) occurs. It is covered by thin, light blue, platy aggregates of Cu-bearing aragonite. Geminite is absent here – it must have been mistaken for rapidcreekite by some former author(s). Aragonite is covered by white to gray protrusions bearing brushite and monohydrocalcite, with some calcite. Rapidcreekite is present locally in the form of sprays of needle-like crystals.



Copper and manganese minerals from “Hans” mine in Przygórze (Lower Silesia, SW Poland) – preliminary results

Łukasz KRUSZEWSKI¹, Rafał SIUDA², Patryk KOSAŁKA³, Paweł ŻOCHOWSKI⁴, Beata MARCINIAK-MALISZEWSKA², Ewa DEPUT¹

¹ Institute of Geological Sciences, Polish Academy of Sciences, Twarda 51/55 Str., Warsaw, Poland; e-mail: lkruszewski@twarda.pan.pl

² Institute of Geochemistry, Mineralogy and Petrology, Faculty of Geology, University of Warsaw, Żwirki i Wigury 93 Str., 02-089 Warszawa, Poland; e-mail: siuda@uw.edu.pl

³ Faculty of Earth Sciences, University of Silesia, Będzińska 60 Str., 41-200 Sosnowiec; pkosalka@o2.pl

⁴ Alterstollen (www.alterstollen.com); e-mail: alterstollen@gmail.com

Samples of baryte veins with poor Cu mineralization were collected on the western slopes of Mt. Golec in Przygórze (Nowa Ruda commune, Lower Silesia, Poland) where “Hans” mine is located. The site is ~600 meters from the Góry Sowie Block contact. The veins cut barren mafic rocks. Baryte is slightly strontian and the enrichment slightly varies within the crystals. Calcite is generally $(\text{Ca}_{0.98}\text{Mg}_{0.02})_{\Sigma 1.00}(\text{CO}_3)_{1.01}$, but may also be ferroan: $(\text{Ca}_{0.81}\text{Fe}_{0.16}\text{Mg}_{0.03}\text{Mn}_{0.01})_{\Sigma 1.00}(\text{CO}_3)_{1.01}$. The associated dolomite is $\text{Ca}_{1.00}(\text{Mg}_{0.96}\text{Mn}_{0.03}\text{Fe}_{0.01})_{\Sigma 1.00}(\text{CO}_3)_{2.16}$. Chalcocite, $\text{Cu}_{2.00}\text{S}_{1.07}$ ($n=11$), is the most common primary ore mineral. It bears some inclusions of chalcopyrite, $\text{Cu}_{1.01}\text{Fe}_{0.99}\text{S}_{1.99}$. Other Cu-S phases are evident and represented by djurleite, $(\text{Cu}_{30.94}\text{Fe}_{0.06})_{\Sigma 31.00}\text{S}_{16.59}$ ($n=11$), digenite/roxbyite, $\text{Cu}_{9.00}\text{S}_{4.97}$ ($n=2$), bornite, $\text{Cu}_{5.09}\text{Fe}_{0.91}\text{S}_{4.25}$ ($n=3$), geerite, $(\text{Cu}_{7.66}\text{Fe}_{0.33}\text{Hg}_{0.01})_{\Sigma 8.00}\text{S}_{4.97}$ ($n=3$), spionkopite, $(\text{Cu}_{33.09}\text{Fe}_{4.89}\text{Hg}_{0.02})_{\Sigma 39.00}\text{S}_{27.64}$, and probable yarrowite, $(\text{Cu}_{6.07}\text{Fe}_{2.93})_{\Sigma 9.00}\text{S}_{7.85}$. Thallium-enriched cinnabar, $(\text{Hg}_{0.98}\text{Tl}_{0.02})_{\Sigma 1.00}\text{S}_{0.84}$ ($n=2$), forms numerous tiny (up to ~15 μm) inclusions in malachite. The latter occurs in three chemical varieties, described by the formulas: $(\text{Cu}_{1.97}\text{Mg}_{0.03})_{\Sigma 2.00}(\text{CO}_3)_{1.00}(\text{OH})_{2.00}$ ($n=10$), $(\text{Cu}_{1.95}\text{Mg}_{0.05})_{\Sigma 2.00}[(\text{CO}_3)_{0.99}(\text{SO}_4)_{0.01}]_{\Sigma 1.00}(\text{OH})_{2.00}$ ($n=20$), and $(\text{Cu}_{1.95}\text{Fe}_{0.03}\text{Mg}_{0.02})_{\Sigma 2.00}[(\text{CO}_3)_{0.90}(\text{SO}_4)_{0.10}]_{\Sigma 1.00}(\text{OH})_{2.00}$ ($n=12$, with mean 2% chukanovite end-member content). Mn oxyhydroxides do not directly contact Cu minerals. They seem to be represented by hollandite, $(\text{Ba}_{0.74}\text{Pb}_{0.14}\text{Ca}_{0.12})_{\Sigma 1.00}\{[\text{Mn}^{4+}[(\text{Mn}^{3+}_{0.78}\text{Cu}_{0.30}\text{Mn}^{4+}_{0.29}\text{Co}^{3+}_{0.24}\text{Fe}^{3+}_{0.1}\text{Ni}^{3+}_{0.12}\text{Si}_{0.07}\text{Mg}_{0.07})_{\Sigma 2.00}]\text{O}_{16.00}\}$ ($n=8$), and possible ranciéite, $(\text{Ca}_{0.03}\text{Ba}_{0.02}\text{Mg}_{0.02})_{\Sigma 0.07}(\text{Mn}^{4+}_{0.53}\text{Fe}^{3+}_{0.29}\text{Co}^{2+}_{0.13}\text{Ni}^{2+}_{0.07}\text{Cu}_{0.07}\text{Si}_{0.04})_{\Sigma 1.13}\text{O}_{1.92}\cdot 0.75\text{H}_2\text{O}$ ($n=6$). The latter is intergrown with Ba- and Mg-rich phases, possibly romanèchite and $(\text{Mn}^{2+}_{0.66}\text{Mg}_{0.15}\text{Ca}_{0.11}\text{Ba}_{0.08})_{\Sigma 1.00}(\text{Mn}^{4+}_{1.67}\text{Fe}^{3+}_{0.15}\text{Co}^{3+}_{0.44}\text{Ni}^{3+}_{0.29}\text{Cu}_{0.28}\text{Si}_{0.16}\text{Al}_{0.01})_{\Sigma 3.00}\text{O}_{6.57}\cdot 2.45\text{H}_2\text{O}$ (4 cations basis, attributed to aurorite). Some of the Ba-rich Mn phases are very locally enriched in W and Bi. Very scarce spinel recast to: $(\text{Fe}^{2+}_{0.89}\text{Zn}_{0.09}\text{Mn}_{0.01}\text{Mg}_{0.01})_{\Sigma 1.00}(\text{Cr}_{1.23}\text{Fe}^{3+}_{0.68}\text{Al}_{0.04}\text{V}_{0.02}\text{Si}_{0.01}\text{Ti}_{0.01})_{\Sigma 2.00}\text{O}_{4.00}$ ($n=2$), corresponding to chromite-magnesian-chromite with 6% zincochromite component. The Mn minerals will be further studied using valency-sensitive techniques, e.g., XANES.



The age of youngest detrital grains of clastic sediments and their interpretation – the cases of active versus passive tectonic settings

Ewa KRZEMIŃSKA¹, Leszek KRZEMIŃSKI¹, Ryszard HABRYN¹, Jolanta PACZEŚNA¹, Grzegorz ZIELIŃSKI¹

¹Polish Geological Institute – National Research Institute, 4 Rakowiecka St., 00-975 Warszawa,
e-mail: ewa.krzeńska@pgi.gov.pl

Introduction

The age of youngest detrital zircon or monazite grain usually are used to constrain the maximum age of sediment deposition. A limitations of this approach are demonstrated in a case studies of the coarse grained clastic rocks from two proximal terranes of Baltica, being active continental margin during Late Neoproterozoic/Cambrian time and passive margin of Baltica.

Results

The U-Pb detrital zircon investigation of conglomerate proximal-type deposits (Potrójna and Raciechowice), from north easternmost margin of Upper Silesian Block (USB) reveal that the youngest cluster of grains ($n > 3$), that overlap within uncertainty yielded similar Late Ediacaran age of 549 Ma. This time has been indicated also by detrital monazite chemical dating method. The geochemical provenance of mostly greywacke source rocks suggest that during Late Ediacaran the USB was controlled by the Cadomian orogenic processes. Thus, these youngest defensible detrital mineral age defines a factual maximum depositional age of sampled conglomerate beds in the area of USB.

Another object of the study was relatively similar coarse-grained sediments from Batowice in southernmost Małopolska Block. These conglomerate beds were usually considered as Late Silurian (< 420 Ma), occurring between the paleontologically recognized Ludlovian and the Lower Devonian sediments. Independently documented youngest detrital zircon age of 474 ± 27 Ma and youngest monazite of 476 ± 25 Ma (Early/Middle Ordovician) seems to be at least fifty million years older than accepted time of this conglomerate bed sedimentation. There are no authigenic grains of monazite. Geochemical provenance studies confirmed a passive margin setting. Usually for such tectonic settings the youngest detritus represents a bit older material than the time of deposition.

The same problem was observed in case of conglomerates from Lublin slope of East European Craton, considered as a passive margin of the Baltica during late Neoproterozoic. The youngest concordant zircon grains detected in Kaplonosy ($n = 5$) gave age of 1452 Ma and in Wisznice ($n = 3$) at 1459 Ma. The stratigraphic position of conglomerates (Żuków Fm) deposited on eroded Palaeo- to Mesoproterozoic basement may suggest their Late Ediacaran age, but they have to be older than rift-related volcanic activity widespread in Volyn-Orsha Aulacogen between 565 and 551 Ma. In this case the radiometric ages reflect only the age of the proximal eroded crystalline basement. Thus, the youngest grains remain tens or hundreds of millions of years older than the real time of sediment accumulation.



Ni,Co-pyrites (bravoites) from the Holy Cross Mountains, Poland

Piotr LENIK¹, Sylwester SALWA², Jakub BAZARNIK¹

¹Polish Geological Institute – National Research Institute, Carpathian Branch;
Address Skrzatów 1, 31-560 Kraków, Poland; e-mail: piotr.lenik@pgi.gov.pl

²Polish Geological Institute – NRI, Holy Cross Mountains Branch; Address Zgoda 21, 25-953 Kielce, Poland

Ni,Co-pyrites are common minerals in epigenetic hydrothermal and early diagenetic ore mineralization in the Holy Cross Mountains. They were noticed for the first time by Muszer et al. in 1995 in hydrothermal vein in the Kostomłoty quarry near Kielce. Their occurrence have been described in many localizations: in Miedzianka near Chęciny, the Józefka quarry near Górnó and the Laskowa quarry near Kielce in the last few years.

Ni,Co-pyrites in Miedzianka were found in fragments of ore collected from the heaps of the former copper mine. Bravoites occur in calcite veins and form small euhedral crystals up to 50 μm , with characteristic zonation and hexagonal shape. They are usually replaced by chalcopyrite. The nickel and cobalt content can reach up to 0.53 apfu and 0.59 apfu, respectively.

Ni-pyrites from the Laskowa quarry occur as thin rims (up to 10 μm) on euhedral crystals of pyrite and product of replacing chalcopyrite along the cracks of crystals copper sulphides. The nickel content in the bravoites is up to 9.8 %wt. (0.2 apfu), while the cobalt content is very low (<1.0 %wt.). Unlike the mineral parageneses from Miedzianka, Ni-pyrites from the Laskowa quarry are younger than chalcopyrite.

Bravoites in the Józefka quarry occur in two different parageneses. A) in hydrothermal veins with Cu-Pb-Zn sulphides, calcite and barite. Ni,Co-pyrites form characteristic hexagonal or orthogonal structures in the centre of euhedral pyrite crystals. The process of replacing bravoites by younger galena has been frequently observed. The nickel and cobalt content achieves 0.61 apfu and 0.24 apfu, respectively. B) the second type of bravoites were observed in black marls, where form small (up to 20 μm) euhedral crystal with characteristic hexagonal bravoite structure. The B type represents synsedimentary – early diagenetic episode of ore mineralization.

Ni,Co-pyrites described from hydrothermal veins represent two different types. Early bravoites show a high variability in chemical composition and a significant content of nickel and cobalt, indicating a transition towards vaesite or cattierite, respectively. Late bravoites contain only nickel, without cobalt.

Acknowledgements. This research is supported by the Ministry of the Environment of Poland from the sources of the National Fund for Environmental Protection and Water Management (no. 22.6605.1601.00.1).

References

- Muszer, A., Salwa, S. & Kowalski, P. (1995). Nowe wystąpienia minerałów niklu (nikielin, gersdorffit, brawoit, annabergite) w paragenzie Zn-Pb-Cu-Fe w Górach Świętokrzyskich. *Acta Universitas Wratislaviensis*, 1739, 229-242.



Thiospinels (siegenite, fletcherite) from the Holy Cross Mountains, Poland – preliminary results

Piotr LENIK¹, Sylwester SALWA², Jakub BAZARNIK¹

¹Polish Geological Institute – National Research Institute, Carpathian Branch;
Address Skrzatow 1, 31-560 Kraków, Poland; e-mail: piotr.lenik@pgi.gov.pl

²Polish Geological Institute – NRI, Holy Cross Mountains Branch; Address Zgoda 21, 25-953 Kielce, Poland

The presence of the minerals from the thiospinel group has been noticed for the first time in the Holy Cross Mountains. Siegenite and fletcherite have been found in the hydrothermal veins in Devonian dolomite in two localizations: in the Józefka quarry near Górnó and in drill core samples from Miedzianka PIG-1 borehole, located in the vicinity of historical copper mine Miedzianka near Chęciny.

The chemical analyses were performed using Cameca SX100 electron microprobe with WDS spectrometer at the Micro-Area Laboratory of the Polish Geological Institute – NRI in Warszawa and TM Hitachi 3030 scanning electron microscope with EDS spectrometer in Holy Cross Branch, Polish Geological Institute – NRI in Kielce.

Siegenite was found within the hydrothermal parageneses in the Józefka quarry. It forms small, anhedral crystals with size up to 50 μm. Usually it occurs as minute inclusions in chalcopyrite. Beside the thiospinel the hydrothermal veins contain mainly chalcopyrite, pyrite, marcasite, barite, galena as well as calcite and Ni-pyrites (bravoites). The formula of siegenite is $(\text{Co}_{1.63}\text{Ni}_{1.23}\text{Fe}_{0.09}\text{Cu}_{0.05})_{3.00}\text{S}_{4.01}$ (based on WDS analyses).

In the second localization, thiospinel forms also small (up to 20 μm), anhedral crystals. It was found in unusual for such mineral parageneses, in intergrowths with secondary copper sulphides (digenite – chalcocite), which are replacing primary, hydrothermal chalcopyrite. Digenite and chalcocite were formed in cementation zone as a product of copper ores oxidation. The presence of thiospinel was detected by scanning electron microscope and its formula is $(\text{Cu}_{0.85-1.11}\text{Co}_{0.84-1.23}\text{Ni}_{0.90-1.36})_{3.00}\text{S}_{3.89-4.09}$ (based on EDS analyses). The chemical composition corresponds to a fletcherite, first time described from the Fletcher Mine in Missouri (USA) in the MVT lead deposits (Craig, Carpenter 1977).

The thiospinel minerals typically are connected with hydrothermal ore mineralization, Siegenite in Józefka quarry is most probably the result of nickel and cobalt mobilization from bravoites in younger stage of ore mineralization, when galena and sphalerite were precipitated. However, the position of fletcherite in cementation zone remains unclear at this stage of investigation and requires further research.

Acknowledgements. This research is supported by the Ministry of the Environment of Poland from the sources of the National Fund for Environmental Protection and Water Management (no. 22.6605.1601.00.1).

References

- Craig, J.M. & Carpenter, A.B. (1977). Fletcherite, $\text{Cu}(\text{Ni},\text{Co})_2\text{S}_4$, a new thiospinel from the Viburnum trend (New Lead Belt), Missouri. *Economic Geology*, 72, 480-486.



Pegmatitic granite from Manikyangsa, Wangdue Phodrang, central Bhutan

Łukasz MACIĄG¹, Bernard CEDRO¹, Anna CEDRO¹

¹*Institute of Marine and Environmental Studies, University of Szczecin, Adama Mickiewicza 18, 70-383 Szczecin, Poland; e-mail: lukasz.maciag@usz.edu.pl; bernard.cedro@usz.edu.pl; anna.cedro@usz.edu.pl*

Introduction

The distinctive syn-Himalayan leucogranite plutons, classified to the Higher Greater Himalayan Section, occur along the South Tibehtian Detachment Section (Gansser 1983). The rocks intruded by granitic plutons are represented by the Greater Himalayan Zone amphibolites, paragneiss, schists and quartzites of Neoproterozoic–Ordovician age (Grujic et al. 2002; Long & McQuarrie 2011).

Representative samples were collected in June 2018 along the fresh road excavation of Wangdue Phodrang-Nobding highway, located nearby Pangkhab, Manikyangsa, central Bhutan. The presented data are especially valuable because of “low impact tourism” policy and necessity of obtaining “restricted-area permit” in several regions in Bhutan.

Preliminary results

Analyzed samples were classified as a LCT pegmatitic leucogranite – aplite, composed of feldspar (albite), quartz, Rb-Cs muscovite, phlogopite, tourmaline (dravite-schörl), petalite, Nb-Ta oxides, hematite and clay minerals. Tourmalines, up to 2 cm long, show weak pleochroism and fine symplectite intergrowths with feldspar.

According to the geochemical results, the bulk pegmatite samples are characterized by high Cs and Rb contents, 77-897 and 387-502 ppm, respectively. The contents of Ta, Nb, Li, Ga, Sn, W and Zr are between 20 and 40 ppm. The Ta/Nb and Zr/Hf mean ratios are 0.57 and 14.62, respectively. The total REY mean content is low (37 ppm) and dominated by Y and Ce. The bulk rock Pb isotope ratios indicate influences of lower mantle protolith.

References

- Gansser, A. (1983). Geology of the Bhutan Himalaya. Denkschriften der Schweizerischen Naturforschenden Gesellschaft, 96, 1-181.
- Grujic, D., Hollister, L. & Parrish, R.R. (2002). Himalayan metamorphic sequence as an orogenic channel: insight from Bhutan. Earth and Planetary Science Letters, 198, 177-191.
- Long, S., McQuarrie, N., Tobgay, T., Grujic, D. & Hollister, L. (2011). Geologic Map of Bhutan. Journal of Maps, 7(1), 184-192.

Ferromanganese crusts from the Clarion-Clipperton polymetallic nodules deposit, equatorial Pacific, Interoceanmetal (IOM) claim area

Łukasz MACIĄG¹, Dominik ZAWADZKI¹

¹*Institute of Marine and Environmental Sciences, University of Szczecin, Adama Mickiewicza 18, 70-383 Szczecin, Poland; e-mail: lukasz.maciag@usz.edu.pl, dominik.zawadzki@usz.edu.pl*

The Clarion-Clipperton Fracture Zone (CCFZ), located in the equatorial northeastern Pacific, is one of the most economically prospective deep-sea deposits of polymetallic nodules, indicating high content of metals, such as Mn, Fe, Ni, Cu, Co, Ti, V, Mo and REY (Kotliński et al. 2015; Zawadzki et al. 2015). The ferromanganese crusts and encrustations are significantly less abundant in the CCFZ compare to nodules, show “sandwich-like” texture and usually form on a consolidated pelagic sediments, mostly zeolite clays.

Analyzed crusts (Fig. 1) are slightly phosphatized (0.13%) and dominated by todorokite, birnessite and vernadite. The thickness vary from 2 to 80 mm.

The external layers show hydrogenous origin and interior indicate diagenetic influences (greater porosity, presence of phillipsite and nontronite). The mean ratios of Mn/Fe and Si/Al are 2.66 and 0.77, respectively. The $\Sigma(\text{Ni, Cu, Co})$ content vary from 0.42 to 1.07%, which is generally lower compared with the nodules. The mean REY content is 1300 ppm.

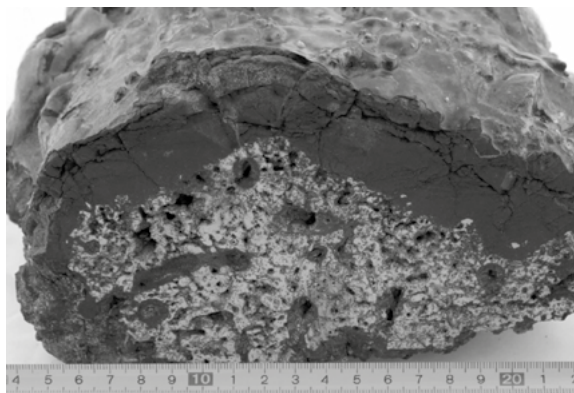


Fig. 1. Representative example of thick ferromanganese crust from the CCFZ, IOM area.

References

- Kotliński, R.A., Maciąg Ł. & Zawadzki D. (2015). Potential and recent problems of the possible polymetallic sources in the oceanic deposits. *Geology and Mineral Resources of World Ocean*, 2(40), 65-80.
- Zawadzki, D., Maciąg, Ł. & Kotliński, R.A. (2015). Osady eupelagiczne Pacyfiku jako potencjalne źródło pozyskiwania pierwiastków ziem rzadkich. *Biuletyn Państwowego Instytutu Geologicznego*, 465, 131-142.



A comparison of vivianite-group minerals from the Kletno and Złoty Stok deposits (SW Poland)

Anna MACIOCH¹

¹Faculty of Geology, University of Warsaw, Żwirki i Wigury 93, 02-089 Warszawa, Poland;
e-mail: macioch.anna@gmail.com

The vivianite group consists of minerals with the general chemical formula $M_3(XO_4)_2 \cdot 8H_2O$, where M is a divalent metal cation (M = Co, Fe, Mg, Ni, Zn) and XO_4 is an arsenate or phosphate anion (X = As or P) (Jambor, Dutrizac 1995; Frost et al. 2003). The occurrence of isomorphic substitutions of metal cations was observed and is a characteristic feature of this mineral group (Jambor, Dutrizac 1995; Frost et al. 2003). One of the solid solutions exists between hörnesite $Mg_3(AsO_4)_2 \cdot 8H_2O$, erythrine $Co_3(AsO_4)_2 \cdot 8H_2O$ and annabergite $Ni_3(AsO_4)_2 \cdot 8H_2O$ (Frost et al. 2003). They form a continuous series, which occur in a triple system including Mg, Co and Ni due to the possible presence of miscibility gaps (Jambor, Dutrizac 1995). The minerals of the vivianite group crystallize under slightly acidic conditions with pH values ranging from 5 to 6 (Drahota, Filippi 2009). They have been recognized in mining and industrial sites associated with As-bearing minerals and in naturally contaminated soils (Drahota, Filippi 2009).

The occurrence of these minerals has been confirmed in the Kletno and Złoty Stok deposits (SW Poland), where the weathering processes have led to the formation of numerous secondary minerals, also from the vivianite group (Siuda, Macioch 2018). This work is to institute a comparison of the physical properties and chemical composition of similar phases from different oxidation zones, which may allow us to determine the geochemical conditions in which these minerals can form.

References

- Drahota, P. & Filippi, M. (2009). Secondary arsenic minerals in environment: A review. *Environment International*, 35, 1243-1255.
- Frost, R. L., Martens, W., Williams, P. A. & Klopogge, J. T. (2003). Raman spectroscopic study of the vivianite arsenate minerals. *Journal of Raman Spectroscopy*, 34, 751-759.
- Jambor, J. L. & Dutrizac, J. E. (1995). Solid solution in the annabergite-erythrite-hörnesite synthetic system. *Canadian Mineralogist*, 33, 1063-1071.
- Siuda, R. & Macioch, A. (2018). Secondary arsenic minerals from the Złoty Stok As-Au abandoned mine (SW Poland). *Geological Quarterly*, 62(4), 925-940.



Could contact metamorphism cause the Marinoan glaciation?

Jarosław MAJKA^{1,2}

¹*Faculty of Geology, Geophysics and Environmental Protection, al. Mickiewicza 30, 30-059 Kraków, Poland; e-mail: jmajka@agh.edu.pl*

²*Department of Earth Sciences, Uppsala University, Villavägen 16, 752 36 Uppsala, Sweden, email: jaroslaw.majka@geo.uu.se*

The Neoproterozoic era is thought to be the most dramatic time in the Earth history when it comes to global climate changes (e.g. Hoffman, Schrag 2002). Both, the Sturtian (ca. 717-660 Ma) and the Marinoan (ca. 645-635 Ma) global glaciations were by far the largest Snowball events known and perhaps the most violent climate change episodes. The direct triggers for these global glaciations are a matter of vivid scientific debate. Several ideas have been proposed including e.g. rapid perturbations to the greenhouse budget and inventory, meteorite impacts and/or voluminous explosive volcanism. Recently, Macdonald and Wordsworth (2017) postulated that the Sturtian global glaciation could have been actually triggered by emplacement of the Franklin Large Igneous Province (LIP) into the evaporate-rich sedimentary basin, which resulted in massive volcanic sulfur aerosol emissions. These emissions could have penetrated the tropopause and formed stratospheric sulfate aerosol, which in turn would have increased albedo. Hence, LIP-sediment interaction due to a development of voluminous contact metamorphic zones could have led to global scale cooling and eventually glaciation. An immediate question arises if a similar process could have triggered the Marinoan glaciation? In this contribution, I will critically evaluate this hypothesis and provide an insight into the Marinoan glaciation recorded in Neoproterozoic section exposed in south-west Svalbard, where there is a record of voluminous mafic volcanism (perhaps of a LIP-scale), associated with contact metamorphism changes, directly preceding and/or coincident with the onset of sedimentation of the Marinoan glacial deposits.

References

- Hoffman, P. F. & Schrag, D. P. (2002). The snowball Earth hypothesis: Testing the limits of global change. *Terra Nova*, *14*, 129-155.
- Macdonald, F. A. & Wordsworth, R. (2017). Initiation of Snowball Earth with volcanic sulfur aerosol emissions. *Geophysical Research Letters*, *44*, 1938-1946.



The critical and associated elements enrichment in cassiterite-sulphide mineralization from the stratiform tin deposits in the Stara Kamienica Schist Belt (Sudetes, SW Poland)

Rafał MAŁEK¹, Stanisław Z. MIKULSKI¹

¹Polish Geological Institute – National Research Institute, 4 Rakowiecka Str., 00-975 Warsaw, Poland;
e-mail: rafal.malek@pgi.gov.pl; stanislaw.mikulski@pgi.gov.pl

The modern geochemical investigation (e.g. ICP-QMS, ICP-OES, WD-XRF and GFAAS) of 42 samples of cassiterite mineralization with additional sulphide mineralization taken from the Sn abandoned mines and documented deposits in the Stara Kamienica Schist Belt in Poland indicates elevated concentrations of critical elements (In, Bi, Ga, Co, Nb, Pt, Pd and Re) as well as some associated elements (Cu, Zn and Pb).

An important critical element occurring in elevated concentrations is indium, whose contents in some samples range from <0.05 ppm to 7.4 ppm (arithmetic mean = 0.92 ppm). The main carriers of indium are sphalerite and chalcopyrite, which according to EPMA studies may have up to a few hundreds of ppm indium admixtures. Besides, the indium mineral – sakuraiite (Cu, Zn, Fe)₃(In, Sn)S₄ has been identified. Gallium was found in the range of about <3 to 84 ppm but the most samples are characterized by gallium content in the range of 20-25 ppm. Cobalt is present in increased quantities in some sulphides (mainly in cobaltite, pyrrhotite and pyrite). The cobalt concentration range from 6 to 168 ppm (arithmetic mean = 37.8 ppm). Another critical element that occurs in samples from tin deposits is bismuth, which occurs in the form of native bismuth or bismuth sulphide. The study shown that bismuth variability is in the range from <0.05 to 1740 ppm. Niobium concentrations of compressed powder samples (WD-XRF) are in the range of <2 to 32 ppm (arithmetic mean = 12.8 ppm). EPMA studies shown that host minerals for Nb admixtures are pyrrhotite, chalcopyrite and arsenopyrite. The interesting concentrations in the studied samples shown also platinum and rhenium. Platinum shows content from <10 to 116 ppb with the arithmetic mean about 56 ppb, while rhenium is present in the samples with the range from 0.21 to 1.03 ppm (arithmetic mean = 0.48 ppm).

In addition, EMPA studies (Cameca SX-100) identified some rare ore minerals in form of small intergrowths in sulphides or mutual mineral overgrowths with them. In general, these minerals occur sporadically and in small amounts but they contain some amounts of interesting metals. These minerals are, inter alia: cobaltite, costibite, gersdorffite, hedleyite, hessite, mimetite, safflorite, sakuraiite, ullmannite and wolframite. Some of these minerals were so far unknown from the tin deposits in the Sudetes (e.g. In-bearing mineral – sakuraiite).

Identified amounts of critical and associated elements may be considering as an added value to cassiterite ores.

Acknowledgements. The project was financed by the National Fund for Environmental Protection and Water Management in accordance with Agreement No. 506/2015.



Single-element geothermobarometry of selected rocks from the Doboszowice Metamorphic Complex (Fore-Sudetic Block)

Dariusz MARCINIAK¹, Jacek SZCZEPAŃSKI¹

¹ Institute of Geological Sciences, University of Wrocław, pl. Maksa Borna 9, 50-204 Wrocław, Poland;
e-mail: darekmarciniak92@gmail.com, jacek.szczepanski@uwr.edu.pl

The Doboszowice Metamorphic Complex (DMC) is situated in the easternmost part of the Fore-Sudetic Block. The complex is composed of a metamorphosed volcano-sedimentary succession comprising the Chałupki paragneiss intercalated with mica schists and amphibolites intruded by the Doboszowice orthogneiss. The volcano-sedimentary succession bear an imprint of Variscan tectonometamorphic reworking previously estimated at maximum ca. 700-740°C and 8-10 kbars (Puziewicz et al. 1999) or 670°C and 8 kbar (Szczepański, Marciniak 2018).

For the purpose of this study we investigated four samples including: 1 mica schist, 1 orthogneiss and 2 paragneiss samples collected in the eastern part of the DMC. We applied a set of single-element geothermobarometers including: Ti-in-biotite and Ti-in-muscovite combined with Si-in-phengite geobarometer. Results of our calculations suggest that investigated samples bear a record of peak of metamorphism at ca. 610-640°C and 1.2-1.5 GPa. Our calculations document slightly lower temperatures and higher pressures compared to previously reported results based on modelling of garnet zoning.

Acknowledgements. The study was financed by the NCN research grant UMO-2015/17/B/ST10/02212.

References

- Puziewicz, J., Mazur, S. & Papiewska, C. (1999). Petrografia i geneza paragnejsów dwułuszczowych metamorfiku Doboszowic (Dolny Śląsk) i towarzyszących im amfibolitów. *Archiwum Mineralogiczne*, 52(1), 35-66.
- Szczepański, J. & Marciniak, D. (2018). PT history preserved in mica schists from the Doboszowice Metamorphic Complex (Bohemian Massif, Fore-Sudetic Block). *Mineralogia – Special Papers*, 48, 86.



Detrital Cr-spinel from Arafura Sea sediments (eastern Indonesia) as a tool in provenance studies of modern sand

Beata MARCINIAK-MALISZEWSKA¹

¹*Institute of Geochemistry, Mineralogy and Petrology, Faculty of Geology, University of Warsaw, ul. Żwirki i Wigury 93, 02-089 Warsaw, Poland, e-mail: b.maliszewska@uw.edu.pl*

Samples of modern sediment were collected along the SW shoreline of the island of New Guinea (water depth 24–82 m, distance to shoreline 5–26 km), eastern Indonesia. They represent the uppermost strata of the seabed sediment of the Arafura Sea shelf. The samples are fine-grained and are mostly sand, muddy sand or gravelly muddy sand. Grains of Cr-spinel were separated by means of a Frantz magnetic separator (0.5A current) from 63–250 µm grain-size class.

Most of the Cr-spinel grains are homogeneous. Electron microprobe (EPMA) analyses have shown that their chemical composition is variable. The Cr₂O₃ content ranges from 22.8–65.7 wt.%, Al₂O₃: 0.3–44.5 wt.%, MgO: 0.9–17.4 wt.% and FeO: 8.8–35.5 wt.%. Additionally, the highest concentration of Fe₂O₃ exceeds 22.0 wt.%. However Fe³⁺ is only present in 28% of the all Cr-spinel analyses. The TiO₂ content reaches 1.8 wt.%, but usually does not exceed 1.0 wt.%. The Cr-spinel grains are also characterized by small amount of MnO (up to 0.8 wt.%) and V₂O₃ (up to 0.4wt.%). The Cr# [Cr/(Cr+Al) atomic ratio] is generally greater than 0.4, and sometimes exceeds 0.9. Therefore, these spinels can be classified as high-Cr. A rather wide range of Al and Cr contents, as well as a small amount of Fe³⁺ in most of the tested grains, suggests an ophiolitic origin (ultramafic cumulate – dunite). At a relatively low Al₂O₃ content, peridotite (ophiolite) spinels show a signature characteristic of a suprasubduction zone. Higher TiO₂ contents in some Cr-spinels from the Arafura Sea are also associated with higher Fe₂O₃ concentrations, which suggests a volcanic origin. The geochemical signature of volcanic spinels is not fully discriminatory: they can be associated with mid-ocean rifts or island arcs.

Certainly, the detrital Cr-spinel grains found in the sediment from the bottom of the Arafura Sea are associated with mafic or ultramafic rocks. Despite the fact that the sampling area is located in a tectonically active region, the nearest ophiolite rocks or island arcs are situated tens or even hundreds of kilometers to the N and NE. Therefore, the source rocks must be located on the southern slopes of the Snowy Mountains, rising above the coast of New Guinea. The Cr-spinel is probably redeposited and comes from the disintegration of sedimentary rocks which record the history and evolution of the northern edge of the Australian plate from the Proterozoic to modern times.



Insights into the origin of organic matter and paleoenvironmental conditions of the Zechstein Limestone basinal facies from the Rudna copper mine (Fore-Sudetic Monocline, Poland) as a potential source of natural gas

Barbara MASSALSKA^{1,2}, Oliwia GRAFKA¹, Anna POSZYTEK¹

¹Faculty of Geology, University of Warsaw, ul. Żwirki i Wigury 93, 02-089 Warsaw, Poland;

²Polish Geological Institute-National Research, ul. Rakowiecka 4, 00-975 Warsaw, Poland;

e-mail: bmas@pgi.gov.pl, oliwia.grafka@uw.edu.pl, anna.poszytek@uw.edu.pl

The presence of a porous dolomite interval, saturated with high pressure natural gas (N₂, CO₂ and CH₄) was revealed within the Zechstein Limestone basinal facies (Upper Permian) situated at the roof of an excavation in the northern area of the Rudna copper mine (Fore-Sudetic Monocline, Poland). The inferred *in situ* source of the accumulated natural gas created a need for detailed organic geochemical research focused on the properties of organic matter preserved in the Zechstein Limestone basinal facies as a potential source of hydrocarbons. This study, therefore, focuses on one of the basic aspects of source rock evaluation, by providing initial insights into the nature of organic activity of the primary producers and the general paleoenvironmental conditions prevailing in the basin during deposition of the Zechstein Limestone unit at this locality, based on the molecular composition of organic matter extracts.

Low molecular weight *n*-alkane and *n*-alkene distribution patterns with an apparent even carbon homologue predominance, very low regular sterane/17 α -hopanes ratio values, and the presence of certain bacterial biomarkers, suggest that organic matter preserved in the studied profile is almost uniformly of dominant marine microbial input with a marginal contribution from terrestrial and algal sources. The presence of isorenieratane and okenane, biomarkers of green and purple sulphur bacteria respectively, indicates a biotope with varying, yet significant, sulfide influx causing prevalent photic zone euxynia. Homohopane distribution patterns and C₃₅S/C₃₄S homohopane ratio values suggest that the bottom waters and the water within the upper layers of the sediment were suboxic or weakly anoxic. Stronger anoxia could have occurred episodically. The gradually decreasing and very low Pr/Ph ratio values probably indicates an increasing input from halophilic bacteria and an associated, gradual increase in salinity while approaching evaporitic sedimentation, rather than gradually decreasing water oxygenation.

The results of the initial organic geochemical studies of the Zechstein Limestone basinal facies at the Rudna mine suggest the prevalence of a relatively oxygen-depleted environment with high salinity and sulfide influx. Such environmental conditions did not support biological activity capable of producing large quantities of biomass, which is the basic prerequisite for a promising hydrocarbon source rock. However, according to the molecular data, the proposed environment facilitated a complex microbial community which could have generated small quantities of biogenic natural gas.



A glance at lower crust beneath S Scotland – preliminary results on pyroxenitic xenoliths from Midland Valley and Southern Uplands

Piotr MATCZUK¹, Magdalena MATUSIAK-MAŁEK¹, Brian G.J. UPTON², Theodoros NTAFLIOS³, Sonja AULBACH⁴

¹Institute of Geological Sciences, University of Wrocław, pl. Maxa Borna 9, 50-204 Wrocław, Poland

²Grant Institute, University of Edinburgh, James Hutton Rd., EH9 3FE Edinburgh, Scotland

³Department of Lithospheric Research, University of Vienna, Althanstraße 14, 1090 Wien, Austria

⁴Department of Geosciences, Goethe University Frankfurt, 60323 Frankfurt am Main, Germany

Carboniferous mafic volcanic rocks occurring in Scotland carry a broad spectrum of mafic and ultramafic xenoliths and megacrysts, which constitute an important primary source of information on the mantle and crust in this area. In this study we present preliminary textural observations and compositional data on pyroxenitic xenoliths from five localities from S Scotland (Midland Valley and Southern Uplands terranes).

Most of the samples are olivine clinopyroxenites, but clinopyroxenites and websterites are also present. Amphibole and dark mica are present in some, whereas magnetite and sulphides occur in majority of the samples. Cores of greenish clinopyroxene are locally enveloped by brownish clinopyroxene; some of the grains enclose exsolution lamellae of orthopyroxene. The pyroxenites have usually meso- to adcumulative textures and are medium to coarse-grained; only one sample is fine-grained and is modally and texturally layered. One sample features a direct, sharp contact between peridotite and clinopyroxenite.

Clinopyroxene in all the rock-types is typically a Ti,Al-diopside/augite with Mg# =0.75-0.85; in samples where clinopyroxene is zoned the rims have lower Mg# and higher Al content. The orthopyroxene is an Al-enstatite with Mg#=0.80-0.84, olivine (Fo₇₉) is relatively NiO-rich (0.18-0.22 wt.%). Clinopyroxene has convex-upward REE patterns (La_N/Lu_N=0.84-2.68).

Some Midland Valley clinopyroxenites were interpreted as precipitates from alkaline magmas whilst websterites were attributed to melts formed during crustal underplating (Downes et al. 2007). Our study suggests that this interpretation may apply to all S Scotland. Nevertheless, the presence of a composite clinopyroxenitic-peridotitic xenolith implies that some of the pyroxenites originated as veins or sills in the lithospheric mantle, probably as a part of a complex crust-mantle transition zone. Presence of zoned clinopyroxene implies reaction of some of the rocks with subsequent batches of melt, possibly during the same magmatic event.

Acknowledgements. Funded by Polish National Science Centre grant no. UMO-2016/23/B/ST10/01905 and supported by the Polish-Austrian project WTZ PL 08/2018.

References

Downes, H., Upton, B.G.J., Connolly, J., Beard, A.D. & Bodinier, J.-L. (2007). Petrology and geochemistry of a cumulate xenolith suite from Bute: evidence for late Palaeozoic crustal underplating beneath SW Scotland. *Journal of Geological Society*, 164, 1217-1231.



Melt-rock reaction and metal enrichment in the subcontinental lithospheric mantle: the Wilcza Góra xenoliths (SW Poland) case study

Hubert MAZUREK¹, Jakub CIAZELA², Magdalena MATUSIAK-MAŁEK¹, Jacek PUZIEWICZ¹, Theodoros NTAFLLOS³, Anna KUKUŁA⁴, Bartosz PIETEREK⁵

¹Institute of Geological Sciences, University of Wrocław, Pl. M. Borna 9, 50-204 Wrocław, Poland; hmaz@o2.pl

²Space Research Centre, Polish Academy of Sciences, ul. Kopernika 11, 51-622 Wrocław, Poland

³Department of Lithospheric Research, University of Vienna, Althanstrasse 14, 1090 Vienna, Austria

⁴Institute of Geological Sciences, Polish Academy of Sciences, ul. Podwale 75, 50-449 Wrocław, Poland

⁵Institute of Geology, Adam Mickiewicz University, ul. Bogumiła Krygowskiego 12, 61-680 Poznań, Poland

Migration of strategic metals such as Au, Ag or Cu, through the lithospheric mantle can be tracked by sulfides in mantle xenoliths. The Wilcza Góra basanite from the SW Poland hosts a variety of subcontinental lithospheric mantle (SCLM) xenoliths giving a unique insight into metal migration through the upper continental mantle.

Three major xenolithic lithologies include 1) peridotites with $Ol_{Fo=89.1-91.5}$ representing depleted mantle (Group A); 2) peridotites with $Ol_{Fo=84.2-89.2}$ representing melt-metasomatized mantle (Group B) and 3) pyroxenites and with $Fo_{77.2-82.5}$ representing fillings of melt migration channels (Group C; Matusiak-Małek et al. 2017).

The three groups of xenoliths differ by sulfide mode and composition. The sulfide modes are enhanced in Group C (1.165-1.631 vol.%) and Group B (0.020-0.111 vol. %) with respect to Group A (0.001-0.010 vol.%). The sulfides from Group A are richer in Cu and Ni than those from Group B and C. This is reflected in mineral composition expressed in vol.% being: $Po_{65-69}Ccp_{1-14}Pn_{17-34}$ in group A, $Po_{73-79}Ccp_{1-9}Pn_{10-26}$ in group B and $Po_{90-97}Ccp_{1-6}Pn_{1-4}$ in Group C, as well as major element composition of sulfides: Ni/(Ni+Fe) in Pn is the lowest in Group C (~0.25) and the highest in Group A (0.54-0.61), whereas Cu/(Cu+Fe) of Ccp is 0.32-0.49 in Group C and ~0.50 in Group A and B.

The sulfide-rich xenoliths of Group C indicate an important role of pyroxenitic veins in transporting Fe-S-rich melts from the upper mantle to the crust. The moderately enhanced sulfide modes in xenoliths of group B show, however, that significant portion of S and metals remains in the mantle never reaching the crust, as has been previously observed in the oceanic lithosphere (Ciazela et al. 2017).

Acknowledgements. This study was supported by the NCN project no. UMO-2014/15/B/ST10/00095 and the Polish-Austrian project WTZ PL 08/2018.

References

- Ciazela, J., Dick, H. J.B., Koepke, J., Pieterrek, B., Muszynski, A., Botcharnikov, R. & Kuhn, T. (2017). Thin crust and exposed mantle control sulfide differentiation in slow-spreading ridge magmas. *Geology*, 45, 935–938.
- Matusiak-Małek, M., Puziewicz, J., Ntafllos, T., Grégoire, M., Kukuła, A. & Wojtulek P.M. (2017). Origin and evolution of rare amphibole-bearing mantle peridotites from Wilcza Góra (SW Poland), Central Europe. *Lithos* 286–287, 302–323.



Cumulate xenoliths from S Sweden – tholeiitic intrusion in deep crust?

Jakub MIKRUT¹, Magdalena MATUSIAK-MAŁEK¹, Theodoros NTAFLSOS², Michel GREGOIRE³, Leif JOHANSSON⁴, Jacek PUZIEWICZ¹

¹ University of Wrocław, Institute of Geological Sciences, Wrocław, Poland,
e-mail: jakub.mikrut7@gmail.com

² University of Vienna, Department of Lithospheric Research, Austria

³ Géosciences Environnement Toulouse, CNRS-CNES-IRD Université Toulouse III, OMP,
Toulouse, France

⁴ Department of Geology, Lund University, Sweden

East European Craton margin in S Sweden was affected by Mesozoic volcanic activity. Volcanic necks contain diverse suite of mantle and crustal xenoliths (Rehfeldt et al. 2007). In this study we discuss origin of gabbroic and pyroxenitic xenoliths from 2 volcanic necks.

We examined 2 websteritic, 2 noritic and 3 gabbronoritic xenoliths with cumulative texture. Norites and gabbronorites exhibit weak foliation. Alterations of Pl and clinopyroxene (Cpx) and melt infiltration are common features, as well as clino-/orthopyroxene (Opx) lamellae in pyroxenes.

Plagioclase modal is >1% in the websterites and from 11 to 70 vol.% in other xenoliths. Modal content of Opx and Cpx in the websterites vary between 26-83 and >53 vol.%, respectively. Plagioclase has An<66, Mg# in Opx and Cpx being 67-78 and 76-83, respectively. Orthopyroxene in all rock-types is LREE-depleted ((La/Lu)_N=0.002-0.060), while that in Cpx is concave-downward ((La/Lu)_N=0.23).

All the samples are of crustal origin, but the gabbronorites were formed at lower pressures (1-2.7 vs. 5.4-9.5 kbar; Nimis, Ulmer 1998). Presence of modal Opx as well as trace element composition of Cpx suggest that the xenoliths may be precipitates from tholeiitic melt. Moreover, the composition of melt in equilibrium with Cpx resembles that of tholeiitic dykes of Permian age from Scania (Obst et al. 2004). The xenoliths suite may be fragments of large magmatic body, evidenced by geophysical data (Thybo 2001).

Acknowledgements. Study funded by Polish National Science Centre grant no. UMO-2016/23/B/ST10/01905 and supported by the Polish-Austrian project WTZ PL 08/2018.

References

- Nimis, P., Ulmer, P. (1998). Clinopyroxene geobarometry of magmatic rocks Part 1: An expanded structural geobarometer for anhydrous and hydrous, basic and ultrabasic systems Contributions to Mineralogy and Petrology, 133, 122-135.
- Obst, K., Solyom, Z. & Johansson, L. (2004). Permo-Carboniferous Magmatism and Rifting in Europe. Geological Society Special Publication 223, London, pp. 259-288.
- Rehfeldt, T., Obst, K., Johansson, L. (2007). Petrogenesis of ultramafic and mafic xenoliths from Mesozoic basanites in southern Sweden: constraints from mineral chemistry. International Journal of Earth Sciences, 96, 433–450.
- Thybo, H. (2001). Crustal structure along the EGT profile across the Tornquist Fan interpreted from seismic, gravity and magnetic data. Tectonophysics, 334, 155-190.



New U-Pb ages of magmatic succession from Los Humeros Geothermal Field (E Mexico)

Magdalena PAŃCZYK¹, Jerzy NAWROCKI¹, Wiesław KOZDRÓJ², Małgorzata ZIÓŁKOWSKA-KOZDRÓJ², Krystian WÓJCIK¹

¹Polish Geological Institute – National Research Institut, 4 Rakowiecka St., 00-975 Warszawa, Poland; e-mail: magdalena.panczyk@pgi.gov.pl

²Polish Geological Institute – National Research Institute, Lower Silesian Branch, al. Jaworowa 19, 53-122 Wrocław, Poland

Los Humeros Geothermal Field is located within the eastern part of Trans-Mexican Volcanic Belt, ca. 180 km east of Mexico City. The 32 samples for geochronological investigations were collected from two areas: Las Minias and Toba, which occur to the east and north-west of Los Humeros caldera, respectively. The analysed profile comprise granitic rocks of basement and outside caldera volcanic successession which contains andesitic and ryodacitic lava flows, pyroclastic rocks (ignimbrites), diorite and basaltic dykes as well as lacustrine volcanoclastic sediments.

Zircons were separated using conventional heavy liquid, magnetic techniques and finally hand-picking. Only three samples were out of zircons. All samples were analyzed using the SHRIMP IIe/MC ion microprobe in the Micro-area Analysis Laboratory of Polish Geological Institute – NRI.

The SHRIMP results for granitic rocks are concordant for each population and form two clusters: Carboniferous and Permian. The ²³⁸U/²⁰⁶Pb ages calculated for zircons from dykes and ignimbrites indicate Miocene age of magma emplacement and volcanic eruption, respectively. The results for younger lava flows as well as for volcanoclastic rocks suggest that the next phase of magmatic activity started in Pleistocene.

Acknowledgements. The GEMex project is supported by the European Union's Horizon 2020 programme for Research and Innovation under grant agreement No 727550.



Dating of charnockite-series rocks from Litynskiy complex (Podolian block, Ukraine) – preliminary results

Magdalena PAŃCZYK¹, Jerzy NAWROCKI¹, Grzegorz ZIELIŃSKI¹

¹Polish Geological Institute – National Research Institut, 4 Rakowiecka St., 00-975 Warszawa, Poland;
e-mail: magdalena.panczyk@pgi.gov.pl

The charnockite-series rocks from Litynski ultra-metamorphic complex (Podolian block) comprise different varieties of charnockites, enderbites and gneisses (Welikanow 2008). The sample for geochronological investigation was taken from the old quarry located north-west of Lityn (Central Ukraine). The coarse-grained charnockite contains plagioclase of oligoclase composition (antiphertite), K-feldspar, orthopyroxene (hyperstene), quartz. Additionally, Cl-amphibole (hastingsite) was identified. Accessory minerals include monazite, zircon, apatite, allanite, magnetite and ilmenite.

The main goal of the present study was to date charnockite rocks using a combination of two methods: monazite dating by EPMA and single zircon U-Pb SHRIMP dating. The obtained results for monazites as well as for zircon rims are very similar and indicate Paleoproterozoic age of metamorphism processes (ca. 2.05 Ga). The SHRIMP results for zircon cores display the mean age ca. 2.8 Ga.

Acknowledgements. This research was supported by the National Science Centre of Poland research project no UMO-2014/15/B/ST10/03695.

References

- Welikanow W. (ed.), (2008). State geological map of Ukraine scale 1: 200 000. Volyn-Podilsky series. Sheets: M-35-XXVIII (Bar), M-35-XXXIV (Mohyliv-Podilsky). Explanatory note. Kyiv. Ministry of Environmental Protection of Ukraine. State Geological Service. UkdGRI. p. 206. [in Ukrainian].



Mineralogy and properties of coal and wood combustion products from home stoves – preliminary results

Artur PEŹZIWIATR¹, Łukasz UZAROWICZ¹, Anna POTYSZ²

¹Department of Soil Environment Sciences, Warsaw University of Life Sciences – SGGW, Nowoursynowska Str. 159, building no. 37, 02-776 Warsaw, Poland; e-mail: artur_pedziwiatr@sggw.pl, lukasz_uzarowicz@sggw.pl

²Department of Experimental Petrology, University of Wrocław, Cybulskiego Str. 32, 50-205 Wrocław; e-mail: anna.potysz@uw.edu.pl

Combustion of bituminous coal and lignite is one of the most important source of electricity and heat worldwide. This process provides variety of wastes like bottom ash and fly ash that can contain elevated amounts of metallic elements (i.e. As, Pb). Disposal of waste materials from combustion process (both from thermal power plants and home stoves) causes environmental risk due to potential leaching of metallic elements into soils. The aim of our study is to identify mineral phases (i.e. using XRD analysis) in products from home stoves where wood and coal have been combusted. Furthermore, chemical composition of samples has been determined. We have collected two types of products: ash remained in the stoves (“bottom ash”- BA), and soot from the chimney (“fly ash” – FA) from three home stoves (H1-H3) located in Central Poland (Dębicze village). Slags (unburned coal) remained on the grid have been also collected from H2. In H1 only wood has been combusted, whereas in H2 and H3 wood and coal together have been combusted.

Common mineral phases in all studied BA are: calcite and quartz. Other phases such as anhydrite (BA from H2 and H3), lime (BA from H1 and H3) are present. Plagioclase is observed only in BA from H1. In FA from H2 and H3 quartz, calcite, and anhydrite are common. In FA from H2 lime is also identified, whereas in H3 plagioclase and hematite. The XRD analysis of magnetic fraction of FA from H3 confirms hematite together with magnesioferrite. Slags from H2 are composed of quartz, plagioclase, and pyroxene. Content of total C in BA is up to 19% (H3) whereas it is 45 and 27% in FA from H2 and H3, respectively. Total N content ranges from 0.11% in BA (H2) up to 6% (FA, H2). Furthermore, FA are characterized by the highest content of S amongst studied samples (up to 3% in H2). The FA are characterized by the highest content of selected metallic elements. For example, FA from H3 contain 9 mg kg⁻¹ of Se, 65 mg kg⁻¹ of As, 3 mg kg⁻¹ of Tl and 178 mg kg⁻¹ of Sb.

Preliminary conclusions from the study are as follows: (1) FA deposition next to the houses (i.e. in gardens) gives higher environmental risk related to soil contamination compared to BA; (2) relatively high content of Sb indicates that polyethylene (i.e. PET bottles) is combusted even though wastes combustion in home stoves is prohibited, and (3) the lack of desulfurization in home stoves may be responsible for relatively high emission of SO_x to the atmosphere compared to thermal power plant stations despite the fact that sulfates are identified in FA.



Sulfide-rich melt-mantle reaction zones in the Balmuccia peridotite massif (NW Italy)

Bartosz PIETEREK¹, Jakub CIAZELA², Riccardo TRIBUZIO³

¹ Institute of Geology, Adam Mickiewicz University, ul. Bogumiła Krygowskiego 12, 61-680 Poznań, Poland; e-mail: barpie@amu.edu.pl

² Space Research Centre Polish Academy of Sciences, ul. Kopernika 11, 51-622 Wrocław, Poland;

³ Department of Earth and Environmental Sciences, University of Pavia, via Ferrata 1 – 27100 Pavia, Italy;

The nature of chalcophile metal migration through the sub-continental lithosphere is not well constrained due to the scarcity of suitable exposures. As sulfides are sensitive to melt-mantle reactions, however, local melt channels are key to understand the behavior of chalcophile metals during melt differentiation, affecting also global mass balances. Here, we use a set of rocks from dunite and pyroxenite veins occurring within the Balmuccia peridotite massif (Ivrea-Verbano Zone, northwest Italy) to better understand potential enrichment in metals upon melt-mantle reactions.

The inherent sulfides are highly concentrated along the contact zones between ultramafic veins (even 2-5 times more sulfide grains than elsewhere) and the host Balmuccia lherzolites. The sulfides form irregular or globular grains up to 2-mm large. Except for rare grains appearing monosulfidic (~8% of all the sulfides), the sulfides are obviously polyphasic and formed after exsolving sulfide liquid. The lherzolite sulfides are dominated by pentlandite (~65 vol.%) with only ~10 vol.% pyrrhotite, while the dunite and pyroxenite veins are markedly enriched in pyrrhotite (up to 25 vol.%). On average, those from dunitic channels are composed of pentlandite ($[\text{Ni,Fe}]_9\text{S}_8$; 63 vol.%), chalcopyrite (CuFeS_2 ; 19 vol.%), and pyrrhotite (Fe_{1-x}S ; 18 vol.%).

First electron microprobe analyses of a contact zone between dunite channel and host lherzolite show pentlandites have a close to stoichiometric metal/S of 1.09-1.10. In addition, pentlandite displays low Co content (0.3 wt.%) and Ni/(Ni+Fe) ranging from 0.39 to 0.43. Chalcopyrite is Cu-poor with Cu/(Cu+Fe) of 0.46. Pyrrhotite is Ni-poor (~0.1 wt.%) and characterized by the low variation of Fe (61.5-62.0 wt.%) and a formula $\text{Fe}_{0.97}\text{S}$ close to the troilitic composition of FeS.

Our first results suggest high efficiency of pyroxenitic pipes in transporting Fe-S-rich melts from the primitive mantle. However, sulfide-rich melt-mantle reaction zones represented by dunite channels demonstrate that uppermost continental mantle is refertilized with these melts during their ascent. Hence, large portion of S and metals returns to the continental mantle never reaching the crust, as has been previously observed in the oceanic lithosphere. *Acknowledgements.* This research is funded by PRELUDIUM 16 grant no. 2018/31/N/ST10/02146 of the NCN.



Biologically and chemically mediated dissolution of copper metallurgical slags

Anna POTYSZ¹, Jakub KIERCZAK¹

¹*Institute of Geological Sciences, University of Wrocław, Cybulskiego 32, 50-205 Wrocław, Poland;
e-mail: anna.potysz@uwr.edu.pl, jakub.kierczak@uwr.edu.pl*

Historical metallurgical slags were formerly considered as useless wastes. However, disposal of such industrial wastes often affected the environment due to the release of metallic elements. In contrast, at the present time, slags are considered as potential metal resources and strong efforts are made towards development of technological process leading to metal extraction and recovery. However, the dissolution pathways of various slags have to be known in order to make the process optimal, efficient and environmentally reasonable.

The aim of this study was to compare susceptibility to dissolution of two copper slags: crystalline slag (CS) and amorphous slag (AS). Chemically mediated dissolution was evaluated with various normality equivalent acids (sulfuric, hydrochloric, nitric, citric and oxalic), whereas biologically mediated dissolution was investigated with acidophilic bacteria *Acidithiobacillus thiooxidans*. Various operating parameters such as: acid concentration (0.1, 0.5 and 1 M) and pulp density (1, 2, 3, 5 and 10%) were applied in the experiments.

This study demonstrated that crystalline and amorphous slags are susceptible to dissolution with the latter being generally more suitable for use in metal extraction. The most efficient treatment for amorphous (AS) and crystalline slag (CS) was bioleaching at 1% PD during 21 days that led to extraction of Cu at 98.7% and 52.1% for AS and CS, respectively. Hydrochloric acid was the most efficient chemical agent that enabled to extract 30.5% of Cu from CS (1% PD, 48 h) and 98.8% of Cu from AS (1% PD, 24 h). Slag residues after biotic treatment had strong alteration features as demonstrated by complete dissolution of fayalite in case of CS and transformation of AS to amorphous silica and secondary gypsum, hence AS in the form of metal-depleted residue. Simulated economic estimation revealed that process can be profitable if optimal conditions are adjusted.

This study highlights the importance of comparing crystalline and amorphous slags in order to properly design reactor operating conditions. Only integrated approach combining many variables may contribute to development of optimal process to be applied in the future at larger scale.

Acknowledgements. This work was financially supported by National Science Centre (NCN) in Poland in the frame of FUGA 5 program under grant agreement UMO-2016/20/S/ST10/00545. Part of this research (mineralogical analyses) has also been supported by statutory funding 0420/2677/18 (Ministry of Science and Education).



Zircon populations in rhyolitic rocks from Central Europe: insight from SEM-MLA analyses

Arkadiusz PRZYBYŁO¹, Anna PIETRANIK¹

¹*Institute of Geological Sciences, University of Wrocław, Maksa Borna 9, 50-204 Wrocław, Poland;
e-mail: arkadiusz.przybylo@uw.edu.pl*

Uranium-lead dating of zircon is the classic method to obtain ages of silicic rocks. However, zircon dating is not straightforward and that it is particularly true for rhyolites, which often give range of ages of over 10-20 million years for a single sample. This may be caused by lead loss during prolonged magmatic activity or by the presence of antecrystic crystals within the zircon cargo (Pietranik et al. 2013). Therefore, it is vital to characterize zircon populations occurring in the rock, which may represent autocrystic and antecrystic grains. To better characterize the population it is interesting to see how they occur in rock structure. However, using traditional microscope and SEM methods is time-consuming. Therefore, we suggest that using SEM equipped with Mineral Liberation Analyzer (SEM-MLA) allows for better and faster analyzes of all grains from a thin section and also gives quantitative information on grains dimensions and mineral association for large number of grains, which is impossible to obtain using traditional methods. The numerical data can be later statistically compared within the sample and between samples (e.g. by STATISTICA software) giving robust information on differences between certain parameters. This study presents information on SEM-MLA characteristic of Central Europe rhyolitic rocks in order to define if the rock contains different zircon populations.

Zircon analyses from Central European rhyolitic rocks by MLA/SEM show that: 1) zircon dominate and occur mostly in one or two minerals (K-feldspar and matrix) and stubby zircons are more regularly distributed in rock than prismatic zircons, 2) dominant zircons do not contain inclusions, 3) modal mineralogy and zircon association data are correlated, however zircon is also associated with other accessory minerals like ilmenite, Fe-oxides, apatite and rutile, particularly in laccoliths zircon seems to predominate in late magmatic assemblage, 4) biotite is also an exception as in general it constitutes only 1% of the rock, but even 17% of zircon border is associated with this mineral and 5) ca. 90% of zircon grains have size less than 75µm. Significant statistical differences in length and angularity are observed between zircons from rhyodacites and rhyolites. These findings have a potential impact on interpretation of zircon ages as two different populations can now be accessed by future zircon dating.

References

- Pietranik, A., Słodczyk, E., Hawkesworth, C.J., Bretkreuz, C., Storey, C.D, Whitehouse, M. & Milke, R. (2013). Heterogeneous Zircon Cargo in Voluminous Late Paleozoic Rhyolites: Hf, O Isotope and Zr/Hf Records of Plutonic to Volcanic Magma Evolution. *Journal of Petrology*, 54(8), 1483–1501.



Organic tracers from Miocene lignite burning

Maciej RYBICKI¹, Leszek MARYNOWSKI¹, Bernd R.T. SIMONEIT²

¹Faculty of Earth Sciences, University of Silesia, Będzińska Str. 60, 41-200 Sosnowiec, Poland;
e-mail: maciej.rybicki@us.edu.pl

²Department of Chemistry, College of Science, Oregon State University, Corvallis, OR 97331, U.S.A.

Levoglucosan, mannosan and galactosan, products from thermal decomposition of cellulose and hemicellulose, are considered as major tracers of contemporary biomass burning. However, a few reports are known, where an alternate source of levoglucosan based on coal combustion was pointed out (Fabbri et al. 2008; Yan et al. 2018). Lignites are often the primary energy source in brown coal mining regions and household furnaces in such regions are the major source of lower temperature emissions of particulate matter (PM).

Here, we performed burn tests of lignite samples from various Polish mines in order to obtain the full geochemical characteristics of Miocene lignite combustion products. Smoke PM samples were taken by high-volume filtration of smoke from low-temperature, open-fire combustion of the Miocene lignites, and then analyzed using gas chromatography coupled with mass spectrometry (GC-MS).

The results confirm that lignite combustion produces significant amounts of levoglucosan, which is generated not only during burning of xylite, but also from other lignite types including detritic and detroxylitic brown coals. Moreover, only trace amounts of mannosan and galactosan have been detected in PM of lignite smoke. This indicates that a portion of the anhydrosaccharides present in aerosols might originate from brown coal combustion, and not, as commonly believed solely from biomass burning.

All lignite smoke PM samples contain thermodynamically unstable $\beta\beta$ -hopanes and hopenes, with values of the homohopane index 22S/(22S+22R) ranging from 0.02 to 0.12. This is characteristic for immature organic matter, and combined with the presence of anhydrosaccharides can be used as tracers for lignite combustion in ambient air. Furthermore, almost all Miocene lignite smoke PM samples contain α -, β -, γ -, and δ -tocopherols, and prist-1-ene. This is the first report of the occurrence of all four tocopherol isomers in the geological record (in lignite extracts) and in lignite smoke PM samples.

References

- Fabbri, D., Marynowski, L., Fabiańska, M.J., Zatoń, M. & Simoneit, B.R.T. (2008). Levoglucosan and other cellulose markers in pyrolysates of Miocene lignites – geochemical and environmental implications. *Environmental Science and Technology* 42, 2957–2963.
- Yan, C., Zheng, M., Sullivan, A.P., Shen, G., Chen, Y., Wang, S., Zhao, B., Cai, S., Desyaterik, Y., Li, X., Zhou, T., Gustafsson, Ö. & Collett, J.L., Jr. (2018). Residential coal combustion as a source of levoglucosan in China. *Environmental Science and Technology* 52, 1665–1674.



The pyrophyllite – a new mineral of the metamorphic rocks from the Holy Cross Mountains, Poland.

Sylwester SALWA¹

¹Polish Geological Institute – National Research Institute, Zgoda 21, 25-953 Kielce, Poland;
e-mail: sylwester.salwa@pgi.gov.pl

Presence of the metamorphic rocks in the Holy Cross Mountains was the first time described only a several years ago by Salwa (2008). The phyllites are composed of: quartz, white mica, chlorite, siderite, pyrite, dolomite, hematite, apatite, xenotime and sporadically monazite. These rocks are intensively tectonized and metamorphism is strictly related to tectonic deformation. The growth and distribution of new minerals was controlled by deformational processes. The phyllites are also cut by numerous, the most often quartz, quartz-kaolinite/dickite, quartz-chlorite-apatite and siderite-dolomite veins.

The research done in recent years have shown the presence of pyrophyllite in described above rocks. The pyrophyllite is not present in the whole profile of phyllites. Its occurrence was found mainly in these parts of metamorphic rocks where there is no chlorite presence or where it is present in small amounts.

The pyrophyllite appears in three forms: as independent, relatively large porphyroblasts dispersed in the rock, within kaolinite/dickite stack structures and in quartz-kaolinite/dickite veins, sometimes also containing a small amount of chlorite. The size of individual minerals reaches up to 1 mm in length and 0.2 mm in thickness, which makes them macroscopically visible.

The pressure at which phyllites were formed, was estimated based on the presence of deformation lamellas in quartz, at over 1.72 kBa. At this pressure the temperature of pyrophyllite formation reaches above 300°C.

References

Salwa S. (2008). Wstępna charakterystyka strukturalno-petrograficzna fyllitów z Podmachocic w regionie łysogórskim Gór Świętokrzyskich. *Przegląd Geologiczny*, 54, 513-520.



Lower Ordovician (Tremadocian) tuffaceous mudstones from the Holy Cross Mountains, Poland: mineral composition and early diagenetic silicification

Sylwester SALWA¹, Wiesław TRELA¹

¹Polish Geological Institute – National Research Institute, Zgoda 21, 25-953 Kielce, Poland;
e-mail: sylwester.salwa@pgi.gov.pl; wieslaw.trela@pgi.gov.pl

The lowermost part of the Ordovician succession in the southern Holy Cross Mountains (SE part of central Poland) consists of the upper Tremadocian glauconite-rich tuffaceous mudstones, siltstones/sandstones and cherts (bedded and nodular). They form the Wysoczki Formation interpreted as the transgressive to highstand unit characterized by the intermittent accumulation of clastic sediment and starved periods operating in the transition from the near- to offshore zone (Trela 2001). The basal contact of this succession is delineated by the angular unconformity with the underlying lower Cambrian strata.

Mudstone beds of the Wysoczki Formation consist of weakly rounded to angular monocrystalline quartz grains, however, the rounded and polycrystalline grains of magmatic origin occur as well. They are accompanied by numerous authigenic and detrital glauconite. Some of angular quartz grains refer to as glass shards and automorphic crystals. It is noteworthy that was the first one who identified the pyroclastic material in these rocks, including pyrogenic quartz, well-preserved plagioclases and biotite as well as abundant montmorillonite in the clay background. The detailed microscopic studies have revealed the unweathered potassium feldspars and plagioclases represented by orthoclases and albites, respectively. Orthoclases occur mostly as isometric grains revealing in some cases the hypidiomorphic shape. Micas are represented by the unweathered muscovite and less common biotite grains. The subordinate mineral components include well-rounded zircons, automorphic apatite crystals and probably analcime.

Chert beds are made up of chalcedonic quartz forming spherulitic growth structures (fibrous fringes and wedge-shaped forms) and microquartz developed as finely crystalline mosaic. Some beds refer to as the composite layers due to the co-occurrence of mudstone, siltstone and chert laminae, lenses and nodules, which in some cases show a soft-sediment deformation and brecciation. A common feature of these rocks is a selective replacement of clay background (with relicts of glass shards) by the chalcedonic quartz and microquartz. Therefore, it seems plausible that the devitrification of volcanic glass and clay transformation were likely sources of silica for the Upper Tremadocian cherts in the Holy Cross Mountains.

References

- Trela, W. (2001). Sedimentary record of changing hydrodynamic conditions in the upper Tremadoc deposits of the Holy Cross Mountains, Poland. *Geological Quarterly*, 45(2), 131-142.



Influence of sorbent texture and structure on sorption properties relative to SO₂ – the case of dolomites

Magdalena SEK¹, Elżbieta Hycnar¹

¹Department of Mineralogy, Petrography and Geochemistry, AGH University of Science and Technology, Mickiewicza 30, 30-059 Cracow, Poland, e-mail: mmsek@agh.edu.pl

The efficiency of the desulphurization process in fluidized bed technology depends on many different factors related to e.g. the type of furnace, place of sorbent feeding to the boiler or fluidized bed temperature, but above all it is related to a sorbent reactivity. Research shows that one of the most important factors affecting the reactivity of a sorbent is the porosity produced at the stage of sorbent thermal dissociation. It mainly depends on the structural-textural character formed as a result of sedimentation, diagenesis and epigenesis (Hycnar 2018). Two different dolomites were studied: dolomitic marble from the Romanowo Górne deposit (Lower Silesia) and the metasomatic dolomite from the Chruszczobród 2 deposit (Upper Silesia). The results of experimental studies have shown that despite similar phase and chemical composition, the samples show different values of SO₂ sorption efficiency. The metamorphosed dolomite was characterized by inferior sorption properties (156 gS/1kg of sorbent) than the secondary dolomite (173 gS/1kg of sorbent). The results of textural studies indicate that the surface area of the sorbent before the decarbonization doesn't have a significant impact on the development of porosity during this process – the values for both dolomites were similar. Whereas, in the case of metasomatic dolomites, the surface area after the decarbonization grows by two orders of magnitude (from 0.47 to 18.57 m²/g), and effective porosity increases at around 30% (from 54.87 to 82.32%). It is related to the structural and textural nature of this dolomite. They are micritic and sparitic dolomites with a porous texture as a result of, among others, dissolving processes. In contrast, dolomitic marble show a much lower surface increase (from 0.28 to 5.59 m²/g) and effective porosity (from 47.85 to 59.17%), which is the result of recrystallization of carbonate minerals during transformations under regional metamorphism conditions (Witek 1976). Despite significant genetic differences, in the case of fluidized bed combustion, both dolomites and dolomitic marble can be successfully used as SO₂ sorbents competing with limestone.

Acknowledgements. This study was supported by project Nr 16.16.140.315 (AGH University of Science and Technology) and Center of Energy AGH infrastructure.

References

- Hycnar E. (2018). The structural and textural characteristics of limestones and effectiveness of SO₂ sorption in fluidized bed conditions. *Gospodarka Surowcami Mineralnymi*, 34(1), 5-24.
- Witek B. (1976). Badania petrograficzne marmurów złoża Wapniarka i Romanowo Górne w NW części pasma Krowiarek. *Geological Quarterly*, 20(2), 241-260.



Remobilization of Ca and Ti during the contact metamorphism of Karkonosze Granite on basis of tourmaline of the Ca-series from Budniki near Kowary

Mateusz SEK¹, Adam PIECZKA¹

¹Department of Mineralogy, Petrography, and Geochemistry, AGH University of Science and Technology, al. Mickiewicza 30, 30-052 Kraków, Poland; e-mail: msek@agh.edu.pl

The Budniki area is located near Kowary town at the NE termination of the Karkonosze Mts. The region is a part of the eastern metamorphic cover of Karkonosze granite belonging to the Kowary-Czarnów metamorphic unit. Two regionally-metamorphosed rocks: amphibolite enriched in Ti-bearing mineralization and surrounding quartzofeldspathic schists, formed from mixed magmatic-sedimentary protoliths, partly connected with basic lavas and tuffs of pre-Variscian bimodal volcanism, which underwent regional Variscan metamorphism under MP-MT conditions. Furthermore, products of the metamorphism were modified by contact metamorphism induced by the intrusion of the Karkonosze Granite pluton. The Ti mineralization (ilmenite, rutile, subordinate titanite) is related to the transformation of primary Ti-bearing minerals of the amphibolite (ilmenite-titanite) during the regional metamorphic event and the superimposed contact metamorphism. The processes resulted in the remobilization of Ca and Al from the primary plagioclase of amphibolites and Ti from ilmenite and titanite and crystallization of the oxides and Al-rich titanite (Mochnacka et al. 2008).

Tourmalines occur in quartz veins crossing out the host amphibolite and schist rock. Crystals of the mineral evolve from Mg-rich/Fe-rich varieties of the alkali series (oxy-dravite to Fe-rich dravite) to members of the calic series (uvite-feruvite), containing up to 1.6 wt% TiO₂ with increasing Fe and F content. It suggests that the tourmalines crystallized in changing condition marked by the increasing role of Fe during the first stage of metamorphism (the first generation) and increasing role of Ca, Ti and F during later stages (the second generation).

The first generation of tourmaline seems to be connected with the mobilization of B-rich fluids during prograde metamorphism. The second one, marked by the increasing role of Ca, Ti and Fe is related to fluid activity and decomposition of plagioclases and associated Ti oxides (ilmenite, rutile) from the host amphibolite during the late stage of regional metamorphism or contact metamorphism of Karkonosze granite intrusion.

Acknowledgements. The study was supported by the National Science Centre (Poland) grant 2017/27/N/ST10/01579 to M.S.

References

- Mochnacka, K., Oberc-Dziedzic, T., Mayer, W. & Pieczka, A. (2010). Ti remobilization and sulphide/sulphoarsenide mineralization in amphibolites: effect of granite intrusion (the Karkonosze-Izera Massif, SW Poland). *Geological Quarterly*, 52(4), 349-368.



Methane inclusions in Western Tatra Mountains mineralization: study by Raman spectroscopy

Magdalena SITARZ^{1,2}, Piotr JELEŃ³, Bożena GOŁĘBIEWSKA², Krzysztof NEJBERT⁴

¹Tatra National Park, ul. Kuźnice 1, 34-500 Zakopane, Poland; e-mail: msitarz@tpn.pl

²AGH University of Science and Technology, Department of Mineralogy, Petrography and Geochemistry, al. Mickiewicza 30, 30-059, Kraków, Poland

³AGH University of Science and Technology, Faculty of Materials Science and Ceramics, al. Mickiewicza 30, 30-059, Kraków, Poland

⁴University of Warsaw, Institute of Geochemistry, Mineralogy and Petrology, Żwirki i Wigury 93, 02-089 Warszawa, Poland

We present a preliminary study of fluid inclusions contained in quartz connected with hydrothermal mineralization from the Polish part of the Western Tatra Mountains, from the “Pyszniańska Valley”, “Pod Banie Gully” and “Baniste Gully”. Copper and silver mineralization is found as abundant polyphase carbonate-quartz and carbonate-quartz-sulphide-barite veins (e.g. Gawęda 2007).

The method of Raman spectroscopy mapping was used to examine the composition of the fluid inclusions. Raman mapping was carried out using a Witec Alpha 300 M+ spectrometer. 488 nm diode laser with 600 grating and 100x ZEISS objective. 40 x 40 μm maps with 80 lines per image x 80 points per line were recorded with an integration time of 1 s. The size of the observed inclusions closed in the range of 2–6 micrometers. Raman scatter peak shifts show that inclusions are mostly made of CH₄ (c.a. 2906–2917 cm⁻¹), but most often ranges from 2909–2911 cm⁻¹, which signifies according to DeHan (2009) a very high density of methane inclusions. Recent microthermometric studies (e.g. Jurewicz, Kozłowski 2003) shows that inclusions are filled with aqueous solutions of salts, mainly NaCl, KCl and CaCl₂ and gas or liquid CO₂. Raman spectroscopy allows us to broaden the number of identified fluid inclusions.

References

- DeHan L., JinXing A., XianMing X., Hui T., Chun Y., AnPing H., JingKui M. & ZhiGuang S. (2009). High density methane inclusions in Puguang Gasfield: Discovery and a T-P genetic study. *Chinese Science Bulletin*, 54, 4714-4723.
- Gawęda A., Jędrysek M. O. & Zieliński G. (2007). Polystage mineralization in tectonic zones in Tatra Mountains, Western Carpathians. *Granitoids in Poland, Archivum Mineralogiae Monograph*, 1, 341-353.
- Jurewicz E. & Kozłowski A., (2003). Formation conditions of quartz mineralization in the mylonitic zones and on the slickenside fault planes in the High Tatra granitoids. *Archiwum Mineralogiczne*, 52, 65-76.



Wallkilldellite-(Fe) from Rędziny (Rudawy Janowickie Mts., SW Poland) – a preliminary report

Rafał SIUDA¹, Bożena GOŁĘBIOWSKA², Adam PIECZKA², Piotr JELEŃ³, Jan PARAFINIUK¹

¹Department of Geochemistry, Mineralogy and Petrology, University of Warsaw, ul. Żwirki I Wigury 93, 02-089 Warsaw, Poland; e-mail: rsiuda@uw.edu.pl

²Faculty of Geology, Geophysics and Environmental Protection, al. Mickiewicza 30, 30-059 Kraków, Poland; e-mail: goleb@agh.edu.pl, pieczka@agh.edu.pl

³Faculty of Materials Science and Ceramics, AGH University of Science and Technology, al. Mickiewicza 30, 30-059 Kraków, Poland; e-mail: pjelen@agh.edu.pl

We report the first Polish occurrence of wallkilldellite-(Fe), a rare hydrated arsenate of calcium and ferric ion. The mineral was found at the third level of Rędziny dolomite quarry in the oxidized ore zone. Wallkilldellite-(Fe) occurs as brown aggregates composed of thin husk-like crystals (up to 100 μm). These aggregates have usually grown on the surface of amorphous, gel-like Fe-Ca arsenate (probably yukonite) or filled fissures in the yukonite-like aggregates. Besides yukonite the analyzed mineral coexists with goethite, conichalcite and chrysocolla.

The empirical formula of the wallkilldellite-(Fe) derived from Electron Microprobe Analysis (EPMA) on the basis of O = 20 is $(\text{Ca}_{3.92}\text{Cu}_{0.02}\text{Zn}_{0.01})_{\Sigma 3.95}\text{Fe}_{5.84}[(\text{As}_{1.00}\text{P}_{0.02})_{\Sigma 1.03}\text{O}_4]_4[(\text{OH})_{7.34}\text{O}_{0.33}]18\text{H}_2\text{O}$. The Raman spectra (RS) were recorded for the same spots, as analyzed previously by EPMA. No RS of wallkilldellite-(Fe) has so far been presented in the literature. Comparing the RS of wallkilldellite-(Fe) to the RS of arseniosiderite, another Ca-Fe arsenate, characteristic three strong bands around 937, 863 and 827 cm^{-1} due to arsenate AsO_4^{3-} symmetric and antisymmetric stretching vibrations (ν_1 and ν_3 mode) can be distinguished. The observed differences between the RS of wallkilldellite-(Fe) and arseniosiderite seem to be attributable to the quantitative relationship between Fe and Ca in the structure of these arsenates and the difference in their atomic weights. The presence of wallkilldellite-(Fe) was confirmed by PXRD analysis.



Numerical simulation of geological CO₂ sequestration: case study of selected mudstones from the Baltic Basin

Piotr SŁOMSKI¹, Jacek SZCZEPAŃSKI¹

¹*Institute of Geological Sciences, University of Wrocław, Plac Maksa Borna 9, Wrocław 50-204, Poland
piotr.slomski@uwr.edu.pl, jacek.szczepanski@uwr.edu.pl*

Geological sequestration of carbon dioxide (CO₂) is one of the ways to reduce the delivery of this greenhouse gas into the atmosphere. CO₂ injected into the rock formations can be immobilised in structural traps, by capillary trapping, by dissolving in brines, adsorption on the surface of organic matter and by mineral trapping. In the latter case CO₂ is bounded as CO₃²⁻ in new carbonate minerals.

In this study numerical modelling of CO₂ sequestration was performed in order to evaluate the effects of CO₂-brine-rock interactions in the early Palaeozoic argillaceous mudstones from the Polish part of the Baltic Basin. Simulations of CO₂ sequestration were conducted using PHREEQC code for 5 samples representing Pelplin and Sasino Formations and Jantar Member. Modelling was performed for a 10 dm³ volume of rock and a period of 3000 years. The other simulation parameters correspond to in situ reservoir conditions and include: temperature of 80 °C, pressure of 40 MPa and the presence of brine being a mixture of NaCl, CaCl₂ and MgCl₂, with total mineralization of 80 mg/L.

Results of simulations indicate that injection of CO₂ will cause dissolution and precipitation of certain minerals and changes in chemistry of brine. Acidification of reservoir water provoked dissolution of feldspars, calcite and chlorite in the studied rock samples. As a result, the cations released from minerals (mostly Ca²⁺, Fe²⁺, Na⁺) together with cations from brines and CO₃²⁻ ions were included into newly precipitated dawsonite and ankerite. The brines after the simulation were characterised by decrease of sodium and magnesium, an increase in calcium, aluminium, iron and silicon and the appearance of various forms of inorganic carbon in the solution. The brine mineralisation increased up to 97 mg/L and its density changed from 1.07 to 1.09 cm³/g. Most mineralogical and chemical changes occurred during the first few hundred years after CO₂ injection.

Performed numerical simulation suggests that the most important mechanisms of CO₂ geological sequestration in the studied set of mudstones would be capturing of this gas: (1) in dissolved form in brine and (2) as CO₃²⁻ in the newly precipitated carbonate minerals, such as ankerite and dawsonite. The modelling results show that 10 dm³ of rocks can absorb ca. 0.5 dm³ of CO₂. Consequently, assuming the reservoir volume of 0.2 km³ (corresponding to 60 m thickness and 1 km radius from the injection site) the investigated rock formations could trap ca. 3 million tons of CO₂ during 300 years. However, the proposed model does not take into account permeability of investigated rocks. Therefore, suggested amount of trapped CO₂ is overestimated. In the future, we plan to design a model taking into account rock permeability and CO₂ flow rate in order to quantify CO₂ sequestration efficiency in the studied mudstones.



Mercury as a proxy for large-scale volcanism during the Late Ordovician mass extinction

Justyna SMOLAREK-LACH¹, Leszek MARYNOWSKI¹, Wiesław TRELA², Paul B. WIGNALL³

¹Faculty of Earth Sciences, University of Silesia, Sosnowiec 41-200, Poland;
e-mail: justyna.smolarek-lach@us.edu.pl; leszek.marynowski@us.edu.pl

²Polish Geological Institute – National Research Institute, 25-953 Kielce, Poland;
e-mail: wtre@pgi.gov.pl

³School of Earth and Environment, University of Leeds, Leeds LS2 9JT, UK;
e-mail: P.B.Wignall@leeds.ac.uk

The Late Ordovician mass extinction (LOME) was the second largest Phanerozoic crisis, but its cause remains elusive. Among others, bioevolutionary events, oceanographic changes, and geotectonic processes have been proposed over the years. Until recently there has been no evidence for large-scale volcanism during the LOME making it one of the few Phanerozoic crises to not have the usual driver. This has changed with recent reports of Hg enrichments from South China and Laurentia at the time of LOME indicating volcanism may indeed have played a role in the crisis (e.g. Jones et al. 2017). Here we extend the known record of Hg spikes in an Upper Ordovician to lowermost Silurian to a peri-Baltic, deep shelf succession from a borehole located in the Holy Cross Mountains (HCM, Poland). To examine the potential role of anoxia in Hg enrichment, we have compared Hg with other trace metals (e.g. Mo), pyrite framboid diameter analysis, and biomarker data. A strong positive anomaly in the lower late Katian (Hg/TOC = 2537.3 ppb/wt.%) was noted. No correlation between Hg and TOC ($R^2 = 0.07$) was distinguished in the Hirnantian, although several positive anomalies were found. The elevated mercury values in the Hirnantian are not caused by anoxia/euxinia because pyrite framboids and euxinic biomarkers (maleimides and aryl isoprenoids) are absent or present in very low abundance. The lack of a strong Hg/TOC correlation, no Hg/TS correlation ($R^2 = 0.02$), Ni enrichments, and the absence of ‘anoxic indicators’ (no biomarkers, no framboids, low Mo concentration) support the interpretation that Hg enrichment is due to enhanced environmental loading (Smolarek-Lach et al. 2019). We conclude that our Hg and Hg/TOC values were associated with volcanic pulses which triggered the massive environmental changes resulting in the Late Ordovician mass extinction.

Acknowledgements. This work was supported by the NCN grant no. 2014/13/N/ST10/03006.

References

- Jones, D.S., Martini, A.M., Fike, D.A. & Kaiho, K. (2017). A volcanic trigger for the Late Ordovician mass extinction? Mercury data from south China and Laurentia. *Geology* 45, 631–634.
- Smolarek-Lach, J., Marynowski, L., Trela, W. & Wignall, P.B. (2019). Mercury Spikes Indicate a Volcanic Trigger for the Late Ordovician Mass Extinction Event: an Example from a Deep Shelf of the Peri-Baltic Region. *Scientific Reports (Nat. Publ. Group)*, 9, art. no. 3139, s. 1-11.



X-ray diffraction and photoelectron spectroscopy studies of chemically complex mineral chevkinite-(Ce)

Marcin STACHOWICZ¹

¹Institute of Geochemistry Mineralogy and Petrology, University of Warsaw, Żwirki i Wigury 93, 02-089 Warsaw, Poland; e-mail: marcin.stachowicz@chem.uw.edu.pl

The crystal structures of natural Nb-rich chevkinite-(Ce) with general formula $A_4BC_2D_2(Si_2O_7)_2O_8$, from the Biraya rare-metal deposit, Russia, crystallising in space groups $C2/m$ and $P2_1/a$, were solved and refined to $R_1=0.03$ and $R_1=0.07$, respectively, from data collected with a single-crystal diffractometer. Annealing at 750 °C of Nb-rich chevkinite-(Ce), resulted in the structural phase transition $C2/m \rightarrow P2_1/a$, which defines chevkinite crystal stability in different environments. This transformation seems to be a rapid version of a naturally occurring process that possibly involves twinning of the crystals. X-ray photoelectron spectroscopy was used to determine the oxidation states of the following ions: Ce^{3+} , Fe^{2+} and Fe^{3+} ; Ti^{4+} and Ti^{3+} . It is proposed that, in addition to the substitution ${}^CFe^{3+} + {}^DTi^{4+} \leftrightarrow {}^CFe^{2+} + {}^DNb^{5+}$, niobium can also be incorporated into chevkinite-(Ce) by the substitution $2{}^DTi^{4+} \leftrightarrow {}^DNb^{5+} + {}^DTi^{3+}$, leading to substantial Nb-enrichment. The use of complementary experimental techniques (electron probe microanalysis, X-ray diffraction, and photoelectron spectroscopy) has delivered information on the structure and transformation of a very complex, highly zoned and partially metamict solid solution. It should be useful in determining the structure of any mineral where cation disorder is present.

References

- Stachowicz, M., Bagiński, B., Welch, M.D., Kartashov, P.M., Macdonald, R., Balcerzak, J., Tyczkowski, J. & Woźniak, K. (2019). Cation ordering, valence states, and symmetry breaking in the crystal-chemically complex mineral chevkinite-(Ce): X-ray diffraction and photoelectron spectroscopy studies and mechanisms of Nb enrichment. *American Mineralogist*, 104, 595–602.



Detrital zircon provenance of volcano-sedimentary succession from the Kamieniec Metamorphic Belt (the Sudetes, SW Poland): preliminary data

Jacek SZCZEPAŃSKI¹, Robert ANCZKIEWICZ², Gabriela KASZUBA¹

¹*Institute of Geological Sciences, University of Wrocław, Plac Maksy Borny 9, Wrocław 50-204, Poland*

²*Institute of Geological Sciences, Polish Academy of Sciences, Research Centre in Kraków, Senacka 1, 31-002 Kraków, Poland*

We performed U-Pb laser ablation ICP-MS isotopic dating of detrital zircons from two samples representing supracrustal formation exposed in the Kamieniec Metamorphic Belt (the Sudetes, SW Poland). Detrital zircon grains from the metaryolite sample reveal one main age density peak at 0.509 Ga and small single peaks at 0.635 and 2.589 Ga. Zircons from the metapelite sample display one main density peak at 0.602, small peaks ranging from 0.77 to 1.024, and between 1.74 and 3.039 Ga and an isolated grain at 1.318. We interpret the main density peak documented in the metarhyolite at 0.509 Ga as indicating the age of felsic volcanism, while the youngest age cluster recognized in the metapelite sample at 0.602 Ga as pointing to a Neoproterozoic maximum depositional age of this rock. Importantly metapelite sample reveals also a few zircons of Grenvillian age. A distinctive feature of both investigated samples is the lack of Mesoproterozoic zircon grains.

Our results indicate that the volcano-sedimentary succession exposed in the Kamieniec Metamorphic Belt represents a Neoproterozoic sedimentary succession injected by Cambrian felsic volcanics. The whole succession has an affinity to the West African Craton of the Gondwana margin. This conclusion seems to be confirmed by negligible amount of zircons with Grenvillian ages documented in the studied samples and lack of zircons with Mesoproterozoic ages. Consequently, crystalline basement of the investigated part of the Fore-Sudetic Block represents fragment of the Saxothuringian zone and most probably forms the easternmost extension of the Saxothuringian terrane.

Acknowledgements. The study was supported from NCN research grant UMO-2015/17/B/ST10/02212.



P-T evolution of HP metapelites from the Kamieniec Metamorphic Belt, the Sudetes, SW Poland: evidence from raman spectroscopy of quartz inclusions in garnet and modelling of garnet zoning

Jacek SZCZEPAŃSKI¹, Xin ZHONG², Marcin DĄBROWSKI^{2,3}, Haozheng WANG⁴, Marcin GOLEŃ¹

¹*Institute of Geological Sciences, University of Wrocław, Plac Maksa Borna 9, Wrocław 50-204, Poland*

²*Physics of Geological Processes, The Njord Centre, University of Oslo, Norway*

³*Computational Geology Laboratory, Polish Geological Institute – National Research Institute, Wrocław, Poland*

⁴*Institute of Geology and Geophysics, China Academy of Sciences, Beijing, China*

HP lawsonite pseudomorph and chloritoid-bearing metapelitic rocks crop out in the the Kamieniec Metamorphic Belt (Sudetes, SW Poland). To characterize the metamorphic history of the studied mica schists we used a combined approach including phase diagram modelling and pressure estimates based on Raman spectra shifts of quartz inclusions in garnet. We conducted detailed study of two samples including: sample PK007 collected in the northern part of the study area in the vicinity of Stolec, and sample PK028 gathered in the southern part of the KMB in the vicinity of Kamieniec Ząbkowicki.

Peak metamorphic assemblages preserved in garnet porphyroblasts are identified and their PT conditions are constrained based on pseudosections produced by Theriak-Domino. For sample PK007 peak metamorphic assemblage consists of Grt1 + [Lws] + Cld + Ph + Pg + Mrg + Chl + Rt + Qz (P: 18-19 kbar, T: 450-470 °C), while for sample PK028 peak metamorphic assemblage comprise Grt + [Lws] + [Cpx] + Cld + Ph + Pg + Rt + Qz (P: 18-20 kbar, T: 500°C). Additionally, for sample PK007 retrograde mineral assemblage related to formation of garnet rims have been identified and comprise Grt2 + Ms + Bt + Pl2 + Chl + Ilm + Qz (P: 5-6 kbar, T: 540-550°C).

To better constrain the P-T history, especially for pressure, independent quartz-in-garnet Raman barometry is applied. About 37 and 65 quartz inclusions in garnet host have been identified with laser Raman spectroscopy for samples PK007 and PK028, respectively. The spectral shifts of three Raman bands at wavenumbers 128, 206 and 464 cm⁻¹ relative to a fully relaxed quartz crystal in the matrix are obtained. All three Raman bands yield very consistent residual pressure. Using the measured garnet composition and a 1D isotropic elastic model, the maximal entrapment pressure is determined to be 1.1 kbar and 15~16 kbar for samples PK007 and PK028, respectively. The entrapment temperature is chosen to be 500 °C but it does not significantly influence the estimated entrapment pressure.

Peak metamorphic assemblages and PT estimates suggest tectonic stacking during Variscan collision, while preserved retrograde assemblage is a record of exhumation most probably during ongoing collision.

Acknowledgements. The study was supported from NCN research grant UMO-2015/17/B/ST10/02212.



First data on mantle xenoliths from Befang (Oku Massif) in the Cameroon Volcanic Line

Sylvin S. T. TEDONKENFACK¹, Jacek PUZIEWICZ¹, Theodoros NTAFLIS², Sonja AULBACH³, Anna KUKUŁA⁴, Magdalena MATUSIAK-MAŁEK¹, Małgorzata ZIOBRO¹

¹Institute of Geological Sciences, University of Wrocław, Pl. Maksa Borna 9, 50-204 Wrocław, Poland
e-mail: jacek.puziewicz@uwr.edu.pl

²Department of Lithospheric Research, University of Vienna, Althanstraße 14, 1090 Vienna, Austria

³Institut für Geowissenschaften, Goethe University, Altenhöferallee 1, 60438 Frankfurt am Main, Germany

⁴Institute of Geological Sciences, Polish Academy of Sciences, ul. Twarda 51/55, 00-818 Warszawa, Poland

Cameroon Volcanic Line (CVL) is a ca. 1600 km long Cenozoic volcanic chain which crosses the boundary between ocean and continent in West Africa. Its origin is still a matter of debate, as is the nature and age of the underlying continental lithospheric mantle (CLM). Some of the CVL lavas contain peridotite xenoliths that help elucidate the role of the CLM in the sustained magma generation along the line. In this abstract we describe xenoliths from Befang pyroclastic cone (< 1Ma) in the Oku Massif in the continental CVL.

Peridotite xenoliths (8 spinel lherzolites, one spinel harzburgite) are between 5 and 21 cm in diameter and have protogranular texture. Olivine is Fo 89.2-90.1 (lherzolites), and 90.3 (harzburgite), it contains 0.36 to 0.42 wt.% NiO. Orthopyroxene has Mg# 0.89-0.91, its Al content is 0.16-0.18 atoms per formula unit (a pfu) in lherzolites and 0.14-0.16 in harzburgite. Clinopyroxene is characterised by Mg# 0.90 - 0.92 and contains 0.24-0.31 a pfu of Al. The Cr# of lherzolite spinel is 0.09-0.15, in the harzburgitic one it is 0.18-0.19. Clinopyroxene occurring in harzburgite and in 5 lherzolites is LREE-depleted ($La_N/Lu_N = 0.26-0.50$), while the remaining lherzolites contain LREE-enriched clinopyroxene ($La_N/Lu_N = 1.36-2.65$). Pyroxenes in all studied rocks record a narrow temperature range of 940 – 985°C (geothermometer of Brey, Köhler 1990), suggesting sampling of a narrow depth interval and highlighting small-scale heterogeneity of the CLM.

Our preliminary data show that the Befang xenoliths represent three mantle spinel peridotite associations: (1) harzburgites recording low degrees (few percent) of melting of DMM (Depleted MORB Mantle); (2) lherzolites metasomatised by melts produced by low-degree melting of DMM, and (3) lherzolites affected by cryptic metasomatism leading to LREE-enrichment.

Acknowledgements. The study was funded by Polish National Centre for Science project UMO-2017/27/B/ST10/00365 to JP. EPMA analyses were done thanks to the Polish-Austrian project WTZ PL 08/2018.

References:

Brey, G.P. & Köhler, T. (1990). Geothermobarometry in four-phase lherzolites II. New thermobarometers and practical assessment of existing thermobarometers. *Journal of Petrology*, 31, 1353-1378.



Micro-Raman spectroscopy of experimentally altered monazite and xenotime

Fabian TRAMM¹, Grzegorz RZEPA², Bartosz BUDZYŃ¹, Gabriela A. KOZUB-BUDZYŃ²

¹*Institute of Geological Sciences, Polish Academy of Sciences (ING PAN), Research Centre in Kraków, Senacka 1, PL–31002 Kraków, Poland; ndrtramm@cyf-kr.edu.pl*

²*AGH University of Science and Technology, Faculty of Geology, Geophysics and Environmental Protection, al. Mickiewicza 30, PL–30059 Kraków, Poland*

Monazite and xenotime are well known U-(Th-)Pb geochronometers used for dating igneous and metamorphic processes. Because both minerals can be altered via fluid-mineral reactions resulting in re-equilibration, it is important to recognize altered domains to avoid geochronological misinterpretations. The micro-Raman spectroscopy provides compositional and structural information, which may supplement commonly used EPMA and LA-ICP-MS methods. However, the availability of monazite and xenotime spectra is limited.

The current study evaluates monazite and xenotime from experiments of Budzyń et al. (2017) by using micro-Raman spectroscopy and EPMA measurements. These will provide data to constrain effects of structural state (radiation damage) and chemical composition (incorporation of non-formula elements) on the features of Raman bands of monazite and xenotime experimentally altered under known P-T conditions, which is commonly difficult (or impossible) to constrain in nature.

Preliminary data have shown good quality Raman spectra of monazite and xenotime within consistent variation in unaltered monazite and xenotime. The spectra, however, show significant differences compared to those for Gd-orthophosphates (Clavier et al., 2018) regarding number of peaks, peak positions, shape and intensities. The project is in progress and future micro-Raman analysis will provide a more detailed insight in the structure of unaltered and altered monazite and xenotime. The resulting Raman spectra database will serve as reference for future geochronological studies on monazite and xenotime, supported by micro-Raman spectroscopy.

Acknowledgements. The project was funded by the National Science Centre of Poland, grant no. 2017/27/B/ST10/00813.

References

- Budzyń, B., Harlov, D.E., Kozub-Budzyń, G.A. & Majka, J. (2017). Experimental constraints on the relative stabilities of the two systems monazite-(Ce) – allanite-(Ce) – fluorapatite and xenotime-(Y) – (Y,HREE)-rich epidote – (Y,HREE)-rich fluorapatite, in high Ca and Na-Ca environments under P-T conditions of 200–1000 MPa and 450–750 °C. *Mineralogy and Petrology*, *111*, 183-217.
- Clavier, N., Mesbah, A., Szenknect, S. & Dacheux, N. (2018). Monazite, rhabdophane, xenotime & churchite: Vibrational spectroscopy of gadolinium phosphate polymorphs. *Spectrochimica Acta Part A: Molecular and Bio-molecular Spectroscopy*, *205*, 85-94



First geochronological evidence for the Finnmarkian orogenic event in the central Scandinavian Caledonides

Katarzyna WALCZAK¹, Jarosław MAJKA^{1,2}, David G. GEE², Iwona KLONOWSKA^{1,2,3}, Christopher BARNES¹

¹ Faculty of Geology, Geophysics and Environmental Protection, AGH University of Science and Technology, al. Mickiewicza 30, 30-052 Kraków, Poland e-mail:kwalczak@agh.edu.pl

² Department of Earth Sciences University of Uppsala, Villavägen 16, 752-36 Uppsala, Swede

³ Department of Earth Sciences, Syracuse University, 204 Heroy Geology Laboratory, Syracuse NY, USA

Scandinavian Caledonides represent an orogen dominated by a nappe stack of far-travelled allochthons (e.g. Gee et al. 2014). Some of these allochthons bear an unequivocal record of deep subduction of the Baltoscandian margin connected to the closure of Iapetus. The Seve Nappe Complex represents a deeply subducted portion of the Baltoscandian rifted margin. The earliest of the deep subduction events is traditionally called the Finnmarkian orogenic phase and has been dated to ca. 500-480 Ma, and it is recognized in the northernmost part of the mountain belt only (approximately north of the Arctic Circle). Farther south, in the central and southern segments of the orogen, (ultra)high-pressure ((U)HP) rocks yield younger ages in the range of ca. 460-440 Ma. This spatially-anchored diachronous age pattern has been a matter of a long-lasting debate.

Here, we present the first geochronological evidence for the Finnmarkian orogenic event from an UHP diamond-bearing gneiss at Tväråklumparna in the central Scandinavian Caledonides (Majka et al. 2014). The ²⁰⁶Pb/²³⁸U age and trace elements patterns, obtained by means of depth profiling of detrital zircon rimmed by metamorphic overgrowths, suggest the first subduction-related zircon rim growth already at ca. 500 Ma followed by more massive formation of another population of metamorphic zircon rim at ca. 450 Ma. Based on these results, we propose that the entire outer margin of Baltica was involved in the Finnmarkian orogeny, but a record of this event may have been (nearly) erased in the vast majority of lithologies by the later pervasive (U)HP event at ca. 460-440 Ma.

Acknowledgements. This research was supported by the NCN research project no. 2014/14/E/ST10/00321.

References

- Gee D.G., Ladenberger A., Dahlqvist P., Majka J., Be'eri-Shlevin Y., Frei D. & Thomsen T. (2014). The Baltoscandian margin detrital zircon signatures of the central Scandes. Geological Society, London, Special Publications, 390, 131–155.
- Majka J., Rosén Å., Janák M., Froitzheim N., Klonowska I., Manecki M., Sasinková V. & Yoshida K. (2014). Microdiamond discovered in the Seve Nappe (Scandinavian Caledonides) and its exhumation by the “vacuum-cleaner” mechanism. *Geology*, 42, 1107–1110.



Bioweathering processes of the Cretaceous joint sandstones from the North-Sudetic Basin

Katarzyna ZBOIŃSKA^{1,2}, Anna POTYSZ¹, Wojciech BARTZ¹, Felix SCHMIDT³, Markus LENZ^{3,4}

¹Institute of Geological Sciences, University of Wrocław, pl. M. Borna 9, 50-204 Wrocław, Poland;
e-mail: katarzyna.zboinska@uwr.edu.pl, anna.potysz@uwr.edu.pl, wojciech.bartz@uwr.edu.pl

²Polish Geological Institute – National Research Institute, Lower Silesian Branch, al. Jaworowa 19, 53-122 Wrocław, Poland

³Institute for Ecopreneurship, School of Life Sciences, University of Applied Sciences and Arts Northwestern Switzerland, Switzerland

⁴Sub-Department of Environmental Technology, Wageningen University, 6700 AA, Wageningen, The Netherlands

Sandstone has been widely used as a building material for centuries. The durability of architectural details made of them was influenced by various external factors, affecting the rate of physical, chemical and biological weathering. The described studies focus on the bioweathering of Cretaceous sandstones from the North Sudetic Basin (Lower Silesia, SW Poland) upon contact with the bacteria *Acidithiobacillus thiooxidans*, water and acidic control solution. The experiment was designed to enable the analysis of the sandstones' behaviour in a long-term exposure to microorganisms and acidic conditions.

Three types of sandstones were subjected to the experiment: the lower joint sandstone from Lwówek Śląski (Cenomanian), the middle joint sandstone from Plakowice (Turonian) and the upper joint sandstone from Żerkowice (Conacian). All types of sandstones were examined for 86 days and then analyzed using scanning electron microscopy (SEM-EDS) and triple quadrupole inductively coupled plasma mass spectrometry (QQQ-ICP-MS).

The studies allow to confirm the research hypothesis suggesting bioleaching as a process intensifying the deterioration of sandstones. Bioleaching had a particularly strong effect on the minerals included in the cement in the studied sandstones: clay minerals and goethite. Based on the example of bioleaching of ferruginous binder, it can be seen that the weathering in biological conditions was as much as 26 times greater than in the case of the least aggressive weathering conditions. In addition, in samples exposed to bacteria new mineral phases associated with accumulations of clay minerals (kaolinite) had developed. During the experiment, significant changes were also noted in the pH value of the samples with bacteria in relation to the relatively stable pH of the reference samples with distilled water.



REE minerals in the cassiterite processing tailings from Indonesian Tin Islands

Karol ZGLINICKI¹, Gustaw KONOPKA¹, Krzysztof SZAMAŁEK¹

¹The Polish Geological Institute – National Research Institute, 4 Rakowiecka Street, 00-975 Warsaw, Poland; e-mail: karol.zglinicki@pgi.gov.pl, gustaw.konopka@gmail.com, krzysztof.szamalek@pgi.gov.pl

The Bangka, Belitung and Singkep Islands are the final, southern fragment of the Southeast Asian Tin Belt, extending from Burma and Thailand to Peninsular Malaysia. In the effect of tectonic evolution, three granite provinces have formed with a different geochemical and petrographic indicators (Schwartz et al. 1995). Granitoids are composed of feldspar, plagioclase, quartz, biotite, hornblende as well as accessory minerals: apatite, titanite, allanite, monazite, xenotime, zircon and others. Granitic magmatism was closely connected to hydrothermal and metasomatic processes, which led to a rich tin mineralization. The intensive weathering processes in tropical conditions from Neogene to the present day have led to the formation of rich cassiterite placer deposits. Artisanal extraction of cassiterite-bearing sands lead to a significant amount of tailing waste accumulated in numerous dumps (Szamałek et al. 2013). As part of prospecting works conducted by a team of Polish geologists, the potential of the tailing deposit was defined. Thirty-five samples of waste from the processing of cassiterite sands were collected. In the tailing samples, economic accumulation of zirconium (up to 84.43 wt.%), monazite (up to 90.60 wt.%) and xenotime (up to 17.20 wt.%) was found. The analyzed material revealed the presence of previously unknown REE phases. EPMA analyses indicate the presence of euxenite group minerals – Y-Ti-W-HREE-Nb. The discovered phases are currently the subject of intensive studies in order to determine the crystallographic structure, chemical composition and physicochemical properties.

References:

- Schwartz, M.O., Rajah, S.S., Askury, A.K., Putthapiban, P. & Djaswadi, S. (1995). The Southeast Asian Tin Belt. *Earth Science Reviews*, 38, 95-293.
- Szamałek, K., Gustaw, K., Zglinicki, K. & Marciniak-Maliszewska, B. (2013). New potential source of rare earth elements. *Gospodarka Surowcami Mineralnymi*, 29(4), 59-76.



Chemical (U-Th-Pb) dating of monazite: standards and application

Grzegorz ZIELIŃSKI¹, Petras JOKUBAUSKAS², Ewa KRZEMIŃSKA¹, Dominik GURBA¹, Paweł DERKOWSKI¹

¹ Micro-area Analysis Laboratory, Polish Geological Institute – National Research Institute, 4 Rakowiecka St., 00-975 Warszawa, Poland; e-mail: grzegorz.zielinski@pgi.gov.pl

² Electron Microprobe Laboratory Joint-Institute Analytical Complex for Minerals and Synthetic Substances University of Warsaw Faculty of Geology, 93 Żwirki i Wigury; 02-089 Warszawa, Poland; e-mail: p.jokubauskas@uw.edu.pl

Standards with well-defined and contrasting ages are routinely used to verify: the accuracy of calibration, quality of data reduction, analytical precision and finally the reliability of chemical dating of each regular sample. The analytical procedures for the chemical dating of monazite, independently set for two Cameca (SX100 and SXFiveFE) electron microprobes (EPMA), have been tested at PGI-NRI and at the Faculty of Geology labs in Warsaw.

A few natural reference monazite standards have been analyzed together with monazite samples as single grain mono-mineral mounts or in situ thin sections. External standards such as 44069 (425 Ma), Thompson Mine (1766 Ma), Moacyr (504 Ma), Namaqualand, South Africa (1040 Ma) were analyzed during several sessions. The results are listed in Table 1. Moreover the chemical ages of monazite grains from the granitogneiss of Prabuty IG-1 and the sillimanite gneiss of Michałowo 1 obtained by EMPA are compared with isotopic ages determined from the same rock samples by the SHRIMP isotopic technique.

Table 1. A comparison of reference age versus chemical Th-U Pb_{total} monazite age, calculated as a weighted average from single regular analytical sessions on EMP; ¹ - SX100, ² - SXFiveFE

Monazite name	TIMS/SIMS Ref. age (Ma)	EPMA Cameca Mean weight (Ma)	Number of analysis	MSWD
Moacyr ¹	504.3 ±0.2	510 ±18	N =23	0.032
44069 ¹	425	415 ±37	N =22	0.065
Thompson Mine ¹	1766	1765 ±59	N =10	0.0094
Namaqualand, South Africa, NMQL ²	(1062) 1045*	1041 ±25	N =21	0.100
Iveland, Norway ¹	903.6 ±1.4	902 ±54	N =8	0.096
Petaca, New Mexico ¹	1425	1425 ±63	N =6	0,094
Prabuty, NE Poland ²	1472 ±9	1469 ±10	N =151	0.12

Despite the lower precision (2-8%) of dates obtained by EPMA on external monazite standards compared to the ID-TIMS (0.5-1%) or SIMS reference data, the results are consistent and accurate but compositional homogeneity has to be controlled by of pre-analysis, high-resolution, chemical maps for U, Th, and Y for each pre-selected monazite grain and external standard.



Retrograde monazite records Early Devonian sinistral strike-slip shearing in the Müllernesset Formation, SW Svalbard

Grzegorz ZIEMNIAK¹, Jarosław MAJKA^{1,2}, Maciej MANECKI¹, Katarzyna WALCZAK¹, Karolina KOŚMIŃSKA¹

¹Faculty of Geology, Geophysics and Environmental Protection, AGH University of Science and Technology, al. Mickiewicza 30, 30-052 Kraków, Poland e-mail: ziemniak.grzegorz@gmail.com

²Department of Earth Sciences, Uppsala University, Villavägen 16, 752-36 Uppsala, Sweden

The breakdown of allanite resulting in monazite growth is a common case in metapelites during the prograde metamorphism, but only a few examples of the same reaction during retrogression has been documented (e.g. Bollinger, Janots 2006). Here, the formation of monazite during retrogressive metamorphism is recorded in the Müllernesset Formation of the Southwestern Basement Province of Svalbard.

The Müllernesset Formation consists of Mesoproterozoic to Neoproterozoic metapelites and metapsammites metamorphosed under amphibolite facies conditions. The amphibolite facies event M1 was followed by the retrogressive event M2 characterized by the mylonitic S2 foliation dipping steeply to SW. Stretching biotite-dominant L2 lineation is dipping moderately-to-shallowly to SE. Observed asymmetric pressure shadows around garnet and stacked porphyroblasts indicate sinistral sense of shear during M2. Retrograde monazite forms tiny blasts (<20µm) surrounding allanite aggregates. It grows within the S2 foliation and shear bands. Th-U-total Pb dating of monazite revealed homogenous population of single spot model dates (n=15) that yield a weighted average age of 410 ±7Ma with MSWD =0.26 and p =0.997. The age is almost identical with 410 ±2Ma ⁴⁰Ar/³⁹Ar cooling age of muscovite reported from the Müllernesset Formation by Dallmeyer (1989).

Petrological observations and coeval formation of monazite and muscovite cooling ages suggest that Early Devonian fast tectonic uplift occurred during a sinistral strike to oblique slip. Late-Caledonian shearing documented in the Müllernesset Formation is another line of evidence advocating for existence of anastomosing set of shear zones within the Southwestern Basement Province and for escape tectonics as a major mechanism of Svalbard assembly.

Acknowledgements. This work is partially funded by NCN research project no. 2015/17/B/ST10/03114, AGH statutory funds 11.11.140.158, AGH research grant 15.11.140.274 and RCN Arctic Field Grant no. 282546.

References

- Dallmeyer, R. D. (1989). Partial thermal resetting of ⁴⁰Ar/³⁹Ar mineral ages in western Spitsbergen, Svalbard: possible evidence for Tertiary metamorphism. *Geological Magazine*, 126(5), 587-593.
- Bollinger, L. & Janots, E. (2006). Evidence for Mio-Pliocene retrograde monazite in the Lesser Himalaya, far western Nepal. *European Journal of Mineralogy*, 18(3), 289-297.



Preliminary data on lithospheric mantle underlying Mid-German Crystalline High Variscan unit: Breitenborn (Vogelsberg) case study

Małgorzata ZIOBRO¹, Jacek PUZIEWICZ¹, Theodoros NTAFLOS², Sonja AULBACH³, Magdalena MATUSIAK-MAŁEK¹

¹*Institute of Geological Sciences, University of Wrocław, Pl. Maksa Borna 9, 50-204 Wrocław, Poland
e-mail: malgorzata.ziobro@uwr.edu.pl*

²*Department of Lithospheric Research, University of Vienna, Althanstraße 14, 1090 Vienna, Austria*

³*Institut für Geowissenschaften, Goethe University, Altenhöferallee 1, 60438 Frankfurt am Main, Germany*

The Cenozoic volcanic field of Vogelsberg (part of CEVP in Central Germany) is located at the northern extension of the Upper Rhine Graben. Three Variscan basement units underlie Vogelsberg from NW to SE: the Rheno-Hercynian Zone, the Northern Phyllite Zone and the Mid-German Crystalline High. Xenoliths from the Breitenborn basanite sample lithospheric mantle (LM) beneath the Mid-German Crystalline High. This study is a part of broader research of LM beneath Vogelsberg.

The Breitenborn suite comprises xenoliths of 3-7.5 cm in diameter: clinopyroxene-poor spinel lherzolites and spinel harzburgites. Peridotites exhibit different degrees of deformation including foliation, grain size reduction and porphyroclastic textures. Mineral components are chemically homogeneous at the grain and xenolith scale. Forsterite content (Fo) in olivine ranges between 89.8 and 91.5% with exception of Fo ~89.0% in one xenolith. Orthopyroxene (opx) is characterized by Mg# of 0.900-0.923, and 0.06-0.18 atoms of Al pfu, whereas clinopyroxene (cpx) by Mg# of 0.894-0.931 and 0.11-0.23 atoms of Al pfu. Spinel (spl) Cr# ranges from 0.18 to 0.45. Positive correlation occurs between Al content in opx and cpx, whereas spl Al content shows no correlation with those of pyroxenes. In most rocks, cpx REE patterns exhibit different degree of enrichment in LREE. Cpx from xenolith 3918 is significantly distinct, having pattern almost flat from Lu to Sm and strongly depleted in lighter REE. Opx from the same xenolith exhibits pattern steeply depleted from HREE to LREE. Rest of opx shows rather mild depletion in LREE relative to HREE.

Similar as in other xenolith suites from the area, mineral major element variations have no correlation with the trace element ones. LREE-enriched cpx patterns suggest metasomatic alteration of LM by alkaline melts, which is typical of other studied sites in Vogelsberg. In contrast, a calculated hypothetical melt in equilibrium with cpx 3918 pattern resembles those of tholeiites occurring in Vogelsberg, testifying to the diversity of melts interacting with the LM during extension.

Acknowledgements. The study was funded by Polish National Centre for Science to MZ (project UMO-2018/29/N/ST10/00259). EPMA analyses were done within the frame of the Polish-Austrian project WTZ PL 08/2018. MZ acknowledges the DAAD fellowship at the Goethe University in Frankfurt.

**XXVIth Meeting of the Petrology Group
of the Mineralogical Society of Poland**

**Hydrothermal and magmatic processes
in the Holy Cross Mountains**

Field trip guide



STOP 1: Miedzianka deposit – one of the oldest mining centres in Poland

Rafał SIUDA¹, Justyna DOMAŃSKA-SIUDA¹

¹*Faculty of Geology, Warsaw University, Żwirki i Wigury 93, 02-089 Warsaw, Poland;
e-mail: siuda@uw.edu.pl; j.domanska@uw.edu.pl*

Introduction

The Miedzianka deposit is one of the most interesting geological features of the Holy Cross Mountains. It is characterized by a very complex geological structure and a rich mineral assemblage. Its centuries-old exploitation record is related to the history of Poland. For over 200 years geological and mineralogical studies have been performed in the deposit. It also represents a place where geology students from many scientific institutions in Poland get their feet wet.

History of the mining activity

In the Holy Cross Mountains the mining of metal ores has a very rich tradition. During the period of Roman influence in central Poland (with the Holy Cross Mountains included) the area was occupied by the Przeworsk culture (related to the Germanic Vandals). One of the most important features of this culture was their perfect development of iron metallurgy. This metal, and Baltic amber, were the main „export products” to the Roman Empire. In the Holy Cross Mountains iron was smelted mainly using bog ore but in Rudki near Nowa Słupia (about 40 km from Miedzianka) an underground mine of iron ore (I – III century AD) existed. Hematite exploitation was carried out using a set of shafts and adits. The exploitation reached down to ca. 40 m (Bielenin 2002). The people of the Przeworsk culture also exploited copper ore in Miedzianka. This may be certified by a find of Roman coins in old mining galleries, at the beginning of the XX century (Fijałkowska, Fijałkowski 1976). Expulsion of the Vandals by Germanic peoples and the migration of various nations led to the termination of copper ore exploitation in Miedzianka about the III century AD. Activity was again undertaken in the Middle Ages. Most likely it began in the XIV century, as the first mentions of lead and other metal ores exploited in the vicinity of Chęciny come from the year 1306. In 1497 a privilege was issued by Polish king Kazimierz Jagiellończyk to a mine manager, Jan Karaś. The privilege mentions a copper ore smelter, the ore coming from Miedzianka. A description of the Chęciny of 1569 reports that not only copper ores (with an elevated content of silver) were exploited in Miedzianka. The raw materials acquired also included malachite and azurite, finding use especially in pigment production. The description’s author also pays attention to a downturn of local mining activity. A recurrence of the exploitation is related to a construction of a drainage adit in the beginning of the XVII century (the year of 1602). The main investor in this enterprise was Polish king Zygmunt III Waza. Unfortunately, the adit collapsed not soon after, and ore exploitation ceased again. The workings were reopened for a short period during the kingship of Jan III Sobieski. A further reopening took place in the mid-XVIII century during the kingship of August III Sas. Dembiński, a governor at that time, employed 12 miners from Hungary. Unfortunately, in view of unfavourable geological conditions the works were closed down after a few years. At the time of the kingship of Stanisław August Poniatowski the Miedzianka deposit

raised the interest of German mineralogist Jan Filip Carosi. He noticed relicts of old mining and positively commented on the possibility of local copper ore gaining. After the partitionings of Poland and formation of the Kingdom of Poland, exploitation was restarted (1817-1821). It was led by the „father of Polish geology”, Stanisław Staszic. The amount of ore produced was low and the mine workings turned out to be loss-making. At that time the first Polish mining school (Mining Academy also known as Academic-Mining School) was established in nearby Kielce. One of its professors, Georg Gottlieb Pusch, was the first to characterize the minerals occurring at Miedzianka. After almost 100 years, mining was reopened at the beginning of the XX century. It was led by Stanisław and Bolesław Łaszczyński. They were the first in the world to develop the technology of electrolytic copper production (Paulewicz 1992). The mining works were kept running until World War I when they were taken over by occupying Austrian authorities. Under Austrian management 4 km of mine galleries were excavated. The then-exploited ore contained some silver. After World War I the two Łaszczyńskis resumed exploitation.. However, due to the scarcity of ore the mine was closed already in 1919. Starting in 1949 Miedzianka was again a place of some exploration work. A new shaft, 60 m deep, represents what was then executed. Also, the total length of mine galleries then formed reached 3 km. During this work about 40 tons of copper ore were mined, the ores having a mean Cu content of 5%. In the end, in view of the exhaustion of the deposit, the mine was closed in 1954.

Geology

The Miedzianka deposit is situated in the southern part of the Chęciny anticline. The deposit is located between the Miedzianka Hill and a village of the same name. The Hill is built of Devonian (Fransian and Famenian) limestones (Szulczewski 1995; Dzik 2006). In the NE part the limestone rocks have a tectonic contact with Lower Cambrian sediments. In the NW part of the Miedzianka Hill, Upper Permian conglomerates are exposed. At the SW side the limestones contact Triassic sediments (sandstones and clays) (Fig. 1).

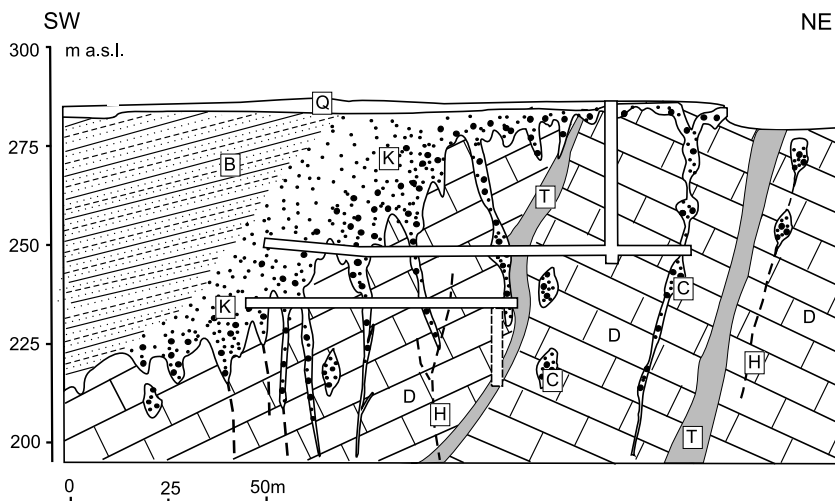


Fig. 1. Geological cross-section across the main exploitation ore field of the Miedzianka deposit (D – Devonian limestones, B – Triassic Buntsandstein sandstone, Q – Quaternary sediments, K – karst zone with secondary copper mineralization, C – caves with copper ore, H – hydrothermal ore veins, T – fault zones with clay minerals). Cross-section after Rubinowski (1971), modified.

Primary hydrothermal mineralization

Calcite veins bearing hydrothermal ore mineralization occur in the Devonian limestones, exclusively. The ore veins use cracks that run parallel to the Chęciny Anticline (NW-SE course). Expressions of mineralization within the younger, NE-SW trending, crack system, are lacking. The dip of the veins is almost vertical. Their length reaches as much as 100 metres and their thickness is from 1 to a dozen or so centimetres. The oldest vein generation is represented by a monomineralic ore-devoid calcite mineralization (Rubinowski 1971). A further generation of calcite veins bears sulfides and sulfosalts. Based on the mineral compositions, three types of ore veins can be distinguished: tennantite-, chalcopyrite- and galena-bearing (Balcerzaki et al. 1992). In the first type the typomorphic mineral is tennantite with an elevated zinc amount (up to 5 wt.% Zn). In the older literature it occurs under the name of "miedziankite". The mineral usually occurs as finely-crystalline aggregates, up to a few cm in diameter. Sometimes also very tiny (up to 0.7 mm) automorphic crystals of this mineral are found growing in calcite (Rubinowski 1971). Evidence of calcite replacing tennantite is not rare. The tennantite coexists with chalcopyrite that usually forms inclusions in the former. The next ore mineral occurring in this kind of vein is gersdorffite. It forms small, grains up to 0.1 mm in diameter. They stick in tennantite, chalcopyrite, or calcite. The aforementioned ore minerals are locally associated with tiny inclusions of galena. The second-type veins have chalcopyrite as the dominant species. It usually forms massive aggregates, up to a few cms in diameter. Automorphic crystals of this mineral are sometimes also found and they reach 0.5 cm in diameter. They grow in calcite. Chalcopyrite is associated with variable amounts of tennantite, galena, gersdorffite, and pyrite. The third-type veins mainly comprise galena, aggregates of which may be a dozen or so cms in size. Galena bears scattered, tiny segregations of chalcopyrite, bornite-I, and sphalerite. The dominant barren mineral in all the vein types is calcite. It sometimes coexists with aggregates of white to pinkish baryte, up to few cms in diameter. Quartz, in the form of tiny (up to do 2-3 mm) transparent crystals, is much rarer. The hydrothermal veins also contain aggregates of covellite, chalcocite, and bornite-II. These minerals arise due to the weathering of the former copper sulfides and sulfosalts. Copper minerals of the hydrothermal veins were formerly under exploitation as so-called vein ores. Their part in the total ore production seems to be subordinate.

Secondary mineralization

Due to karstic processes the Miedzianka limestones were cut by a set of caves and sinkholes. In silt-covered areas of these formations weathered debris of the hydrothermal veins was deposited (Fig. 2a). These ore fragments already contained secondary Cu sulfides (chalcocite, digenite, covellite, bornite-II) and malachite (Rubinowski 1971). However, secondary copper sulfides, mainly chalcocite, were also formed within the silts filling the karst formations. The accumulations could reach a mass of several dozen tons (Rubinowski 1958). Copper ions mobilized during the primary sulfide mineralization weathering were carried away from the limestones with ground waters and were absorbed at the contact between the Devonian limestones and the Triassic sediments (Rubinowski 1955). There the so-called contact ores were formed, comprising Triassic clays and sandstones impregnated by copper carbonates (Fig. 2b).

The most diverse parageneses of the weathering minerals occur above the secondary copper sulfides precipitation zone. There, a set of secondary minerals occurs, being mainly represented by copper carbonates and arsenates. The most common representative of the first group is malachite. It usually forms earthy cryptocrystalline aggregates with mass reaching several dozen of kgs. Malachite also forms flowstone-like, dark green aggregates. This type of malachite may have been used for pigment production. The last variety of malachite occurs as rounded aggregates, up to 2 cms in diameter. Malachite-after-azurite pseudomorphs are

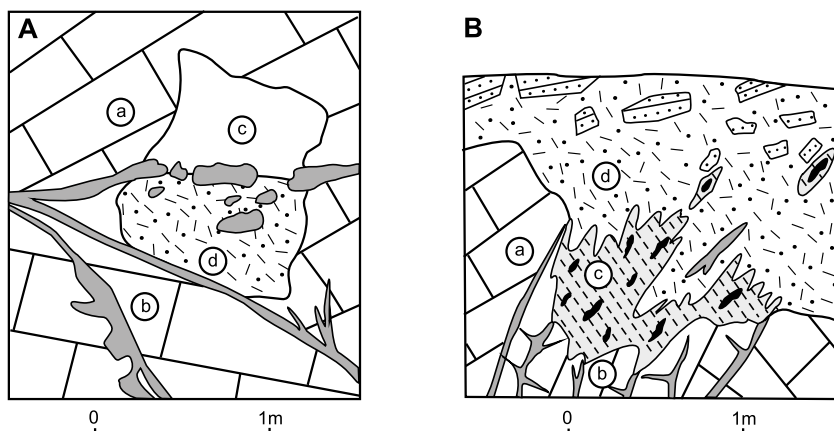


Fig. 1. Geological cross-section across the main exploitation ore field of the Miedzianka deposit (D – Devonian limestones, B – Triassic Buntsandstein sandstone, Q – Quaternary sediments, K – karst zone with secondary copper mineralization, C – caves with copper ore, H – hydrothermal ore veins, T – fault zones with clay minerals). Cross-section after Rubinowski (1971), modified.

very common (Łaskiewicz 1928). The malachite-associated azurite usually forms small, up to several mm long crystals with a very rich morphology (Łaskiewicz 1928). They are, indeed, usually replaced by malachite. However, both malachite and azurite may be replaced by chrysocolla. This mineral is also found as botryoidal aggregates, up to a dozen or so cms in size. Arsenates are often represented by conichalcite. It forms green encrustations on the surfaces of fractured Devonian limestones. One may also find botryoidal and dripstone-like aggregates of this mineral occurring in voids in the earthy malachite. They are otherwise found at surfaces of druzey malachite and azurite crystals. Conichalcite also forms green coatings on the surfaces of weathering-undergoing galena. There it coexists with green aggregates of duftite that reach 0.2 cm in diameter. Also olivenite may be found associated with olivenite. (TWO olivenites!) It forms botryoidal crusts comprising very tiny crystals (up to 0.3 cm in diameter). Olivenite also occurs as veinlets cutting strongly weathered tennantite. A much more rarely found arsenate is tyrolite (Wieser, Żabiński 1986). It usually forms radiating aggregates of a diameter reaching a few cms. They fill cracks cutting yellow-green, porous malachite. Austinite is also a rare arsenate at Miedzianka. Its rounded aggregates (up to 0.3 cm in diameter) may sometimes be found as larger assemblages, a dozen or so cms large. Secondary Cu phosphates also exist in Miedzianka. They are represented by hentschelite and pseudomalachite. This is also true for hydrous Cu sulfates – antlerite and brochantite (Bzowska et al. 2003; Wisser, Żabiński 1986). The subsurface part of the deposit is where variable amounts of tenorite, cuprite and native copper were found (Wojciechowski 1958). Karwowski (2009) has determined cuprite and native copper to be associated with small amounts of marshite. Weathering of galena of the primary mineralization led to the formation of a set of secondary lead minerals. The most common is cerussite. Sometimes, the surfaces of decomposed galena are covered by prisms of mimetite and pyromorphite, and rounded aggregates of duftite. In the Miedzianka deposit weathering zone small amounts of gold were also described. They occur within limonite (Balcerzak et al. 1992; Kozłowski 2011).

References

- Bielenin, K. (2002). Kilka dalszych uwag dotyczących starożytnego hutnictwa świętokrzyskiego [Some further notes regarding ancient Holy Cross metallurgy]. [In:] *Hutnictwo świętokrzyskie oraz inne centra i ośrodki starożytnej metalurgii na ziemiach polskich* [Holy Cross metallurgy and other centres and stations of ancient metallurgy in Poland]. Akademia Świętokrzyska, Kielce, 197-216 [in Polish].
- Balcerzak, E., Nejbert, K. & Olszyński, W. (1992). Nowe dane o paragenezach kruszcowych w żyłach siarczków pierwotnych złoża Miedzianka (Góry Świętokrzyskie) [New data on ore parageneses in primary sulfide veins of Miedzianka deposit (Holy Cross Mountains)]. *Przegląd Geologiczny*, 11, 659-663 [in Polish].
- Bzowska, G., Karwowski, Ł. & Juzaszek, A. (2003). New phosphate and arsenate minerals from Miedzianka near Chęciny (Holy Cross Mts). *Mineralogical Society of Poland Special Papers*, 22, 25-29.
- Fijałkowska, E. & Fijałkowski, J. (1976). Historia eksploatacji kruszców na Miedziance [The history of ore exploitation at Miedzianka]. *Informator Towarzystwa Przyjaciół Górnictwa, Hutnictwa i Przemysłu Staropolskiego w Kielcach*, 1-43 [in Polish].
- Karwowski, Ł. (2009). Marshite—copper iodide from Miedzianka in the Holy Cross Mts. *Mineralogia Special Papers*, 35, 89.
- Kozłowski, A. (2011) Native gold from Miedzianka Mountain, Świętokrzyskie Mts. Gold in Poland, *Archivum Mineralogiae*, 2, 339-349.
- Łaskiewicz, A. (1928). Morfologia azurytów Łysogórskich [Morphology of the Łyse Góry azurites]. *Archiwum Mineralogiczne*, 3, 129-158 [in Polish].
- Paulewicz, M. (1992). Chęcińskie górnictwo kruszcowe (XIV do połowy XVII wieku) [The Chęciny ore mining (XIV to mid-XVII century)]. Eds: *Kieleckie Towarzystwo Naukowe*, 1-152 [in Polish].
- Rubinowski, Z. (1955). Nowe obserwacje okruszcowania na Miedziance Świętokrzyskiej [New observations of mineralization in Holy-Cross Miedzianka]. *Przegląd Geologiczny*, 6, 299-301 [in Polish].
- Rubinowski, Z. (1958). Wyniki badań geologicznych w okolicy Miedzianki Świętokrzyskiej [Results of research around Holy-Cross Miedzianka]. *Biuletyn Instytutu Geologicznego*, 126, 143-153 [in Polish].
- Rubinowski, Z. (1971). Rudy metali nieżelaznych w Górach Świętokrzyskich i ich pozycja metalogiczna [Non-iron metal ores in the Holy Cross Mountains and their metallogenic position]. *Biuletyn Instytutu Geologicznego*, 247, 1-166 [in Polish].
- Wieser, T. & Żabiński, W. (1986). Copper arsenate and sulphate minerals from Miedzianka near Kielce (Poland). *Mineralogia Polonica*, 17 (1), 17-41.
- Wojciechowski, J. (1958). Minerale miedzi pod Chęcynami [Copper minerals near Chęciny]. *Prace Muzeum Ziemi*, 1, 134-156 [in Polish].



STOP 2: Hematite mineralization in Zachełmie quarry, Holy Cross Mts.

Piotr LENIK¹, Sylwester SALWA²

¹Polish Geological Institute – National Research Institute, Skrzatów 1, 31-560 Kraków;
e-mail: piotr.lenik@pgi.gov.pl

²Polish Geological Institute – National Research Institute, Zgoda 21, 25-953 Kielc;
e-mail: sylwester.salwa@pgi.gov.pl

The Zachełmie Quarry is located in the western part of Chełmowa Mountain near Zagnańsk in the Holy Cross Mountains. In the quarry Devonian dolomites were exploited, forming an „island“ of Palaeozoic formations emerging from under the cover of Permian-Mesozoic rocks (Fig. 1). This area belongs structurally to the Łysogóry region of the Palaeozoic core of the Holy Cross Mountains. The quarry is known primarily for two reasons. The first is the presence of a Postvariscan unconformity between the middle Devonian and Permian-Triassic rocks. The second is to find traces of tetrapods in this quarry. Another interesting phenomenon in the Zachełmie quarry is the presence of hydrothermal hematite mineralization (Fig. 2). This fact has been known since the beginning of the existence of the quarry. Before World War II hematite was even mined as an accompanying mineral (Czarnocki 1950).

The dolomites dip at an angle of about 40° towards the NNE. They are locally brecciated and cut by a few vertical strike-slip faults on a NNE-SSW trend. The faults are associated with narrow, rarely exceeding 0.5 m thickness, zones of tectonic breccia. Devonian rocks are covered by horizontal Permian and Triassic claystones, mudstones and sandstones which do exhibit almost no tectonic involvement, except for a single, normal fault trending WNW-ESE.

The hydrothermal veins in the Zachełmie quarry formed at two stages. Its older stage represents iron (hematite) mineralization defined by Rubinowski (1971) as the Zagnańsk type. The younger stage of mineralization is ore-free and is represented by dolomite-barite-calcite veins with ankerite, (aragonite?) and quartz.

Hematite mineralization occurs only in the northern part of the Zachełmie quarry and has a veinous and nest character. Vertical and steep hematite veins used the NNE-SSW and N-S joint sets. The richest accumulations of hematite, in the form of massive nests up to 60 cm in diameter, occur in places where the joint sets intersect the interlayer spaces.

The ore mineral in this paragenesis is hematite, which occurs as two species. The first is t phaneric – specularite. In this form, hematite forms polycrystalline aggregates in which the size of individual hematite plates reaches up to 2 mm (Fig. 3a). Large nest accumulations of hematite are composed mainly of this type of hematite.

The second is cryptocrystalline type hematite – red ochre. In microscope images, the massive hematite clusters usually have a cellular structure, where the walls are made of more solid hematite aggregates and the inner parts are made of more dispersed hematite aggregates. Most often the outlines of such cells are irregular (boxwerk type). The clusters of small (up to 1 mm) hematite crystals show structures which could have been formed by displacement and replacement of earlier minerals (Fig. 3b). Some of the forms indicate that they could have been dolomite (or ankerite) crystals or by replacing the colomorphic structures, possibly also composed of iron minerals (goethite or colomorphic hematite). The replacement of primary dolomite I crystals

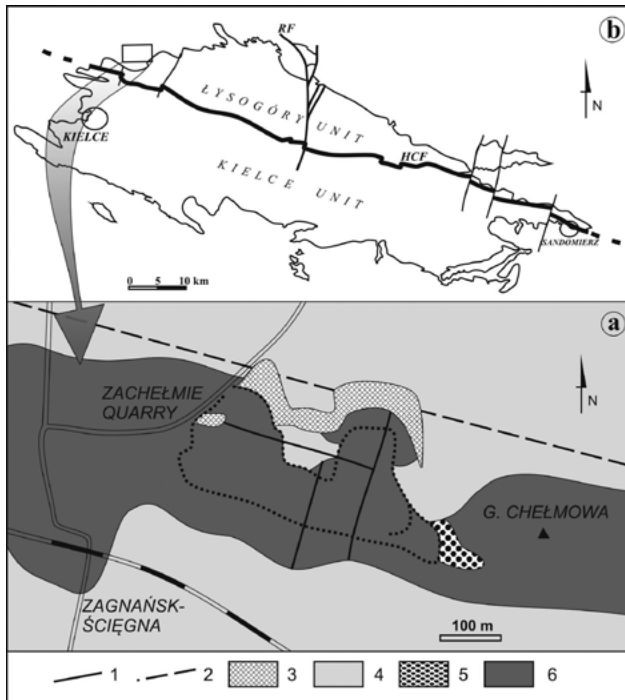


Fig. 1. Geological sketch of the Zachełmie quarry vicinity (a) in relation to the main structural units of the Holy Cross Mountains (after Czarnocki, 1950). Explanations: 1 – faults, 2 – probably faults, 3 – dumps, 4 – Triassic, 5 – Permian, 6 – Devonian.

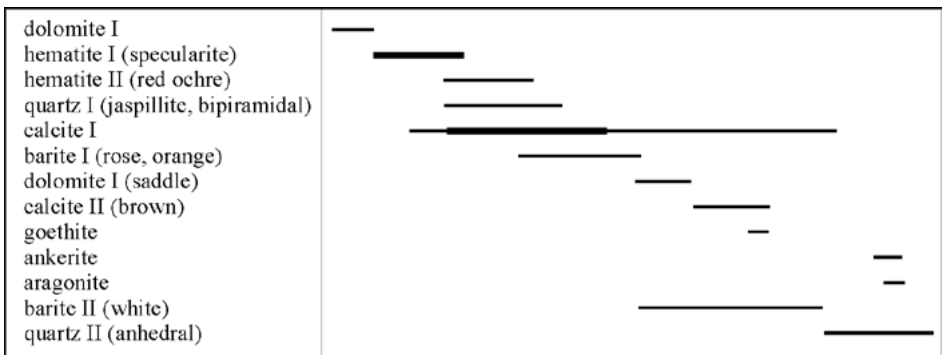


Fig. 2 Mineral succession of hydrothermal mineralization from Zachełmie quarry.

by hematite was selective. Preserved pseudomorphs of hematite clusters show a zonal structure, such as the original dolomites. Probably, individual zones in dolomites differed in chemical composition, especially in manganese and iron content. The effects of dedolomitisation of younger saddle dolomites, visible in the samples, show that the zones containing manganese were first dissolved and metasomatized in the dolomites and only then enriched in iron. Phaneric hematite may also replace carbonates (mainly dolomite) of the rock hosting ore mineralization. The replacement of the sparite and dolomite microsparite took place along the edge of the dolomite crystals until they were completely replaced. Typical metasomatic ores were then formed (Fig. 3c, d).

The second variety of hematite, cryptocrystalline in the form of red ochre, most often forms impregnating occurrences in the host rock, where dolomite microsparite penetrates between the dolomite microsparites or impregnates minerals younger than the nanocrystalline hematite, such as calcite, quartz or barite, giving them a characteristic red or cherry color. The position in which red ochre occurs indicates that it is generally younger than the specularite and completes the stage of iron mineralisation.

The hematite is mainly accompanied by quartz, which forms two morphological types. The first is amorphous, anhedral-shaped quartz deposits replacing dolomite microsparite that builds the rock that hosts ore mineralization. They form irregular, cherry coloured (dispersed hematite) jasper zones around hematite nests in the dolomites. In this type of quartz aggregates, there are also inclusions of specularite in quartz as small, needle-shaped crystals up to several dozen micrometers in size. The second form of quartz occurrence is associated with the final hydrothermal mineralization processes. Idiomorphic quartz crystals (bipyramidal), up to 7 cm long, are present in druses and voids. They grew on rock fragments as well as on hematite and often contain specularite inclusions.

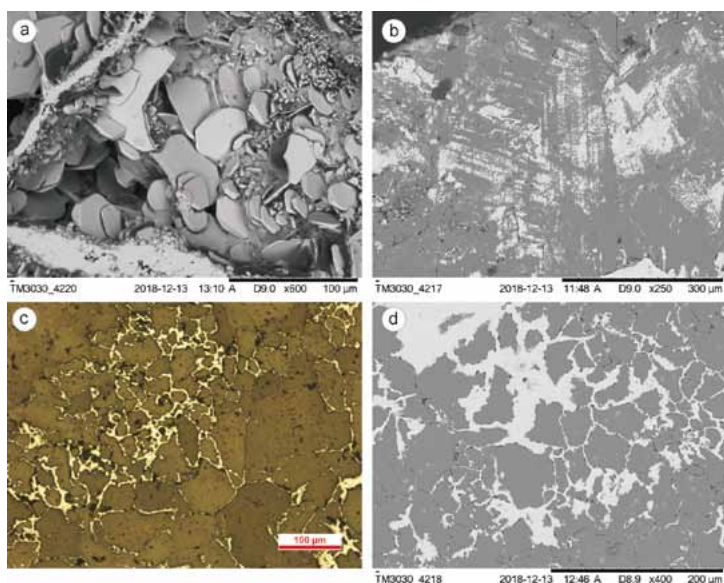


Fig. 3 The forms of hematite mineralization: a – specularite, BSE image; b – selective metasomatism of hydrothermal dolomite by hematite, BSE image; c, d – metasomatism of sparite dolomite by hematite, c – reflected light, d – BSE image.

The younger stage of formation of the mineral veins is ore-free. It is represented by dolomite II-barite-calcite veins with ankerite, aragonite and quartz II. The second generation of dolomite forms euhedral crystals of saddle shape and zonal structure. These dolomites may yield dedolomitization processes with the separation of goethite at the levels of scaling or at the boundaries of crystals. Dolomite and calcite are the most common minerals in the hydrothermal veins. There are both red calcites, whose colour comes from minor hematite inclusions. This indicates their simultaneous formation with the final phases of hematite increasing. Very often they are a cement for breccias made of an older variety of hematite – specularite. There are also brown calcites, after dolomite, formed as a result of dedolomitization of saddle dolomites. The presence of the youngest, white calcites as well as aragonite and ankerite, which coexist with them, was also noted. Calcites rarely form euhedral crystals, but most often anhedral ones or pseudomorphs after dolomite and aragonite. Aragonite (calticic calcitic ??? pseudomorphs) and ankerite are most commonly found in druses, forming well shaped crystals up to several cm long. Some of the calcite clusters show crushes forming the characteristic pattern of colomorphic structures. It is possible that aragonite could have been the precursor for this type of calcite, which tends to form such structures and only later transformed into calcite. However, it cannot be precluded that this type of calcite, with outlines of colomorphic structures, are pseudomorphs after other minerals that form such structures, e.g. goethite. Quartz II, occurring rarely, forms anhedral fillings druses crystals of calcite. (Rewrite this last sentence) This variety of quartz has no hematite appendages and can reach up to 2 cm in size.

The last barren mineral associated with the hydrothermal mineralization processes present in the Zachełmie quarry is barite. It forms two types of clusters. The older one, associated with the final processes of hematite mineralization, forms irregular, nest accumulations, sometimes cementing the aggregations of nanocrystalline hematite. It is in the form of small (up to a few mm) plate crystals of orange or reddish color, coming from the dispersed hematite pigment. The younger generation of barite forms large, white, plate-like crystals, the size of which reaches several centimeters. On the surface they may be cherry in colour, probably as a result of weathering of hematite.

The issue of age of both stages of mineralization seems to be clear. In no case was the presence of mineral veins in Permian-Triassic rocks observed. This indicates that both its stages are Variscan.

References

- Czarnocki, J. (1950). Geologia regionu łysogórskiego w związku z zagadnieniem złoża rud żelaza w Rudkach. Prace Instytutu Geologicznego, *6a*, 1-153.
- Rubinowski, Z. (1971). Rudy metali nieżelaznych w Górach Świętokrzyskich I ich pozycja metalogeniczna. Biuletyn Instytutu Geologicznego, *247*, 1-140.



Stop 3: Bardo diabase – Prągowiec

Jerzy NAWROCKI¹, Magdalena PAŃCZYK²

¹Maria Curie Skłodowska University, Faculty of Earth Sciences and Spatial Management, Lublin, Kraśnicka 2cd, 20-718, Poland

²Polish Geological Institute – National Research Institut, 4 Rakowiecka St., 00-975 Warszawa, Poland; e-mail: magdalena.panczyk@pgi.gov.pl

The most extensive magmatic intrusion of the Holy Cross Mts. occurs in the Bardo syncline. It is widely named the Bardo diabase (e.g. Czarnocki 1919; Kowalczewski 1974). One of the exposures occurs on the northern limb of the Bardo Syncline on the bank of the Bardzianka river (Fig. 1). According to Krzemiński (2004), the CIPW normative composition classifies the Bardo diabase as olivine tholeiite. It shows strong chemical similarity to continental flood basalts, which are associated with extensional tectonics (op. cit). The Bardo diabase contains not only a geochemical record but it also documents some features of the ancient geomagnetic field. It can give information about the age of the diabase and the geographical location of the Holy Cross Mts. during emplacement of the magma. On the other hand, the Bardo diabase can be considered as a possible raw material and we should search for the best place enabling its exploitation.

The diabase intrusion penetrates the Silurian rocks of the Bardo Syncline, close to the stratigraphic boundary between Lower Ludlow graptolite shales and Upper Ludlow greywackes. The overall thickness of the intrusion varies between 20 and 30 m. The first magnetic survey of the Bardo Syncline was performed between 1937 and 1942. It proved an almost continuous diabase body surrounding the Bardo Syncline (Czarnocki 1958; Kowalczewski, Lisik 1974).

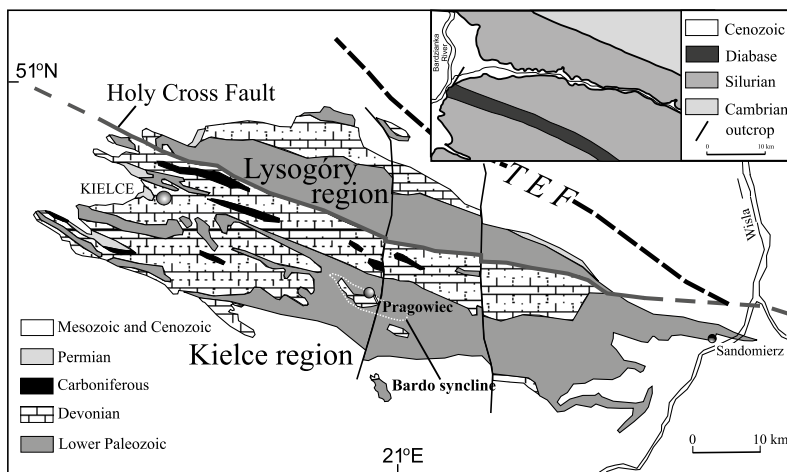


Fig. 1 Geological sketch map of the Holy Cross Mountains (after Kowalczewski et al. 1990) with location of Prągowiec diabase outcrop.

Spatial image of the diabase is more complex in the western part of the syncline where the authors draw more than two dykes. A detailed magnetic survey was performed in that part of the syncline (Nawrocki et al. 2007a). According to the geological map of Czarnocki (1958) the roots of the diabase intrusion should occur at the surface just in the area studied.

The tectonic and stratigraphic observations point to a Late Ludlowian – Siegenian age interval for the Bardo intrusion. The Ludlowian strata along with the diabases were folded and discordantly covered by Lower Devonian (Emsian) sediments, equivalent to the Old Red facies (Kowalczewski, Lisik 1974). In the vicinity of Prągowiec the unconformity is 30 – 50° of dip (Kowalczewski, Migaszewski 1994). A paleomagnetic study described below provides a pre-folding paleomagnetic pole concordant with the Ludlow segment of the Baltic APWP (Nawrocki 2000). However, preliminary isotope studies did not exclude their Variscan age (Migaszewski, 2002). Younger ⁴⁰Ar-³⁹Ar studies (Nawrocki et al. 2007b, 2013) provided more consistent age data. The combined Ar-Ar and magnetostratigraphic age of the Bardo diabase intrusion (425 – 417 Ma; Nawrocki et al. 2013) is comparable with the U-Pb age of a diorite intrusion (420 ± 2 Ma) from the northern part of the Brunovistulian terrane (Sosnowiec IG-1 borehole; Nawrocki et al. 2019). These intrusions were emplaced during the same event of regional tectonic extension at the Silurian/Devonian boundary. This event was most probably associated with the Rheic Ocean closure in this part of Europe and with the onset of extension forming the Rheno-Hercynian Basin (Nawrocki et al. 2019).

References

- Czarnocki J. (1919). Stratygrafia i tektonika Gór Świętokrzyskich. Prace Towarzystwa Naukowego, 28, 77-81.
- Czarnocki J. (1958). Mapa rozmieszczenia diabazów w okolicy Łagowa. Surowce mineralne w Górach Świętokrzyskich, z.3 Surowce Skalne, Prace Instytutu Geologicznego 21.
- Kowalczewski, Z. & Lisik R. (1974). New data on diabases and geological structure of the Prągowiec area in the Góry Świętokrzyskie Mts. (in Polish with English summary), Bulletin of Polish Geological Institute, 275, 114-158.
- Kowalczewski, Z. & Migaszewski, Z. (1994). Excursion stop: Bardo – Prągowiec Ravine, in Europrobe, Trans-European Suture Zone Workshop, Kielce, Poland, 24th September – 1st October, Excursion Guidebook: 39-45.
- Kowalczewski Z., Romanek A. & Studencki M. (1990). Mapa geologiczna odkryta paleozoiku Gór Świętokrzyskich (uproszczona). Archiwum PIG-PIB, Kielce.
- Krzemiński, L. (2004). Geochemical constraints on the origin of the mid-Paleozoic diabases from the Holy Cross Mts. and Upper Silesia, southeastern Poland. Geological Quarterly, 48, 147-158.
- Migaszewski, Z.M. (2002). Datowanie diabazów i lamprofirów Świętokrzyskich metodą K-Ar i Ar-Ar. Przegląd Geologiczny, 50, 227-229.
- Nawrocki, J. (2000). Late Silurian paleomagnetic pole from the Holy Cross Mountains: constraints for the post-Caledonian tectonic activity of the Trans-European Suture Zone. Earth and Planetary Science Letters, 179, 325-334.
- Nawrocki J., Polechońska O. & Salwa S. (2007a). Model przestrzenny intruzji bardziańskiej w okolicach Zagorza (region kielecki Gór Świętokrzyskich) w świetle wyników nowych badań magnetycznych. Przegląd Geologiczny, 55, 1136-1142.

- Nawrocki J., Dunlap J., Pecskey Z., Krzemiński L., Żylińska A., Fanning M., Kozłowski W., Salwa S., Szczepanik Z. & Trela W. (2007b). Late Neoproterozoic to Early Palaeozoic palaeogeography of the Holy Cross Mountains (Central Europe): an integrated approach. *Journal of Geological Society, London*, *164*, 405-423.
- Nawrocki, J., Salwa, S. & Pańczyk, M. (2013). New ^{40}Ar - ^{39}Ar age constrains for magmatic and hydrothermal activity in the Holy Cross Mts. (southern Poland) *Geological Quarterly*, *57*, 551-560
- Nawrocki J., Pańczyk M. & Szrek P. (2019). Magmatic activity at the Silurian/Devonian boundary in the Brunovistulia and Małopolska Terranes (S Poland): possible link with the Rheic Ocean closure and the onset of the Rheno-Hercynian Basin. *Geological Magazine*, DOI: <https://doi.org/10.1017/S0016756819000384>

Authors' Index

Talat AHMAD	43	Piotr GUNIA	40
Robert ANCZKIEWICZ	87	Ryszard HABRYN	57
Sonja AULBACH	31, 68, 89, 96	Thomas HADLARI	44
Bogusław BAGIŃSKI	22, 27, 34, 40	Daniel HARLOV	27
Kamila BANASIK	42	Elżbieta HYCYNAR	80
Christopher BARNES	91	Sławomir ILNICKI	45, 46
Wojciech BARTZ	28, 41, 92	Janusz JANECZEK	37
Jakub BAZARNIK	58, 59	Zdzisław JARY	51
Zdzisław BELKA	40	Piotr JELEŃ	82, 83
Łukasz BIRSKI	29	Mariusz O. JĘDRYSEK	30
Michał BUCHA	30	Leif JOHANSSON	70
Daniel BUCZKO	31	Petras JOKUBAUSKAS	27, 47, 94
Bartosz BUDZYŃ	29, 32, 90	Dominik JURA	48
Jolanta BURDA	20, 33	Maciej KAŁASKA	49
Anna CEDRO	60	Gabriela KASZUBA	87
Bernard CEDRO	60	Katarzyna KĄDZIOLKA	50
Małgorzata CEGIEŁKA	34	Piotr KENIS	51
Andrzej CHMIELEWSKI	35	Jakub KIERCZAK	50, 75
Aleksandra CHOJNACKA	30	Iwona KLONOWSKA	91
Jakub CIAZELA	36, 69, 74	Urs KLÖTZLI	20, 33
Justyna CIESIELCZUK	37, 48	Gustaw KONOPKA	93
Matthew COBLE	52	Patryk KOSAŁKA	56
Anna CZARNECKA-SKWAREK	38	Karolina KOŚMIŃSKA	52, 95
Marcin DĄBROWSKI	88	Jakub KOTOWSKI	49, 53
Ewa DEPUT	56	Wiesław KOZDRÓJ	71
Paweł DERKOWSKI	94	Gabriela A. KOZUB-BUDZYŃ	90
Anna DETMAN	30	Łukasz KRUSZEWSKI	54, 55, 56
Justyna DOMAŃSKA-SIUDA	39, 99	Ewa KRZEMIŃSKA	43, 57, 94
Mateusz DULSKI	37	Leszek KRZEMIŃSKI	57
Daniel J. DUNKLEY	15	Tomasz KRZYKAWSKI	37
Monika FABIAŃSKA	48	Anna KUKUŁA	69, 89
David G. GEE	91	Monika A. KUSIAK	15
Miłosz GIERSZ	49	Piotr LENIK	58, 59, 104
Grzegorz GIL	40, 45	Markus LENZ	92
Jane GILOTTI	52	Quili LI	20, 33
Marcin GOLEŃ	88	Yan LIU	45
Bożena GOŁĘBIEWSKA	82, 83	Ray MACDONALD	27, 34
Magdalena GORYL	42	Łukasz MACIĄG	60, 61
Maciej GÓRKA	41	Anna MACIOCH	62
Anna GRABARCZYK	43	Stanisław MADEJ	40
Marta GRABOWSKA	36	Jarostaw MAJKA	63, 91, 95
Oliwia GRAFKA	67	Rafał MAŁEK	64
Michel GREGOIRE	31, 70	Maciej MANECKI	95
Dominik GURBA	94		

Dariusz MARCINIAK	65	Anna SIKORA	30
Beata MARCINIAK-MALISZEWSKA	56, 66	Laurynas SILIAUSKAS	22
Leszek MARYNOWSKI	30, 42, 77, 85	Bernd R.T. SIMONEIT	77
Barbara MASSALSKA	67	Magdalena SITARZ	82
Piotr MATCZUK	68	Rafał SIUDA	55, 56, 83, 99
Magdalena		Grazina SKRIDLAITE	22
MATUSIAK-MAŁEK	31, 68, 69, 70, 89, 96	Alisa SKURIDINA	41
Witold MATYSZCZAK	27	Jacek SKURZYŃSKI	51
Hubert MAZUREK	36, 69	Jiří SLÁMA	32
William MCCLELLAND	52	Piotr SŁOMSKI	84
Jakub MIKRUT	70	Justyna SMOLAREK-LACH	42, 85
Magdalena MISZ-KENNAN	48	Marcin STACHOWICZ	86
Stanisław Z. MIKULSKI	64	Krzysztof SZAMAŁEK	93
Andrzej MUSZYŃSKI	36	Jacek SZCZEPAŃSKI	46, 65, 84, 87, 88
		Marcin SYCZEWSKI	49
Jerzy NAWROCKI	71, 72, 108	Eligiusz SZEŁĘG	37, 55
Krzysztof NEJBERT	39, 82		
Joanna NOWIK	48	Mateusz ŚWIERK	55
Theodoros NTAFLIOS	31, 68, 69, 70, 89, 96		
		Sylvin S. T. TEDONKENFACK	89
Sławomir OSZCZEPALSKI	35	Fabian TRAMM	90
		Wiesław TRELA	79, 85
Jolanta PACZEŚNA	57	Riccardo TRIBUZIO	74
Magdalena PAŃCZYK	71, 72, 108		
Jan PARAFINIUK	83	Brian G.J. UPTON	31, 68
Levente PATKO	36	Łukasz UZAROWICZ	73
Artur PĘDZIWIATR	73		
Adam PIECZKA	81, 83	Katarzyna WALCZAK	91, 95
Bartosz PIETEREK	36, 69, 74	Haozheng WANG	88
Anna PIETRANIK	50, 76	Paul B. WIGNALL	85
Mikołaj PIETRAS	30	Martin J. WHITEHOUSE	15
Łukasz PLEŚNIAK	30	Simon A. WILDE	15
Anna POTYSZ	41, 50, 73, 75, 92	Richard WIRTH	29
Anna POSZYTEK	67	Janina WISZNIEWSKA	43
Sabina PRUSINSKIENE	22	Beata WOSKOWICZ-ŚLĘZAK	33
Arkadiusz PRZYBYŁO	76	Krzysztof WOŹNIAK	23
Jacek PUZIEWICZ	31, 69, 70, 89, 96	Emilia WÓJCIK	38
		Krystian WÓJCIK	71
Jolanta RATUSZNA	28		
Agnieszka ROŻEK	38	Dominik ZAWADZKI	61
Maciej RYBICKI	77	Katarzyna ZBOIŃSKA	92
Grzegorz RZEPA	90	Karol ZGLINICKI	93
		Xin ZHONG	88
Sylwester SALWA	58, 59, 78, 79, 104	Grzegorz ZIELIŃSKI	57, 72, 94
Felix SCHMIDT	92	Grzegorz ZIEMNIAK	95
Anja SCHREIBER	29	Małgorzata ZIOBRO	89, 96
Ilona SEKUDEWICZ	45	Małgorzata ZIÓŁKOWSKA-KOZDRÓJ	71
Magdalena SĘK	80		
Mateusz SĘK	81	Paweł ŻOCHOWSKI	56
Wojciech SIERNY	54		



Mineralogy in the modern world

emc² 2020
6 - 10 september

3rd European Mineralogical Conference
Cracow Poland

The third European Mineralogical Conference will be held in Poland at the Auditorium Maximum Jagiellonian University in Kraków 6-10 September 2020 and will cover a broad range of themes:

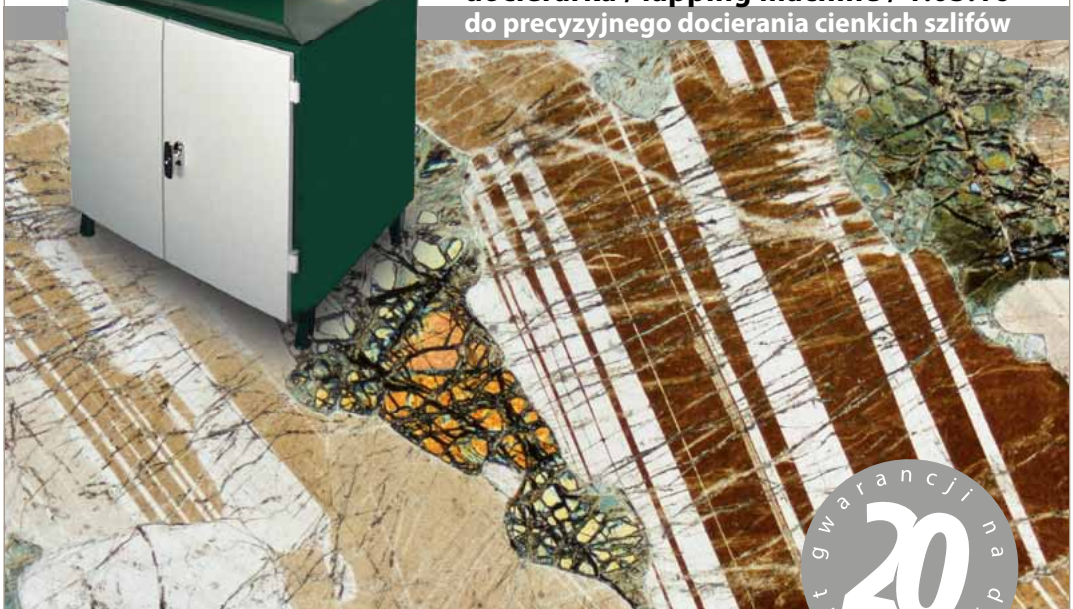
- T1. Advanced analytical techniques
- T2. Applied mineralogy
- T3. Archaeometry, care and preservation
- T4. Atomistic and thermodynamic modelling
- T5. Education and mineralogy
- T6. Environmental mineralogy and low T geochemistry
- T7. Experimental mineralogy and petrology
- T8. Geobiochemistry, Geomicrobiology and Biomineralogy
- T9. Geochronology
- T10. Magmatism and volcanology
- T11. Mantle petrology and geochemistry
- T12. Metamorphism
- T13. Mineral deposits and raw materials
- T14. Mineral diversity and evolution
- T15. Mineral physics
- T16. Mineralogical crystallography
- T17. Planetary materials and processes
- T18. Radioactive materials

www.emc2020.ptmin.eu



BROTLAB®
od skały do szlifu

docierarka / lapping machine / 1.03.16
do precyzyjnego docierania cienkich szlifów



fotografia szlifu z zasobów prof. B. Bagińskiego Wydział Geologii UW

BROT Technologies od ponad 50 lat zajmuje się projektowaniem i produkcją urządzeń służących do przygotowywania próbek geologicznych. Gama oferowanych narzędzi pokrywa zapotrzebowanie laboratoriów geologicznych w takich sektorach jak: górnictwo, wydobywanie ropy i gazu, ośrodki badawcze i naukowe. Tworzy następujące rodziny aparatów: przecinarki, docierarki i szlifierki, polerki oraz przyrządy do spajania i impregnacji, które można zestawić w kompletną linię do przygotowywania cienkich szlifów dla geologii, mineralogii gleboznawstwa, petrologii i archeologii. W ofercie znajdują się również szereg materiałów eksploatacyjnych i akcesoriów do produkowanych urządzeń w tym: diamentowe narzędzia skrawające, pasty diamentowe, materiały ściernie, kleje, żywice i inne.

Przedstawiciel w Polsce

EMDER

EMDER Sp. z o.o., Dziekanów Leśny, ul. Rolnicza 262, 05-092 Łomianki, e-mail: biuro@emder.pl



**BUREAU
VERITAS
MINERALS**

BUREAU VERITAS Upstream Minerals



INDUSTRY LEADING SOLUTIONS FOR THE EXPLORATION AND MINING COMMUNITY

- Sample Preparation
- Geochemical and Assay Laboratory
- Laser Ablation, XRF, Ore & High Grade Analysis
- Fast Turnaround Fire Assay Testing
- Customer Web Access to our Enterprise Management System (LIMS/EMS)
- MineDSi, Core logging and Spectral
- Full On-Site Services Packages



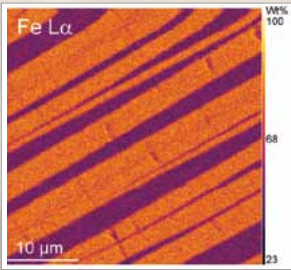
AcmeLabs Polska Sp. z o.o.
ul. Magazynowa 3
30-858 Kraków, Poland
adam.potoczek@pl.bureauveritas.com
+48 601 306 201
www.bureauveritas.com/um

World-leading analytical instruments for geo & environmental sciences

EPMA

SXFive-TACTIS

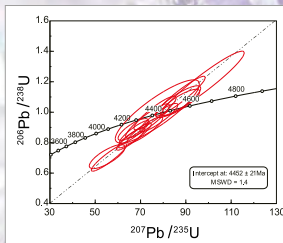
A unique touchscreen **Electron Probe MicroAnalyzer**, specifically designed for multi-user facilities to take full advantage of a single tool. High resolution trace element mapping and reproducible quantitative analysis of the most challenging geological samples. Shown here: quantitative X-ray map from intensely brecciated Howardite meteorite (Tindouf area, Sahara). High spatial resolution is achieved using a focused electron beam (7 keV / 30 nA).



SIMS

IMS 1300-HR³

Large Geometry **Secondary Ion Mass Spectrometer** with unequalled analytical performance for a wide range of geoscience applications: tracking geological processes using stable isotopes, dating minerals, determining the distribution of trace elements... Shown here: U-Pb dating in apatite grains. *Data from O. P. Popova et al., Science (2013).*

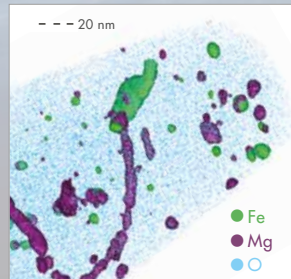


Also in our SIMS product lines:
NanoSIMS 50L: High spatial resolution multicollection SIMS
IMS 7F-GEO: High throughput SIMS for geoscience laboratories

APT

LEAP[®] 5000

State-of-the-art **Atom Probe Tomography** system delivering sub-nanometer chemical analysis of trace elements in complex mineral systems and extra-terrestrial samples. Shown here: 3-D nanoscale analysis of igneous zircon from Martian meteorite NWA 7475, revealing a complex nano-structure of trace element enrichment within multiple linear features and numerous clusters. *Courtesy of Prof. D. Moser, Univ. of Western Ontario.*

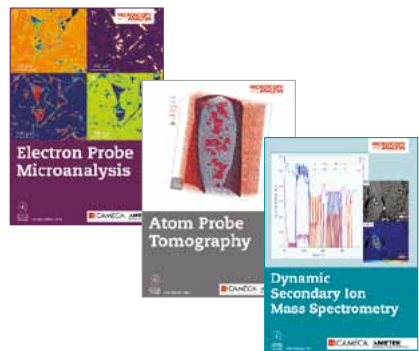


Expand your knowledge with our free guides!

Co-edited with Wiley, *Essential Knowledge Briefs on Electron Probe Microanalysis, Secondary Ion Mass Spectrometry and Atom Probe Tomography* are available for **free download** from cameca.com. Each booklet provides a simple introduction to the analytical technique, details some of its specific implementations and explores the developments that are likely to be seen in the future. Case studies provide examples of how each technique is used in the real world by leaders in geo- and cosmochemistry, vulcanology, geochronology, and more!

Scan to the QR code →
to download your free guides

or visit www.cameca.com/focus/tuto



Dystrybutor aparatury badawczej i naukowej od 1993 roku

Aparatura technologiczna, m.in:

- **Neocera** - PLD (Pulsed Lased Deposition)
- **Riber** - MBE (Molecular Beam Epitaxy)
- **Aliance Concept** - nanoszenie warstw metodami sputteringu
- **Annealsys** - szybka obróbka cieplna RTP
- **Plasma-Therm** - trawienie plazmowe
- **FCT Anlagenbau GmbH** - obróbka cieplna przy podwyższonym ciśnieniu
- **Memsstar** - wytrawianie i osadzania w procesach półprzewodnikowych, MEMS oraz technologiach pokrewnych
- **TPT Wire Bonder** - wykonywanie połączeń drutowych

Aparatura badawcza, m.in:

- **Cameca** - spektroskopy mas jonów wtórnych SIMS i mikroskopy elektronowe EPMA, APT (Atom Probe Tomography)
- **Hitachi** - mikroskopy elektronowe SEM, TEM, STEM, FIB, Dual Beam, Triple Beam, mikroskopy sił atomowych AFM, urządzenia do przygotowywania próbek (flat milling, cross-section)
- **Thermo Fisher Scientific** - systemy EDS, WDS, EBSD, XPS (ESCA)
- **Horiba Scientific** - spektrometry Ramana, spektrometry emisyjne: ICP-OES, GD-OES, GD-MS, monochromatory, siatki dyfrakcyjne, elipsometry spektroskopowe, spektrometry VUV
- **Bruker-microCT** - mikrotomografy komputerowe do badań z zakresu Material Science i Life Science (in-vivo i ex-vivo)
- **Neaspec** - systemy nano-FTIR, neaSNOM
- **Setaram** - analizatory termiczne: DTA, DSC, TG, TMA
- **C-therm** - urządzenia do pomiarów przewodnictwa cieplnego
- **JANIS Research Company** - kriosystemy
- **Riber** - systemy MBE
- **Solartron Analytical** - potencjostaty/galwanostaty
- **Newport Spectra-Physics** - fotonika, optyka i optomechanika systemy laserowe

COME F SP. Z O.O. SP. K.

Główne biuro:
ul. Gdańska 2, 40-719 Katowice
Tel: +48 32 428 38 20
Fax: +48 32 428 38 30
Email: comef@comef.com.pl

www.comef.com.pl

Biuro w Warszawie:
ul. Niedźwiedzia 10B, 02-737 Warszawa
Tel: +48 22 848 18 44
Fax: +48 22 233 01 11
Email: warszawa@comef.com.pl



INTELIгентNY
DYFRAKTOMETR



www.malvernpanalytical.com/empyrean

EMPYREAN

Trzecia generacja wielofunkcyjnego
dyfraktometru z **MultiCore Optics**

Malvern Panalytical B.V.
Branch Poland
ul. Ostrobramska 101 A
04-041 Warszawa
szymon.stolarek@malvernpanalytical.com.
Tel + 48 22 8632009

 **Malvern
Panalytical**
a spectris company



Polish Geological Institute
National Research Institute



MICRO-AREA ANALYSIS LABORATORY



SHRIMP
IIe/MS



HITACHI
SU 3500



CAMECA
SX 100

Laboratorium Analiz w Mikroobszarze
Państwowy Instytut Geologiczny
- Państwowy Instytut Badawczy
ul. Rakowiecka 4, 00-975 Warszawa
tel. 22 45 92 232; fax 22 45 92 001



SCAN CODE SMARTPHONE
AND LEARN MORE...

Retsch®

MILLING SIEVING ASSISTING

PRZEGLĄD PRODUKTÓW RETSCH

Więcej informacji na stronie www.retsch.pl. Znajdą tam Państwo nowości, informacje o poszczególnych produktach, broszury, filmy video do pobrania, wyszukiwarke aplikacji i wiele innych.



Kruszarki szczękowe
BB 50/BB 100/BB 200/BB 250/
BB 300/BB 400/BB 500/BB 600



Młyn ultra odśrodkowy
ZM 200



Młyn bijakowy
SR 300



Młyn krzyżakowo bijakowy
SK 300



Młyn z cyklonem
TWISTER

Mielenie



Młyn nożowe
GRINDMIX GM 200/GM 300



Młyny tnące SM 100/SM 200/
SM 300/SM 400



Ucierak móżdżerowy
RM 200



Młyny dyskowe
DM 200/DM 400



Wibracyjne młyny dyskowe
RS 200/RS 300



Młyn do XRD
McCrone



CryoMill



Młyn miksujące
MM 200/MM 400/MM 500



Młyn wysokoenergetyczny
Emax



Młyny planetarno kulowe
PM 100 CM/PM 100/PM 200/
PM 400

Przesiewanie



Przesiewacze wibracyjne
AS 200/AS 300/AS 400/AS 450



Przesiewacz wibracyjny
AS 200 tap



Przesiewacz Air Jet
AS 200 jet



Sita testowe
Oprogramowanie EasySieve®



Optyczne analizatory cząstek
CAMSIZER® P4/CAMSIZER® X2/
CAMSIZER® M1

Urządzenia
Pomocnicze



Dzielniki prób
PT 100/PT 200/PT 300/PT 600



Podajnik wibracyjny
DR 100



Suszarka fluidalna
TG 200



Myjnie ultradźwiękowe
UR 1/UR 2/UR 3



Prasy hydrauliczne
PP 25/PP 40

part of **VERDER**
scientific

www.retsch.pl